(2)

NPS55-90-21

NAVAL POSTGRADUATE SCHOOL

Monterey, California

Co

A STUDY OF UNDERWATER SOUND RAY
TRACING METHODOLOGY

Robert R. Read

September 1990

Approved for public release; distribution is unlimited.

Prepared for:
Naval Postgraduate School,
Monterey, CA 93955

7

NAVAL POSTGRADUATE SCHOOL
MONTEREY, CALIFORNIA

Rear Admiral R. W. West, Jr.
Superintendent

Harrison Shull
Provost

This report was prepared under the joint support of Naval Undersea Warfare Engineering Station, Keyport, Washington and the Naval Postgraduate School Research Program.

This report was prepared by:

ROBERT R. READ
Professor of Operations Research

Reviewed by:

PETER PURDUE
Professor and Chairman
Department of Operations Research

Released by:

Dean of Faculty and Graduate Studies

Unclassified

Security Classification of this page

REPORT DOCUMENTATION PAGE

1a Report Security Classification UNCLASSIFIED	1b Restrictive Markings
2a Security Classification Authority	3 Distribution Availability of Report
2b Declassification/Downgrading Schedule	Approved for public release; distribution is unlimited
4 Performing Organization Report Number(s) NPS55-90-21	5 Monitoring Organization Report Number(s)
6a Name of Performing Organization Naval Postgraduate School / 6b Office Symbol *(If Applicable)* OR	7a Name of Monitoring Organization NUWES
6c Address *(city, state, and ZIP code)* Monterey, CA 93943-5000	7b Address *(city, state, and ZIP code)* Code 512, Keyport, WA 98345
8a Name of Funding/Sponsoring Organization Naval Postgraduate School / 8b Office Symbol *(If Applicable)* OR/Re	9 Procurement Instrument Identification Number N0002488WX48044AC
8c Address *(city, state, and ZIP code)* Monterey, California Monterey, CA 93943	10 Source of Funding Numbers

Program Element Number	Project No	Task No	Work Unit Accession No

11 Title *(Include Security Classification)* A Study of Underwater Sound Ray Tracing Methodology

12 Personal Author(s) Read, Robert R.

13a Type of Report	13b Time Covered	14 Date of Report *(year, month,day)*	15 Page Count
Technical	From To	1990, September	

16 Supplementary Notation The views expressed in this paper are those of the author and do not reflect the official policy or position of the Department of Defense or the U.S. Government.

17 Cosati Codes		
Field	Group	Subgroup

18 Subject Terms *(continue on reverse if necessary and identify by block number)* Ray tracing; calibration; underwater tracking; short baseline systems; systematic errors

19 Abstract *(continue on reverse if necessary and identify by block number*

An operational study has been made of the algorithms employed by the Naval Undersea Weapons Engineering Station in ~~their~~ short base line underwater position location systems. Some important sources of systematic error have been uncovered. The issues studied include isospeed vs. isogradient ray tracing, effect of the depth velocity profile and water layer thickness, approximate vs. exact array tilt corrections, and ray tracing initialization methodology.

It is shown that the practice of constant speed extrapolation of depth-velocity information can cause considerable mischief. The best remedy is to measure speed all the way to the bottom. It is further shown that the systematic errors are periodic functions of the azimuth direction of the sound ray from the receiver array. The amplitudes of these functions are greater for the more severely tilted arrays. An alternative algorithm is proposed that reduces these errors by at least an order of magnitude.

20 Distribution/Availability of Abstract [X] unclassified/unlimited [ ] same as report [ ] DTIC users	21 Abstract Security Classification Unclassified	
22a Name of Responsible Individual R. R. Read	22b Telephone *(Include Area code)* (408) 646-2382	22c Office Symbol OR/Re

DD FORM 1473, 84 MAR 83 APR edition may be used until exhausted security classification of this page

All other editions are obsolete Unclassified

Acknowledgements

This report had the partial support of the Naval Undersea Weapons Engineering Station, Keyport, Washington. The computer programming and graphical work was performed by Colin Cooper. The manuscript was processed by Hania La Born.

1. INTRODUCTION

The purpose of this report is to discover and quantify the systematic errors in the algorithms employed by NUWES in their short base line underwater position location system. Systematic error can have a number of sources and previous works [6,7] have treated other issues. The present work deals with the algorithms used in sound ray tracing. There are a number of aspects to be treated, and some background is necessary in order to explain them.

Figure 1 contains a schematic diagram of a short base line hydrophonic array and of the signals it may receive. Sharply pulsed signals, or pings, are sent by the sound source vehicles (surface craft, submarine, torpedo) and they are received by the four transducers (called the X, Y, Z and C-phones) of the array. These four hydrophones form a right angled coordinate system with origins at the C-phone and arm lengths D (=30 feet) to each of the other three phones.

The ray paths from a source to the four receivers are synchronously timed with great precision (10^{-7} secs) and the differentials of arrival times are used to construct the direction of the source. But due to variability of the speed of sound at various water depths, the ray paths themselves are not straight lines. Also the paths may change from day to day as the water depth-velocity profile changes. Knowledge of the current profile allows one to perform a ray tracing computation. Recovery of the three-dimensional position of the sound source is accomplished by reconstructing the ray path and following it for the given amount of time. Each source vehicle has a phase coded "ping" so that its signals can be discriminated from those of other vehicles.

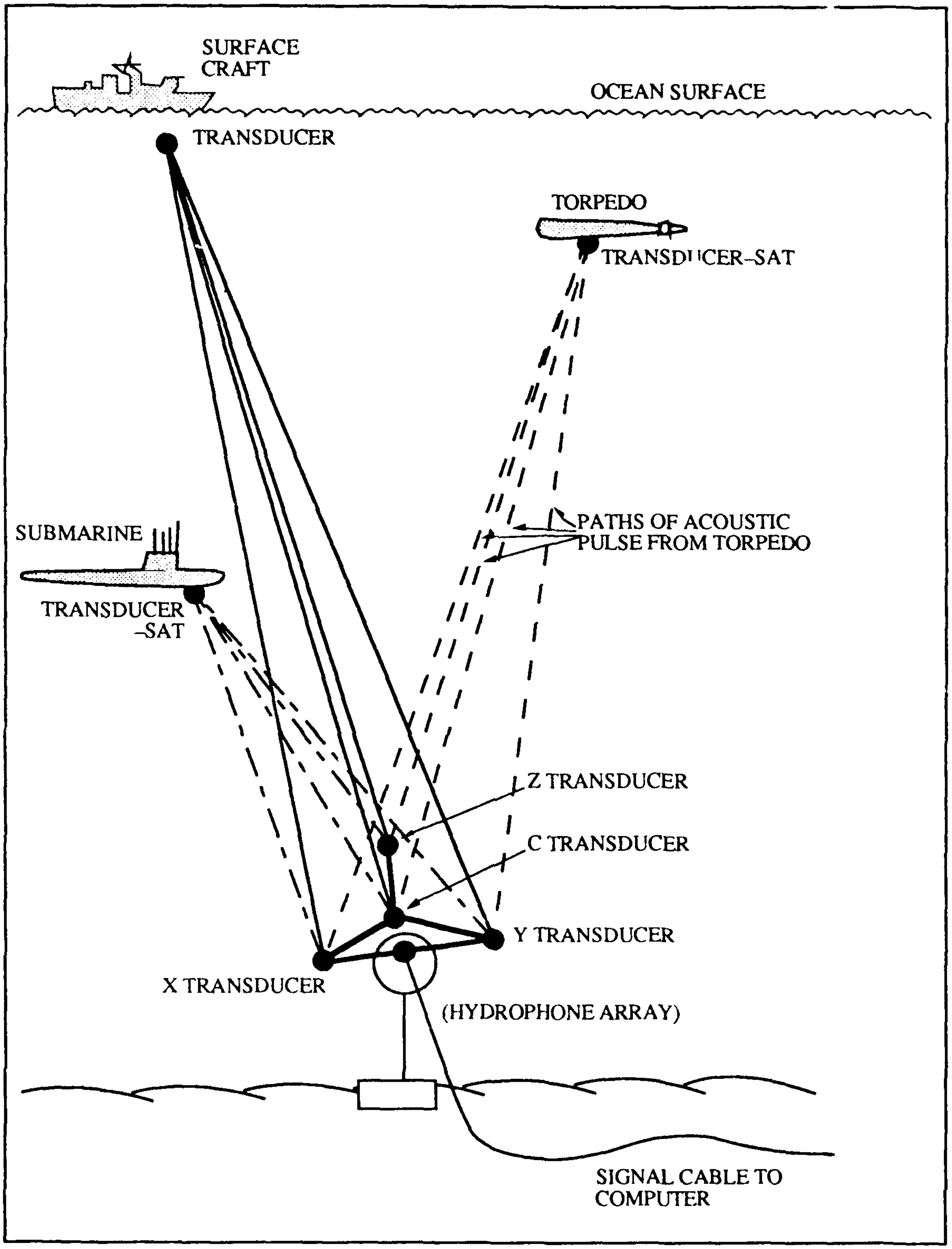

Figure 1. Short Baseline Array and Signal Sources

Each hydrophonic array is placed on the sea floor by lowering it over the side of a utility ship. Each has a self-leveling capability. When finally resting on the bottom, they are not perfectly level, but the X and Y arms have tilt meters that measure the angles that are made with the horizontal. An array surveying activity checks these angles and measures the rotation of the vertical. Thus the local coordinate system can be reconciled with the master range coordinate system.

The currently employed ray tracing methodology partitions the water column into a number of equal thickness layers and treats the speed of sound as constant in each layer. This leads to the use of isospeed ray tracing [1, 5]. Presently the layer thicknesses at Nanoose are 25 feet. In those instances for which the measured depth-velocity profile does not go as deep as the array, a constant speed extrapolation is used. In effect the thickness of the deepest layer is larger, perhaps 50 or 75 feet.

Now the issues can be detailed:

i) How accurate is iso-speed raytracing using a 25 foot water layer increment?

ii) What is the effect when it is necessary to use a thicker deepest layer?

iii) How well are the ray tracing directions and transit times determined?

iv) What effect does the various depth velocity profiles have upon the answers to i), ii) and iii)?

The treatment of these questions requires a valid sound ray construction methodology and a representative set of depth-velocity profiles. To satisfy the latter requirement we have selected twelve experimental days at the Nanoose range spanning the period May 1988 to June 1989. They are presented (in graphical form) in Appendix A. We note that the more interesting ones seem

to appear in the Spring. Two of the experimental days, 23-24 April, 1989 are consecutive. This allows us a glimpse into the question of day to day variability.

To treat the former requirement, we have developed an isogradient ray fitting algorithm. It fits a sound ray connecting two given points (in the horizontal-vertical plane) assuming direct path propagation. The depth velocity profile is partitioned into five foot equi thickness layers and within each layer the slope of sound speed vs. depth is constant. Thus the DV profile is represented as a continuous function consisting of a sequence of straight line segments. Within each layer the ray path is a circle arc because of Snell's law, [2,3,8]. The outputs of this algorithm are the angles that the ray makes with the horizontal at each of the endpoints, and the transit time of the ray from the initial point to the final one.

Section 2 of the report presents some theoretical material and formulas. The distinctions between isospeed and isogradient ray tracing are explained. Snell's law is introduced and supported.

Section 3 of the report deals with the accuracy of pure ray tracing in two dimensions, the horizontal-vertical plane. Computations are made for a number of initial angle–transit time pairs and for all twelve depth velocity profiles. Errors from this source are generally small but can be as large as a foot or more. The situation is more difficult when extrapolation of the water column is necessary. This occurs when the sounding does not extend as deep as the receiver. In such cases we cannot be definite about the nature of the errors, but several equally defensible methods lead to results that disagree by five or ten feet and even more. We state that there is a problem with

extrapolation. The soundings should be made at the deepest part of the range and to full depth. Failing that, a careful development of an extrapolation policy should be made.

Section 4 deals with the three dimensional problem of locating the position of the source based upon the transit times to each of the four hydrophones. Hence the question is one of finding the azimuth and initial elevation angles of the ray, and a matching transit time to stop the ray tracing algorithm. Also there are confounding sources of variability. The depth-velocity profile plays a role, as mentioned before. But the arrays themselves have directional properties that would interact with the algorithm even if they were fully level and aligned with the range. The fact that the arrays are tilted and rotated in a variety of ways has contributed to the puzzle of interpreting the mismatches in the array overlap areas. Taken altogether it is shown that systematic error from these sources can be as large as ten or twelve feet. Moreover errors of this magnitude are unnecessary. An alternative method is proposed which can reduce them by at least an order of magnitude.

The conclusions are summarized in Section 5. Section 6, an addendum, addresses an issue raised in the review process. Also a number of appendices are included. They hold the depth-velocity profiles, supporting mathematical details, details of the algorithms, and the source code for the FORTRAN programs.

A brief general statement of conclusions is as follows:

i) The error in iso-speed raytracing is an increasing function of horizontal range, but is seldom more than one foot.

ii) The error due to constant speed extrapolation in the deepest layer can range up to 10 or more feet.

iii) The error due to initializing the ray tracing is a periodic function of the azimuth direction and can be substantial for tilted arrays and at the greater horizontal ranges. The effect of the determination of azimuth is especially noticeable.

Greater details are presented as the various issues are developed.

2. PERTINENT ITEMS FROM RAY TRACING

The sound source pings and sends out an isotropic wave front, which is a fixed phase point on the pressure cycle. A receiving transducer measures the time of arrival of the wave front. A ray is a path normal to the wave front and extending in space back to the source. Our goal is to trace a ray from the receiver for a fixed amount of time and thereby locate the source. To do this we must construct the azimuth and elevation angles of the ray at the receiver and then bend the ray back through the various speed layers until the measured transit time is consumed.

If the speed of sound in water were constant then the ray path would be a straight line. But it is not. Speed is a function of temperature, pressure and salinity. These variables interact in interesting ways for the water layer that affects our problem. Speed is not necessarily a monotone function of depth. Conditions change with time, and water sounding drops are made daily. They provide a depth-velocity profile which is assumed to be fixed for the entire day's exercises. Further, these values are assumed constant throughout each horizontal plane; i.e., the field is homogeneous.

Our immediate goal is to justify the use of a ray invariant in a horizontal-vertical plane and to establish the circular arc nature of ray paths

in water layers for which the speed of sound is a straight line function of depth.

Let us begin with Snell's law. Consider two adjacent layers with speed s_1 in the lower layer and speed s_2 in the upper. The ray enters the lower layer at elevation angle θ_1 and the upper layer with angle θ_2. Given s_1 and s_2 let us find the relationship between θ_1 and θ_2 that will minimize the transit time from (0,0) to (c,a+b).

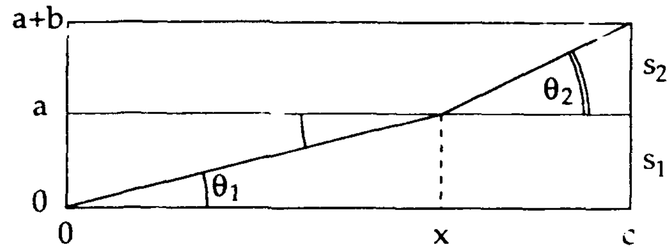

Proposition. For a ray to traverse from (0,0) to (c,a+b) in minimum time, we must have the relationship

$$\frac{\cos(\theta_1)}{s_1} = \frac{\cos(\theta_2)}{s_2} \tag{2.1}$$

Proof. The transit time of a path from (0,0) to (c,a+b) that goes through (x,a) is given by

$$T(x) = \frac{1}{s_1}\sqrt{a^2 + x^2} + \frac{1}{s_2}\sqrt{b^2 + (c-x)^2}.$$

Further, it has derivative

$$T'(x) = \frac{1}{s_1}\frac{x}{\sqrt{a^2 + x^2}} - \frac{1}{s_2}\frac{c-x}{\sqrt{b^2 + (c-x)^2}}.$$

The relationship (2.1) is a consequent of setting $T'(x) = 0$.

Now suppose the point c is not fixed but variable. It follows that a ray entering the lower layer at an angle θ_1 (with the horizontal) will seek the path

of minimum transit time and exit the upper layer at an angle of θ_2; the two angles are related by (2.1).

Next suppose that a number of layers are stacked vertically; within each layer the speed of sound is constant. The relationship (2.1) must hold for every successive pair of layers and hence the ratio

$$rv = \frac{\cos(\theta)}{s} \tag{2.2}$$

must be constant for the entire ray path. This value characterizes the ray path and is called the ray invariant. This is Snell's law.

Consider the vertical plane containing the source and the receiver. Call this is (h,z) plane with the depth z taken as positive downward. Our ray tracing problem is two dimensional in this plane. Given the depth velocity profile we need only the elevation angle at the receiver and the transit time to locate the source.

The depth-velocity profile can be approximated with a series of thin layers each having constant (internal) sound speed. Thus ray tracing can be enacted using such an approximation. This approach is called isospeed ray tracing [1].

A sharper approximation is available through the use of water layers whose sound speed structure can be represented with a linear function of depth

$$\upsilon(z) = \upsilon_0 + \upsilon_1 z \tag{2.3}$$

Proposition. If (2.3) holds then the ray path is a circle arc of radius $z_m + \upsilon_0/\upsilon_1$. If $\upsilon_1 > 0$ then the arc is a distance υ_0/υ_1 above $z = 0$.

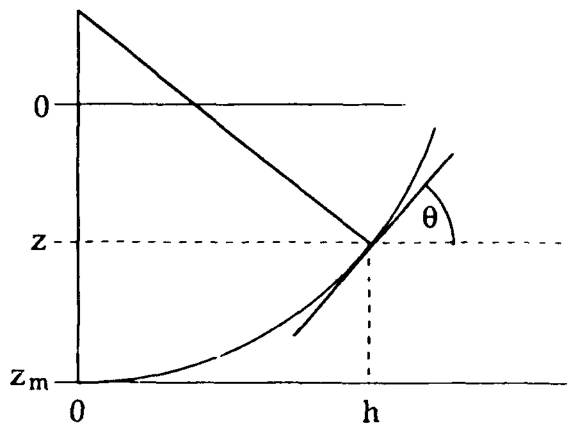

Proof. Referring to the diagram, let (h,z) be an arbitrary point on the ray path and θ is the angle of the tangent line.

Because of Snell's law we must have

$$\frac{\cos(\theta)}{\upsilon_0+\upsilon_1 z} = \frac{1}{\upsilon_0+ \upsilon_1 z_{max}} = rv \tag{2.4}$$

and the ray path can be described parametrically in terms of

$$\{h(\theta), z(\theta)\} \qquad \text{for } 0 < \theta$$

The radius of curvation can be found from the general formula

$$r = \frac{\{[h'(\theta)]^2 + [z'(\theta)]^2\}^{3/2}}{|h'(\theta)z''(\theta) - h''(\theta)z'(\theta)|}.$$

Using (2.3), $\frac{dh}{dz} = \cot(\theta)$, and implicit differentiation we find

$$z'(\theta) = -\sin(\theta)/\upsilon_1 rv \qquad h'(\theta) = -\cos(\theta)/\upsilon_1 rv$$

$$z''(\theta) = -\cos(\theta)/\upsilon_1 rv \qquad h''(\theta) = \sin(\theta)/\upsilon_1 rv$$

and hence

$$r = 1/\upsilon_1 rv = \frac{\upsilon_0}{\upsilon_1} + z_{max}$$

which is a constant, independent of θ. Hence the path is a circle arc; the radius is as specified; and the center of the circle is on a line above zero at a distance υ_0/υ_1. This proof follows those found in [4,8].

If $\upsilon_1 < 0$, then the $[h(\theta), z(\theta)]$ curve is concave, still a circle arc, and the circle's center is still on the line $z = -\upsilon_0/\upsilon_1$. But now this line is below $z=0$. If $\upsilon_1 = 0$, the circle radius is infinite, the sound speed is constant, and the ray path is a straight line.

Now, the numerical construction of the ray path can also be accomplished by representing each layer's sound speed as a straight line segment (function of depth) and piecing together the consequent circle arcs. Since each layer has a constant speed gradient with depth, this is called isogradient ray tracing, [1].

The question of efficiency of the two methods, isospeed and isogradient ray tracing, is really a question of how well the depth-speed function in a layer can be represented by a constant on the one hand, or by a linear function on the other. For thick layers there may be oscillations that make the choice difficult. For thin layers it seems that the straight line fit should perform better.

The algorithm for isogradient ray tracing is presented in Appendix C. A corresponding algorithm for isospeed ray tracing can be extracted from it by making a number of deletions. Fortran source codes for each are shown in Appendix G. Inputs for these algorithms include the depth-velocity table; the layer depths; the depth of the receiver; the elevation (layer entrance) angle at the receiver; the ray transit time. The outputs are the horizontal and vertical end points of the ray, and the final elevation (exit layer) angle of the ray. This latter quantity is needed in the timing synchronization model, [7].

For isospeed ray tracing the pertinent formulae are

$$\Delta h = \Delta z \cot(\theta)$$

$$\Delta t = \Delta z / \upsilon \sin(\theta)$$

where θ is the angle that the ray enters the layer; Δz is the layer thickness; Δh is the horizontal distance transversed in the layer; Δt is the transit time through the layer. The next layer entrance angle is computed from the ray invariant equation (2.1).

For isogradient tracing the pertinent formulas are more complicated. For a ray that enters a layer at depth z_0; horizontal displacement h_0; and angle θ_0 we must first compute the coordinate (q_1, q_0) of the center of the circle arc $(\upsilon_1 \neq 0)$

$$\begin{aligned} q_2 &= -\upsilon_0/\upsilon_1 \\ q_1 &= h_0 + (q_2 - z_0) \sin(\theta_0)/\cos(\theta_0) \end{aligned} \tag{2.5}$$

and the radius of the arc

$$r = \operatorname{signum}(q_2)\,(q_2 - z_0)/\cos(\theta_0). \tag{2.6}$$

The new horizontal displacement is

$$h_1 = q_1 - \operatorname{signum}(q_2)\, r \sin(\theta_0) \tag{2.7}$$

and the increase in transit time is the line integral $\Delta t = \int \frac{ds}{\upsilon_0 + \upsilon_1 z(s)}$ along the circular path. This integral is most easily managed using $ds = \sqrt{(dz)^2 + (dh)^2} = d\theta / \upsilon_1 r \upsilon$ and $\upsilon_0 + \upsilon_1 z = \cos(\theta)/r\upsilon$ so that

$$\Delta t = \frac{1}{\upsilon_1} \int_{\theta_0}^{\theta_1} \frac{d\theta}{\cos(\theta)} = \frac{1}{\upsilon_1} \left\{ \ln\left[\frac{1+\sin(\theta_1)}{\cos(\theta_1)}\right] - \ln\left[\frac{1+\sin(\theta_0)}{\cos(\theta_0)}\right] \right\}$$

and the layer exit angle is computed from the ray invariant equation (2.1),

$$\cos(\theta_1) = rv \cdot \upsilon(z_1)$$

The layer exit angle is the entrance angle for the next layer.

The above equations form the heart of direct path ray tracing. The organizational questions that arise when developing a ray tracing algorithm are treated in Appendix C. Basically one proceeds upwards through the layers until the specified total transit time is consumed. An end correction is normally necessary because of the requirement to stop part way through a layer.

3. QUALITY OF ISOSPEED RAY TRACING

We are concerned with the quality of the currently employed isospeed ray tracing algorithm, which uses a uniform water layer thickness of 25 feet. The receiver depths range from about 1100 to 1350 feet. The elevation angle can range from 90° (directly overhead) to some rather small but positive values. Of course a variety of water columns (depth-velocity profiles) can be encountered. We have selected twelve (see Appendix A) spanning the period May, 1988 to July 1989.

Our first problem is to establish a standard ray to serve as a basis for comparison. To this end we are limited by the resolution of the water column data available. The information depicted graphically in Appendix A provides sound speed averages for every five feet. That is, at level l the corresponding velocity value represents

$$\upsilon_l = \frac{1}{5} \int_{\ell}^{\ell+5} \upsilon(z)dz \tag{3.1}$$

and we have no information concerning the amount of variability that may exist within the layer. It is presumed small and is neglected. (A model for assessing such variability is presented in Appendix D, and this author is concerned about the issue for small entrance angles.)

The most expedient standard available is to employ the ray established by isogradient ray tracing utilizing the five foot layer thicknesses with the straight line segments as depicted (and exaggerated) in Figure 2. These rays are used to judge the rays formed by the isospeed method with 25 foot layer thickness. The corresponding depth-velocity table is formed by partitioning the $\{v_l\}$ into consecutive sets of size 5 and, within each set, average the five values.

With the above as background, the remainder of this section deals with numerical comparisons treating three issues: the computational noise generated by the processing of a large number of layers on the computer; the basic precision of the current isospeed ray tracing; the effects of extrapolation policies when the measured water column does not go sufficiently deep.

i. The adopted standard generally processes over 200 water layers (20 for each 100 feet separating source and receiver). The buildup of computational noise can be checked by using an artificial but linear depth velocity profile: An exact ray can be developed from the theory presented in the previous section and applied to a single layer of great thickness. Then the isogradient programs can attempt to match this ray by tracing through the usual five foot layers. This was done for the depth layer 150, 1200 ft. and intercepts 4250, 4800,

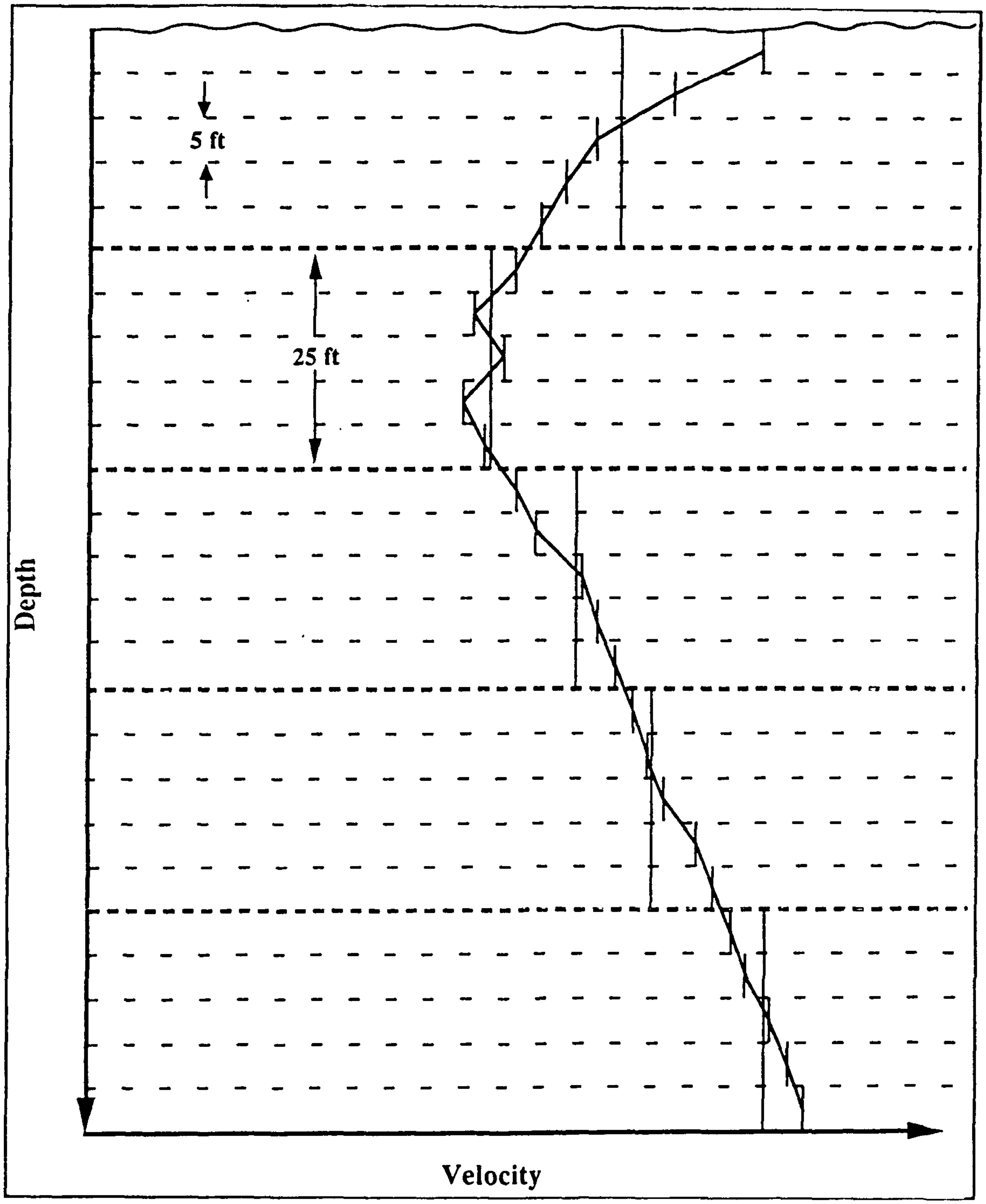

Figure 2. Schematic Diagram Comparing Isogradient and Isospeed Representations of Depth-Velocity Information

4850 ft/sec matched with slopes .1, .05, .01 ft/sec·ft respectively. The two methods produce virtually identical results. All computations are in double precision arithmetic.

ii. The ray fitting technique produces transit time, and entrance and exit angles of the ray connecting two points (source and receiver coordinates) in the horizontal-depth plane. When isogradient ray tracing is applied starting at the receiver, using the entrance angle and stopping when the transit term is consumed, then the coordinates of the source are reproduced to within some small preassigned value ϵ (we used $\epsilon = 10^{-6}$).

The accuracy of isospeed raytracing using 25 foot layer increments is compared against isogradient ray tracing using five foot-layer increments. A fixed set of entrance angle (θ_0 in radians) and transit time (t_0 in seconds) pairs have been selected. Generally they produce horizontal distances of 1000 to 6000 feet and depths of less than 50 to over 500 feet. The distance, d, between the two versions of sound source is compared for each input pair (θ_0, t_0) and each of the twelve DV profiles. The values are recorded in Table 1 along with the source coordinates (h_c, z_c) for currently utilized isospeed methodology, and (h_s, z_s) for the standard (isogradient). An additional computation (h_g, z_g) was performed using isogradient ray tracing with 25 ft layer thicknesses. (The purpose was to provide an indication of the relative importance of layer thickness and the two types of ray tracing.) In all cases the receiver depth is 1300 feet.

The errors are computed using

$$d = \sqrt{(h_s - h_r)^2 + (z_s - z_r^2)} \tag{3.2}$$

with the subscript r replaced by c and g, respectively, in order to identify the current and 25 ft isogradient computations.

Examination of Table 1 shows that the errors, d, grow with range and the majority of the total error is in the vertical component. The effect of varying DV profiles is quite noticeable. The larger errors can exceed one foot. Generally isogradient ray tracing with 25-foot layer thicknesses is noticeably better than the current methods.

iii. Some measure of the effect of extrapolation techniques is given in Table 2. The same cases are developed as found in Table 1, but the sensor depth has increased to 1350 feet. The DV profiles seldom goes below 1300 feet so extrapolation of speed information is necessary. There are quite a few arrays deeper than 1300 feet and several (2, 3, 7, 13, 14 see Table B-1) considerably so. Moreover, the C-phones are even deeper, see Table B-2. (Fourteen of the C-phones are deeper than 1325 ft.) The methods of extrapolation are explained in Appendix A along with the visual effect of their use. In some instances the visual effect is appealing and in others it is not. See the insets in Appendix A. Thus the values for the standard (h_s,z_s) are not always well supported. Even so, the effect is substantial and this is an important source of systematic error.

Table 2 is similar to Table 1 in the qualitative sense. The effect of the DV profile is greater and at the greater ranges the discrepancies can be quite large.

4. ERROR ASSESSMENT FOR THREE DIMENSIONAL METHODS

The ability to locate a sound source position from the transit times (t_1, ..., t_4) needs to be assessed in three dimensions because of the directional properties of the array cubes. Our approach is to place the acoustic center at a

depth a_2, and at the center of a right circular cylinder of radius h. The sound sources (k in number) are equally spaced on a section of the cylinder at depth z. Figure 3 shows a plan view. Azimuth is measured counter clockwise with zero at "3 o'clock."

The ray fitting methodology is used to construct true elevation angles (θ_1, ..., θ_5) and true transit times (t_1, ..., t_5) to each of the k sound sources from the four hydrophones and the acoustic center (θ_5, t_5). We also need the azimuth from the acoustic center (origin of circle) to the sources. These latter are

$$\phi_j = 2\pi(j-1)/k \text{ for } j = 1, ..., k. \qquad (4.1)$$

Since the ray fitting methodology is two-dimensional, we must characterize the vertical planes connecting each sound source on the cylinder to each of the five points in the array cube. The technique for doing this is developed in Appendix B. One needs only the horizontal separations and the vertical positions of source and receiver. Thus five rays are fit to each sound source; one to each of the four phones and one to the acoustic center. Also five elevation angles are generated; but we retain only the last, the true elevation angle at the acoustic center.

During operations, the information collected consists of the set of transit times (t_1, ..., t_4) from sound source to receiver array, (see Figure 1). For our purposes these four values are regarded as exact. Thus we can use the values produced in the ray fitting process. They must be converted to a ray tracing direction (azimuth angle, ϕ and elevation angle, θ) and a single transit time (t_{ac}) to stop the ray tracing. The currently employed procedure is described in [5]. It is convenient to present certain aspects , and this is done in Appendix E.

TABLE 1. Comparison of Two Dimensional Ray Tracing. Sensor at 1300 FT.

05/12/88 θ_0 rad	deg	t_0	h_c	h_s	h_g	z_c	z_s	z_g	d_c	d_g	06/22/88 h_c	h_s	h_g	z_c	z_s	z_g	d_c	d_g
.85	48.70	.35	1122.68	1122.69	1122.71	16.02	16.04	16.05	.022	.021	1122.47	1122.47	1122.51	18.47	18.50	18.50	.026	.047
.80	45.84	.30	1017.32	1017.33	1017.35	248.61	248.63	248.64	.021	.020	1015.79	1015.81	1015.82	250.85	250.87	250.88	.030	.013
.70	40.11	.25	931.32	931.33	931.35	512.58	512.60	512.61	.021	.021	930.19	930.21	930.22	514.42	514.44	514.45	.031	.013
.55	31.51	.50	2071.77	2071.81	2071.84	17.58	17.62	17.67	.059	.057	2071.29	2071.31	2071.38	22.28	22.34	22.40	.062	.092
.50	28.65	.45	1922.11	1922.14	1922.17	241.14	241.20	241.25	.060	.057	1919.24	1919.28	1919.30	244.21	244.28	244.32	.085	.038
.40	22.92	.40	1794.59	1794.61	1794.64	533.58	533.64	533.70	.065	.070	1792.48	1792.52	1792.54	536.89	536.98	537.02	.100	.043
.35	20.05	.65	2971.47	2971.51	2971.56	197.04	197.16	197.27	.126	.123	2967.24	2967.31	2967.34	201.90	202.08	202.15	.188	.080
.30	17.19	.65	3023.22	3023.27	3023.32	345.83	345.97	346.11	.146	.152	3018.72	3018.79	3018.82	350.72	350.93	351.02	.219	.100
.25	14.32	.65	3067.42	3067.47	3067.52	496.72	496.89	497.06	.177	.182	3063.70	3063.77	3063.80	503.51	503.78	503.89	.271	.114
.25	14.32	.85	4008.63	4008.69	4008.75	244.93	245.16	245.38	.238	.229	4002.69	4002.78	4002.82	251.93	252.27	252.41	.346	.150
.20	11.46	.80	3818.79	3818.85	3818.91	495.53	495.80	496.08	.274	.281	3814.19	3814.28	3814.32	505.42	505.84	506.01	.423	.178
.20	11.46	1.05	5008.80	5008.88	5008.96	236.59	236.96	237.31	.375	.355	5001.47	5001.59	5001.64	246.66	247.18	247.41	.536	.232
.15	8.59	1.00	4816.40	4816.47	4816.55	524.15	524.60	525.07	.457	.475	4810.92	4811.04	4811.09	540.54	541.24	541.55	.717	.306
.15	8.59	1.25	6017.31	6017.42	6017.51	320.71	321.28	321.84	.583	.560	6008.53	6008.68	6008.74	335.43	336.31	336.66	.894	.354

07/21/88 θ_0 rad	deg	t_0	h_c	h_s	h_g	z_c	z_s	z_g	d_c	d_g	08/03/88 h_c	h_s	h_g	z_c	z_s	z_g	d_c	d_g
.85	48.70	.35	1122.76	1122.76	1122.83	17.65	17.67	17.70	.027	.070	1122.16	1122.17	1122.23	16.69	16.73	16.75	.041	.053
.80	45.84	.30	1015.52	1015.54	1015.57	250.15	250.17	250.20	.034	.041	1015.19	1015.23	1015.25	249.23	249.27	249.28	.051	.026
.70	40.11	.25	929.48	929.50	929.53	513.64	513.66	513.70	.033	.045	929.45	929.48	929.50	512.77	512.81	512.83	.051	.027
.55	31.51	.50	2071.78	2071.79	2071.91	20.92	20.98	21.10	.061	.173	2070.73	2070.75	2070.85	18.28	18.37	18.46	.095	.133
.50	28.65	.45	1918.75	1918.80	1918.85	242.31	242.39	242.49	.097	.115	1918.13	1918.20	1918.23	239.85	239.98	240.04	.143	.072
.40	22.92	.40	1791.07	1791.11	1791.17	533.80	533.91	534.03	.111	.135	1791.04	1791.10	1791.14	531.52	531.67	531.75	.167	.082
.35	20.05	.65	2956.60	2966.68	2966.76	197.97	198.16	198.39	.207	.245	2965.63	2965.74	2965.79	192.72	193.01	193.15	.312	.148
.30	17.19	.65	3017.24	3017.32	3017.41	344.92	345.16	345.44	.244	.298	3016.54	3016.65	3016.71	339.20	339.53	339.71	.348	.196
.25	14.32	.65	3061.32	3061.39	3061.49	494.93	495.21	495.57	.290	.369	3061.16	3061.26	3061.33	489.03	489.44	489.67	.422	.240
.25	14.32	.85	4001.56	4001.66	4001.78	244.21	244.58	245.01	.383	.452	4000.30	4000.45	4000.52	234.70	235.24	235.51	.564	.283
.20	11.46	.80	3811.18	3811.27	3811.39	492.00	492.43	492.99	.442	.571	3810.96	3811.10	3811.18	483.08	483.73	484.07	.660	.356
.20	11.46	1.05	5000.08	5000.21	5000.35	234.81	235.38	236.06	.590	.692	4998.49	4998.67	4998.77	220.30	221.14	221.57	.858	.440
.15	8.59	1.00	4806.81	4806.93	4807.10	517.44	518.16	519.11	.725	.974	4806.55	4806.75	4806.86	503.25	504.36	504.95	1.126	.599
.15	8.59	1.25	6005.51	6005.62	6005.85	312.94	313.72	314.93	.789	1.238	6004.17	6004.40	6004.51	292.46	293.79	294.45	1.352	.669

10/27/88 θ_0 rad	deg	t_0	h_c	h_s	h_g	z_c	z_s	z_g	d_c	d_g	01/13/89 h_c	h_s	h_g	z_c	z_s	z_g	d_c	d_g
.85	48.70	.35	1123.93	1123.98	1123.99	15.74	15.78	15.79	.059	.015	1121.61	1121.65	1121.66	16.17	16.21	16.21	.053	.008
.80	45.84	.30	1017.74	1017.78	1017.79	248.50	248.54	248.55	.056	.013	1016.66	1016.70	1016.70	248.64	248.67	248.68	.050	.008
.70	40.11	.25	931.67	931.71	931.72	512.55	512.59	512.61	.058	.014	931.26	931.30	931.30	512.57	512.61	512.62	.058	.006
.55	31.51	.50	2074.06	2074.14	2074.16	18.48	18.61	18.64	.155	.040	2069.82	2069.89	2069.90	16.63	16.75	16.76	.143	.021
.50	28.65	.45	1922.89	1922.98	1922.99	241.42	241.56	241.60	.163	.036	1920.86	1920.93	1920.94	240.37	240.49	240.51	.144	.021
.40	22.92	.40	1795.28	1795.35	1795.37	534.00	534.16	534.21	.180	.050	1794.57	1794.64	1794.65	533.57	533.72	533.74	.164	.026
.35	20.05	.65	2972.48	2972.60	2972.64	197.78	198.10	198.19	.339	.093	2969.42	2969.53	2969.54	194.70	194.99	195.04	.311	.043
.30	17.19	.65	3024.47	3024.59	3024.62	347.10	347.48	347.58	.397	.106	3021.60	3021.71	3021.73	343.58	343.92	343.97	.364	.054
.25	14.32	.65	3068.58	3068.71	3068.74	498.17	498.64	498.76	.480	.133	3067.06	3067.18	3067.19	496.10	496.53	496.59	.443	.060
.25	14.32	.85	4010.31	4010.48	4010.52	247.12	247.74	247.88	.646	.147	4006.06	4006.21	4006.23	240.52	241.08	241.16	.582	.082
.20	11.46	.80	3820.23	3820.39	3820.44	497.89	498.61	498.81	.744	.206	3818.32	3818.47	3818.49	494.53	495.20	495.30	.693	.102
.20	11.46	1.05	5010.85	5011.08	5011.13	240.02	241.02	241.25	1.034	.230	5005.57	5005.77	5005.79	229.63	230.51	230.63	.901	.124
.15	8.59	1.00	4818.25	4818.46	4818.52	528.23	529.46	529.80	1.249	.343	4816.26	4816.46	4816.48	523.77	524.93	525.07	1.171	.142
.15	8.59	1.25	6019.88	6020.13	6020.20	326.48	327.99	328.39	1.533	.407	6014.01	6014.26	6014.30	311.49	312.89	313.10	1.423	.213

TABLE 1 (Continued)

03/08/89											03/22/89							
θ_0		t_0	h_c	h_s	h_g	z_c	z_s	z_g	d_c	d_g	h_c	h_s	h_g	z_c	z_s	z_g	d_c	d_g
rad	deg																	
.85	48.70	.35	1119.58	1119.60	1119.62	16.40	16.42	16.43	.027	.019	1119.01	1119.06	1119.05	18.90	18.94	18.93	.063	.013
.80	45.84	.30	1014.59	1014.61	1014.62	248.67	248.69	248.70	.025	.019	1014.20	1014.24	1014.23	250.86	250.90	250.89	.059	.012
.70	40.11	.25	929.94	929.96	929.97	512.32	512.34	512.35	.032	.014	929.38	929.41	929.41	514.24	514.28	514.27	.058	.010
.55	31.51	.50	2066.02	2066.07	2066.09	14.66	14.72	14.77	.073	.051	2065.01	2065.10	2065.08	19.09	19.23	19.20	.167	.036
.50	28.65	.45	1916.93	1916.96	1916.99	237.83	237.89	237.94	.067	.057	1916.20	1916.28	1916.27	242.21	242.35	242.32	.167	.035
.40	22.92	.40	1792.11	1792.15	1792.17	531.15	531.22	531.28	.082	.059	1791.08	1791.17	1791.14	535.45	535.63	535.59	.206	.053
.35	20.05	.65	2963.18	2963.24	2963.27	187.45	187.59	187.69	.162	.105	2962.24	2962.37	2962.34	195.98	196.32	196.24	.368	.088
.30	17.19	.65	3016.16	3016.21	3016.25	335.82	336.00	336.12	.182	.132	3014.60	3014.71	3014.71	344.72	345.10	345.06	.397	.047
.25	14.32	.65	3062.48	3062.58	3062.59	487.97	488.24	488.35	.290	.105	3060.85	3060.99	3060.96	498.26	498.78	498.67	.534	.114
.25	14.32	.85	3997.87	3997.94	3998.00	226.28	226.55	226.76	.283	.209	3996.45	3996.63	3996.59	240.82	241.48	241.33	.684	.159
.20	11.46	.80	3812.53	3812.63	3812.67	481.64	482.04	482.24	.415	.201	3810.64	3810.83	3810.79	497.16	497.98	497.79	.841	.190
.20	11.46	1.05	4995.26	4995.36	4995.43	207.24	207.67	207.98	.445	.313	4993.63	4993.87	4993.81	229.09	230.14	229.88	1.073	.265
.15	8.59	1.00	4809.51	4809.64	4809.68	504.20	504.84	505.16	.651	.322	4807.02	4807.30	4807.22	528.38	529.88	529.48	1.525	.411
.15	8.59	1.25	6002.68	6002.82	6002.91	279.68	280.42	280.89	.746	.483	6000.25	6000.56	6000.47	311.16	312.90	312.42	1.762	.488

04/26/89											04/27/89							
θ_0		t_0	h_c	h_s	h_g	z_c	z_s	z_g	d_c	d_g	h_c	h_s	h_g	z_c	z_s	z_g	d_c	d_g
rad	deg																	
.85	48.70	.35	1118.30	1118.29	1118.33	18.59	18.60	18.61	.020	.047	1118.49	1118.52	1118.53	18.59	18.62	18.62	.043	.009
.80	45.84	.30	1012.89	1012.91	1012.92	250.54	250.56	250.57	.020	.021	1013.02	1013.06	1013.06	250.56	250.59	250.59	.042	.003
.70	40.11	.25	928.47	928.48	928.50	513.75	513.77	513.78	.021	.021	928.53	928.56	928.56	513.78	513.82	513.82	.043	.003
.55	31.51	.50	2063.68	2063.66	2063.75	17.59	17.61	17.69	.032	.118	2064.05	2064.11	2064.12	17.83	17.93	17.94	.113	.018
.50	28.65	.45	1913.73	1913.75	1913.78	239.86	239.91	239.96	.057	.058	1913.97	1914.03	1914.04	240.07	240.17	240.18	.118	.010
.40	22.92	.40	1789.38	1789.41	1789.43	532.95	533.02	533.08	.071	.063	1789.48	1789.53	1789.54	533.11	533.24	533.25	.139	.009
.35	20.05	.65	2958.31	2958.35	2958.40	189.90	190.02	190.14	.121	.128	2958.67	2958.76	2958.77	190.43	190.67	190.68	.256	.018
.30	17.19	.65	3011.15	3011.20	3011.24	338.08	338.22	338.36	.151	.145	3011.58	3011.68	3011.68	338.80	339.10	339.11	.313	.013
.25	14.32	.65	3057.73	3057.78	3057.83	490.69	490.87	491.04	.186	.180	3057.95	3058.06	3058.06	491.24	491.60	491.62	.378	.023
.25	14.32	.85	3991.28	3991.34	3991.41	229.18	229.40	229.63	.232	.233	3991.79	3991.91	3991.92	230.23	230.70	230.72	.480	.031
.20	11.46	.80	3806.72	3806.78	3806.85	485.37	485.66	485.93	.293	.279	3807.01	3807.14	3807.15	486.24	486.82	486.85	.595	.032
.20	11.46	1.05	4987.13	4987.21	4987.29	211.00	211.35	211.70	.365	.354	4987.74	4987.91	4987.92	212.58	213.31	213.36	.748	.044
.15	8.59	1.00	4802.24	4802.34	4802.42	509.72	510.22	510.69	.514	.470	4802.55	4802.74	4802.75	510.97	511.98	512.03	1.031	.045
.15	8.59	1.25	5993.00	5993.12	5993.21	284.82	285.43	285.97	.613	.553	5993.78	5994.01	5994.02	287.36	288.56	288.62	1.221	.062

05/10/89											06/06/89							
θ_0		t_0	h_c	h_s	h_g	z_c	z_s	z_g	d_c	d_g	h_c	h_s	h_g	z_c	z_s	z_g	d_c	d_g
rad	deg																	
.85	48.70	.35	1118.66	1118.66	1118.69	18.58	18.58	18.60	.009	.039	1119.89	1119.93	1119.95	18.65	18.68	18.70	.054	.025
.80	45.84	.30	1012.56	1012.57	1012.59	250.59	250.59	250.61	.001	.028	1013.21	1013.25	1013.26	250.77	250.81	250.82	.052	.023
.70	40.11	.25	927.95	927.95	927.97	513.70	513.70	513.72	.002	.027	928.37	928.41	928.42	513.96	514.00	514.02	.053	.023
.55	31.51	.50	2064.37	2064.35	2064.41	18.01	18.01	18.08	.017	.098	2066.59	2066.66	2066.69	19.59	19.71	19.77	.140	.063
.50	28.65	.45	1913.10	1913.10	1913.14	239.54	239.55	239.62	.003	.079	1914.33	1914.40	1914.44	240.76	240.89	240.95	.147	.064
.40	22.92	.40	1788.29	1788.29	1788.33	532.01	532.01	532.10	.007	.088	1789.06	1789.13	1789.16	533.23	533.38	533.45	.171	.073
.35	20.05	.65	2957.41	2957.41	2957.47	189.01	189.02	189.17	.005	.170	2959.35	2959.46	2959.51	192.11	192.41	192.54	.318	.136
.30	17.19	.65	3009.93	3009.94	3010.00	336.52	336.53	336.72	.010	.200	3011.54	3011.64	3011.71	339.77	340.11	340.28	.357	.182
.25	14.32	.65	3056.00	3056.01	3056.07	487.85	487.86	488.10	.015	.242	3057.47	3057.60	3057.65	491.57	492.02	492.21	.470	.191
.25	14.32	.85	3989.87	3989.87	3989.96	226.92	226.93	227.24	.016	.317	3992.43	3992.59	3992.66	232.84	233.41	233.66	.589	.256
.20	11.46	.80	3804.51	3804.52	3804.60	480.71	480.73	481.10	.023	.375	3806.34	3806.51	3806.57	486.43	487.15	487.43	.738	.294
.20	11.46	1.05	4985.31	4985.31	4985.42	207.23	207.24	207.72	.015	.491	4988.52	4988.73	4988.82	216.35	217.25	217.63	.921	.388
.15	8.59	1.00	4799.06	4799.07	4799.18	500.74	500.78	501.40	.040	.630	4801.23	4801.45	4801.55	509.53	510.73	511.24	1.217	.524
.15	8.59	1.25	5990.30	5990.31	5990.45	277.21	277.26	278.00	.049	.756	5993.80	5994.06	5994.17	290.12	291.57	292.17	1.480	.602

TABLE 2. Comparison of Two Dimensional Ray Tracing. Sensor at 1350 FT.

05/12/88											06/22/88							
θ_0 rad	θ_0 deg	t_0	h_c	h_s	h_g	z_c	z_s	z_g	d_c	d_g	h_c	h_s	h_g	z_c	z_s	z_g	d_c	d_g
.85	48.70	.35	1123.35	1123.23	1123.27	65.93	65.82	65.86	162	.061	1122.53	1122.39	1122.41	68.47	68.34	68.36	.189	.036
.80	45.84	30	1017.63	1017.53	1017.57	298.60	298.50	298.54	153	057	1016.04	1015.92	1015.94	300.84	300.71	300.74	.179	035
.70	40.11	.25	931.64	931.55	931.58	562.64	562.52	562.56	.155	.058	930.52	930.41	930.43	564.47	564.33	564.36	.181	.033
.55	31.51	50	2073.01	2072.79	2072.87	68.19	67.82	67.96	.433	.162	2071.45	2071.19	2071.25	72.36	71.94	72.02	.500	.096
.50	28.65	.45	1922.71	1922.51	922.58	291.53	291.14	291.29	433	.161	1919.72	1919.48	1919.53	294.51	294.07	294.15	.505	.097
.40	22.92	.40	1795.24	1795.05	1795.12	584.20	583.74	583.91	493	.183	1793.12	1792.90	1792.94	587.50	586.97	587.06	.567	098
.35	20.05	65	2972.48	2972.16	2972.27	248.21	247.33	247.66	.934	.345	2967.95	2967.57	2967.64	252.72	251.70	251.90	1.087	.204
.30	17.19	65	3024.17	3023.85	3023.97	397.19	396.14	396.53	1.098	.409	3019.77	3019.38	3019.46	402.22	400.98	401.22	1.296	.250
.25	14.32	.65	3068.49	3068.16	3068.28	548.62	547.33	547.82	1.327	.497	3064.80	3064.41	3064.48	555.49	553.97	554.25	1.565	.289
.25	14.32	.85	4009.90	4009.46	4009.63	297.20	295.51	296.14	1.739	.647	4003.72	4003.21	4003.31	303.78	301.81	302.19	2.040	.394
.20	11.46	.80	3820.13	3819.71	3819.87	548.60	546.59	547.34	2.054	.768	3815.58	3815.08	3815.17	558.59	556.20	556.64	2.439	.450
.20	11.46	1.05	5010.43	5009.86	5010.07	290.28	287.65	288.63	2.692	1.003	5002.76	5002.11	5002.24	299.61	296.52	297.11	3.151	.603
.15	8.59	1.00	4818.21	4817.66	4817.86	579.68	576.29	577.55	3.432	1.272	4812.66	4812.02	4812.12	595.86	591.85	592.54	4.054	.696
.15	8.59	1.25	6019.27	6018.57	6018.83	376.64	372.43	374.00	4.261	1.586	6010.63	6009.75	6009.92	391.77	386.64	387.62	5.209	.999

07/21/88											08/03/88							
θ_0 rad	θ_0 deg	t_0	h_c	h_s	h_g	z_c	z_s	z_g	d_c	d_g	h_c	h_s	h_g	z_c	z_s	z_g	d_c	d_g
.85	48.70	.35	1122.47	1122.22	1122.31	67.68	60.54	67.54	7.143	6.993	1122.02	1121.96	1121.94	66.71	66.65	66.63	.089	.030
.80	45.84	.30	1015.70	1015.45	1015.56	300.14	293.00	299.99	7.143	6.994	1015.51	1015.45	1015.43	299.22	299.16	299.14	.081	.031
70	40.11	25	929.87	929.61	929.74	563.70	556.53	563.54	7.176	7.011	929.93	929.87	929.85	562.85	562.79	562.76	.082	.032
.55	31.51	.50	2071.33	2070.86	2071.04	70.68	63.05	70.20	7.646	7.146	2070.52	2070.40	2070.36	68.17	67.98	67.90	.233	.080
50	28.65	.45	1919.10	1918.63	1918.83	292.53	284.86	292.03	7.692	7.172	1918.72	1918.61	1918.57	290.23	290.03	289.95	.226	.090
.40	22.92	.40	1791.85	1791.33	1791.59	584.55	576.66	583.94	7.906	7.282	1791.97	1791.87	1791.83	582.43	582.17	582.08	.260	.103
35	20.05	.65	2967.26	2966.53	2966.83	248.73	240.08	247.56	8.679	7.488	2966.49	2966.32	2966.25	243.72	243.27	243.09	.487	.191
.30	17.19	.65	3018.26	3017.42	3017.82	396.38	387.28	394.98	9.149	7.717	3017.86	3017.68	3017.62	391.07	390.52	390.30	.577	.228
.25	14.32	.65	3062.60	3061.70	3062.15	547.21	537.54	545.48	9.709	7.952	3062.73	3062.55	3062.48	541.80	541.13	540.86	.693	.282
.25	14.32	.85	4002.32	4001.33	4001.75	295.57	285.37	293.37	10.247	8.010	4001.56	4001.34	4001.25	286.94	286.08	285.73	.894	.358
.20	11.46	.80	3812.78	3811.63	3812.20	545.63	534.41	542.93	11.280	8.537	3812.92	3812.70	3812.60	537.49	536.45	536.02	1.070	.436
.20	11.46	1.05	5001.05	4999.81	5000.34	287.03	275.04	283.61	12.056	8.594	5000.07	4999.78	4999.66	273.88	272.54	272.00	1.375	.551
.15	8.59	1.00	4809.00	4807.49	4808.24	574.05	559.88	569.49	14.248	9.637	4809.23	4808.92	4808.80	561.19	559.42	558.72	1.793	.718
.15	8.59	1.25	6007.41	6005.67	6006.47	368.70	353.16	363.14	15.635	10.007	6006.41	6006.04	6005.91	349.20	347.04	346.24	2.183	.812

10/27/88											01/13/89							
θ_0 rad	θ_0 deg	t_0	h_c	h_s	h_g	z_c	z_s	z_g	d_c	d_g	h_c	h_s	h_g	z_c	z_s	z_g	d_c	d_g
.85	48.70	35	1124.18	1124.04	1124.00	65.71	65.59	65.55	.180	063	1122.59	1122.49	1122.47	66.04	65.95	65.93	.130	.029
.80	45.84	.30	1018.06	1017.95	1017.90	298.49	298.37	298.33	.168	.063	1017.05	1016.97	1016.95	298.63	298.54	298.52	.123	.026
70	40.11	25	931.98	931.87	931.84	562.60	562.47	562.42	.171	.062	931.68	931.60	931.58	562.64	562.55	562.53	.124	.027
.55	31.51	.50	2074.50	2074.25	2074.17	68.70	68.30	68.15	.475	.166	2071.63	2071.45	2071.40	67.51	67.21	67.15	.348	078
50	28.65	.45	1923.53	1923.31	1923.22	291.82	291.41	291.25	.469	.180	1921.61	1921.44	1921.41	290.84	290.53	290.47	.347	.073
40	22.92	.40	1795.88	1795.68	1795.60	584.58	584.08	583.90	.541	.201	1795.34	1795.19	1795.15	584.30	583.93	583.85	.392	.089
.35	20.05	.65	2973.68	2973.33	2973.19	249.18	248.21	247.84	1.031	.393	2970.65	2970.40	2970.34	246.14	245.43	245.28	.749	.162
30	17.19	.65	3025.28	3024.92	3024.79	398.26	397.11	396.69	1.207	.436	3022.84	3022.58	3022.52	395.34	394.51	394.32	.873	.199
.25	14.32	.65	3069.62	3069.25	3069.11	550.02	548.61	548.08	1.459	.538	3068.54	3068.27	3068.21	548.72	547.68	547.46	1.077	.232
25	14.32	.85	4011.61	4011.12	4010.94	299.42	297.58	296.88	1.902	.716	4007.66	4007.30	4007.22	293.34	291.99	291.71	1.398	.296
.20	11.46	.80	3821.53	3821.07	3820.90	550.86	548.65	547.83	2.259	.833	3820.20	3819.85	3819.77	548.75	547.12	546.77	1.674	.360
.20	11.46	1.05	5012.56	5011.96	5011.71	293.88	291.02	289.92	2.924	1.123	5007.61	5007.15	5007.05	284.22	282.10	281.65	2.168	.465
.15	8.59	1.00	4819.95	4819.34	4819.11	583.42	579.69	578.32	3.777	1.396	4818.45	4818.00	4817.89	580.36	577.63	577.02	2.765	.624
.15	8.59	1.25	6021.52	6020.76	6020.49	381.50	376.89	375.23	4.668	1.685	6016.51	6015.94	6015.80	368.95	365.57	364.83	3.436	.751

TABLE 2 (Continued)

03/08/89											03/22/89							
θ_0 rad	θ_0 deg	t_0	h_c	h_s	h_g	z_c	z_s	z_g	d_c	d_g	h_c	h_s	h_g	z_c	z_s	z_g	d_c	d_g
.85	48.70	.35	1120.41	1120.39	1120.32	66.29	66.27	66.21	.031	.085	1119.83	1119.64	1119.58	68.79	68.61	68.57	.261	.072
.80	45.84	.30	1015.20	1015.18	1015.12	298.65	298.63	298.58	.030	.082	1014.64	1014.46	1014.42	300.84	300.67	300.62	.246	.067
.70	40.11	.25	930.54	930.52	930.47	562.42	562.39	562.33	.030	.082	929.96	929.80	929.76	564.34	564.14	564.09	.250	.069
.55	31.51	.50	2067.57	2067.53	2067.41	65.42	65.35	65.16	.083	.227	2066.53	2066.16	2066.06	69.84	69.25	69.08	.696	.193
.50	28.65	.45	1918.07	1918.03	1917.92	288.55	288.47	288.27	.082	.230	1917.05	1916.72	1916.62	292.74	292.13	291.96	.694	.193
.40	22.92	.40	1793.28	1793.23	1793.14	582.25	582.16	581.92	.105	.252	1792.17	1791.89	1791.77	586.48	585.77	585.54	.754	.270
.35	20.05	.65	2964.89	2964.82	2964.65	239.41	239.24	238.78	.184	.490	2963.53	2963.71	2962.86	247.48	246.07	245.68	1.504	.417
.30	17.19	.65	3018.03	3017.97	3017.78	388.45	388.26	387.69	.204	.595	3016.51	3015.97	3015.79	397.40	395.71	395.21	1.781	.531
.25	14.32	.65	3064.71	3064.65	3064.46	541.86	541.61	540.92	.255	.714	3062.79	3062.22	3062.05	551.66	549.54	548.93	2.194	.636
.25	14.32	.85	4000.29	4000.20	3999.95	280.48	280.16	279.26	.332	.935	3998.26	3997.54	3997.32	293.99	291.29	290.53	2.795	.795
.20	11.46	.80	3815.44	3815.36	3815.12	538.04	537.66	536.57	.397	1.116	3813.08	3812.34	3812.11	552.58	549.21	548.23	3.444	1.009
.20	11.46	1.05	4998.31	4998.19	4997.87	263.91	263.40	261.98	.529	1.450	4995.94	4995.01	4994.72	284.23	280.00	278.76	4.339	1.267
.15	8.59	1.00	4812.90	4812.79	4812.45	564.07	563.40	561.53	.679	1.899	4810.08	4809.18	4808.81	587.36	581.88	580.02	5.553	1.901
.15	8.59	1.25	6006.72	6006.58	6006.14	341.26	340.46	339.11	.820	2.384	6003.69	6002.29	6001.91	371.15	363.72	361.67	7.565	2.084

04/26/89											04/27/89							
θ_0 rad	θ_0 deg	t_0	h_c	h_s	h_g	z_c	z_s	z_g	d_c	d_g	h_c	h_s	h_g	z_c	z_s	z_g	d_c	d_g
.85	48.70	.35	1118.79	1118.54	1118.68	68.52	57.49	68.43	11.037	10.940	1118.91	1118.87	1118.77	68.53	68.51	68.41	.044	.138
.80	45.84	.30	1013.48	1013.24	1013.39	300.52	289.47	300.43	11.049	10.952	1013.61	1013.58	1013.49	300.54	300.51	300.42	.041	.131
.70	40.11	.25	929.18	928.92	929.10	563.87	552.78	563.76	11.089	10.981	929.23	929.20	929.12	563.90	563.87	563.76	.042	.134
.55	31.51	.50	2064.58	2064.13	2064.38	68.04	56.68	67.72	11.374	11.047	2064.80	2064.74	2064.55	68.21	68.11	67.80	.117	.367
.50	28.65	.45	1914.93	1914.37	1914.65	290.55	279.13	290.22	11.429	11.088	1915.08	1915.02	1914.84	290.76	290.66	290.33	.117	.372
.40	22.92	.40	1790.75	1790.24	1790.58	584.25	572.65	583.85	11.615	11.203	1790.85	1790.80	1790.63	584.41	584.29	583.89	.129	.437
.35	20.05	.65	2959.94	2959.24	2959.65	241.78	229.72	241.01	12.089	11.305	2960.30	2960.21	2959.93	242.31	242.07	241.32	.254	.804
.30	17.19	.65	3013.14	3012.33	3012.84	390.87	378.46	389.94	12.445	11.497	3013.50	3013.40	3013.11	391.50	391.21	390.30	.299	.957
.25	14.32	.65	3060.15	3059.23	3059.83	544.89	531.98	543.72	12.930	11.747	3060.30	3060.20	3059.89	545.31	544.96	543.81	.362	1.194
.25	14.32	.85	3993.64	3992.63	3993.23	283.27	270.06	281.78	13.251	11.737	3994.14	3994.02	3993.61	284.32	283.86	282.41	.474	1.513
.20	11.46	.80	3809.77	3808.60	3809.35	542.06	528.01	540.20	14.100	12.214	3809.96	3809.84	3809.42	542.72	542.16	540.33	.568	1.878
.20	11.46	1.05	4990.08	4988.80	4989.54	267.47	252.98	265.12	14.549	12.167	4990.70	4990.54	4990.01	269.07	268.36	266.05	.728	2.371
.15	8.59	1.00	4806.20	4804.66	4805.61	571.09	554.87	567.85	16.287	13.010	4806.45	4806.28	4805.69	572.18	571.20	568.01	.987	3.245
.15	8.59	1.25	5997.06	5995.34	5996.34	346.45	329.49	342.56	17.052	13.115	5997.85	5997.63	5996.91	348.99	347.82	343.98	1.177	3.912

05/10/89											06/06/89							
θ_0 rad	θ_0 deg	t_0	h_c	h_s	h_g	z_c	z_s	z_g	d_c	d_g	h_c	h_s	h_g	z_c	z_s	z_g	d_c	d_g
.85	48.70	.35	1118.73	1118.70	1118.69	68.57	68.55	68.54	.032	.019	1119.54	1119.49	1119.37	68.69	68.56	68.53	.063	.173
.80	45.84	.30	1013.14	1013.12	1013.10	300.57	300.55	300.54	.027	.021	1013.70	1013.67	1013.54	300.76	300.72	300.60	.045	.178
.70	40.11	.25	928.61	928.60	928.58	563.81	563.79	563.77	.026	.023	928.94	928.91	928.80	564.05	564.02	563.88	.044	.182
.55	31.51	.50	2064.47	2064.42	2064.40	68.06	67.99	67.95	.084	.050	2065.96	2065.86	2065.65	69.26	69.14	68.74	.159	.452
.50	28.65	.45	1914.18	1914.15	1914.12	290.22	290.16	290.10	.076	.060	1915.26	1915.20	1914.96	291.35	291.24	290.80	.124	.504
.40	22.92	.40	1789.58	1789.55	1789.52	583.23	583.15	583.09	.083	.074	1790.16	1790.11	1789.88	584.28	584.15	583.61	.143	.580
.35	20.05	.65	2958.98	2958.92	2958.88	240.82	240.67	240.55	.165	.129	2960.76	2960.66	2960.28	243.74	243.48	242.47	.274	1.082
.30	17.19	.65	3011.89	3011.83	3011.78	389.27	389.08	388.93	.193	.156	3013.29	3013.19	3012.80	392.25	391.93	390.71	.329	1.283
.25	14.32	.65	3058.26	3058.20	3058.15	541.78	541.56	541.37	.233	.195	3059.40	3059.30	3058.90	544.96	544.58	543.07	.393	1.568
.25	14.32	.85	3992.18	3992.11	3992.04	280.95	280.65	280.42	.303	.247	3994.42	3994.29	3993.76	286.32	285.84	[illegible]	.497	2.028
.20	11.46	.80	3807.37	3807.30	3807.23	537.00	536.64	536.35	.363	.305	3808.80	3808.67	3808.14	541.88	541.28	538.90	.611	2.443
.20	11.46	1.05	4988.21	4988.10	4988.02	263.59	263.12	262.75	.473	.380	4991.05	4990.88	4990.19	271.94	271.17	268.11	.786	3.138
.15	8.59	1.00	4802.81	4802.70	4802.61	561.55	560.95	560.42	.608	.532	4804.41	4804.24	4803.51	568.84	567.83	563.74	1.019	4.160
.15	8.59	1.25	5994.26	5994.12	5994.00	338.55	337.80	337.18	.765	.624	5997.10	5996.87	5995.98	349.75	348.49	343.55	1.279	5.024

Finally the values (θ, t_{ac}) together with the array depth and DV information are fed into the ISOSPEED ray tracing program. The output consists of the (h,z) values. Upon combining these with the azimuth ϕ_c, the estimated position of the sound source can be computed.

A number of error calculations can be made. First the error in estimating transit time

$$tim_{er} = t_{ac} - t_5 \tag{4.2}$$

affects the rule for stopping the ray tracing algorithm. An error of 10^{-4} seconds translates to about half a foot in horizontal range, h, (i.e., $\upsilon \approx 4800$ ft./sec.). Next, the horizontal error is measured directly

$$h_{er} = h_c - h_1 \tag{4.3}$$

The values tim_{er} and h_{er} should be strongly correlated.

In a similar fashion, the error in the elevation angle is correlated with the error in the vertical component

$$\begin{aligned} \theta_{er} &= \theta_c - \theta_o \\ z_{er} &= z_c - z_1 \end{aligned} \tag{4.4}$$

but, because of ray bending, the relationship is non-linear. The value z_{er} is measured directly in feet. The value θ_{er} is more difficult to interpret. It is a function of the water layers involved. See [7].

Finally we have the error in azimuth

$$\phi_{er} = \phi_c - \phi_o. \tag{4.5}$$

These values are in radians and, when multiplied by h_1, measure how far off the mark (see Figure 3) in feet, along the cylinder perimeter.

It is a rather incipient fact that our errors are periodic functions of the true azimuth. This is illustrated in Figure 4. We suspect that this is at the root some earlier attempts to treat possible causes of systematic error, [6,7].

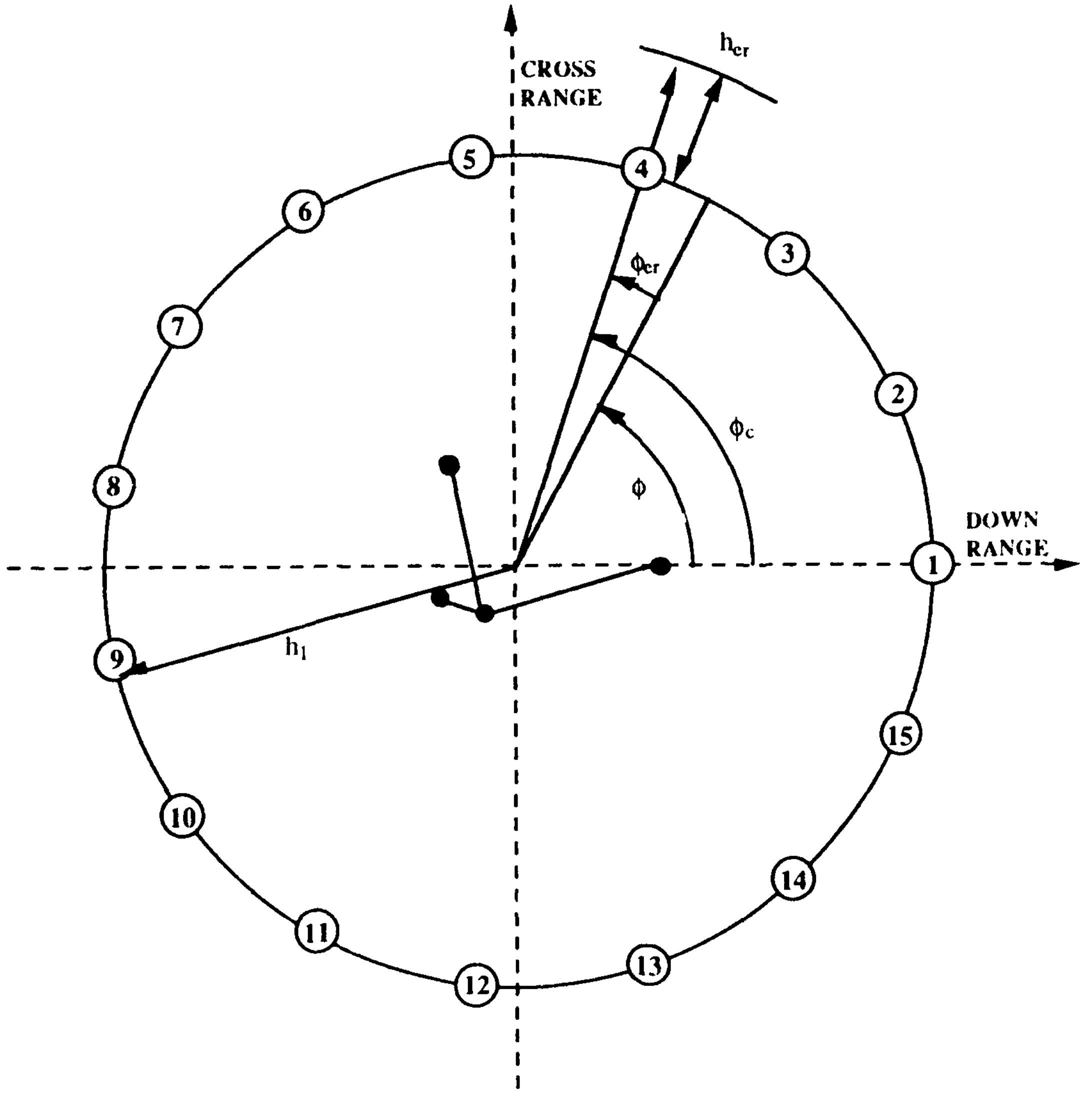

Figure 3. Cylinder Cross Section Illustrating Sound Source and Receiver Positions

Many tabulations of these errors have been made. Four sets, each with 15 points around the cylinder and four radii (h_1 = 2000, 3000, 40000, 5000 ft.),

Figure 4. Periodic Nature of Errors as a Function of Azimuth

Case: DV of 3/22/89 and Array No. 1. Ref. Table 3.

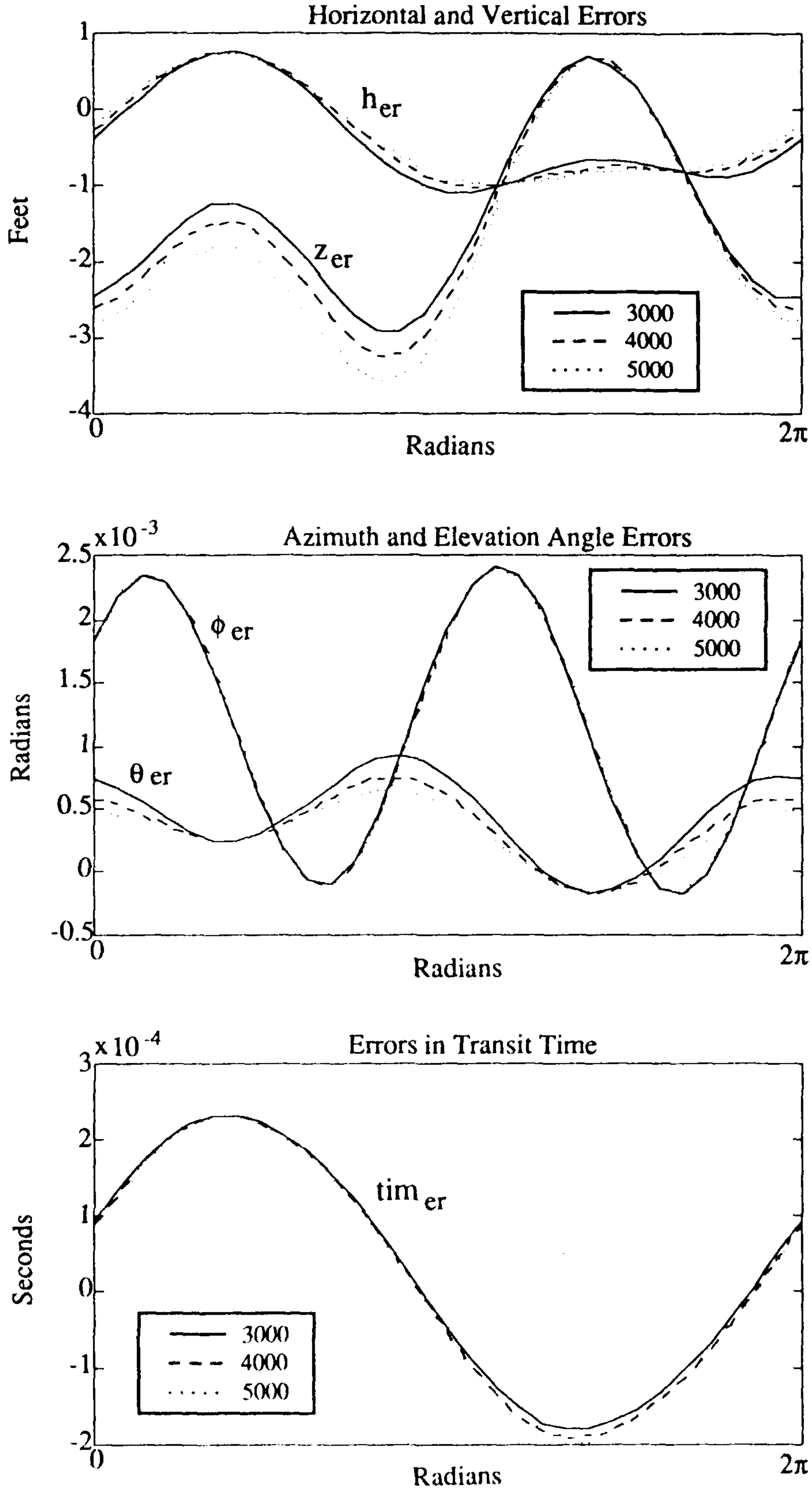

have been selected for display and they appear in Table 3. The basis of selection was to choose two of the more interesting water columns (10/27/88 and 3/22/89, see Appendix A) each matched with two of the more severely tilted arrays: Number 1 and 56, see Table B-1. The tilts for array number 1 have opposite signs while those for array 56 are of the same sign.

Let us make a sample calculation in order to aid in the interpretation of these errors. The total error offset is essentially

$$d = \sqrt{z_{er}^2 + h_{er}^2 + \left(h_1 \phi_{er}\right)^2}.$$

Thus for the case of Array No. 1 on 10/27/88 at h_1 = 5000 ft. and azimuth 0.418879 radians (i.e., 24 deg. north of east) we have $\sqrt{(2.45)^2 + (.28)^2 + (5 \cdot 2.3525)^2} = 12.02$ ft. The dominant portion of the error is in the azimuth, which (measured along the arc) contributes 2.3525 ft. of error for every 1000 ft. of horizontal range. A scan of Table 3 shows generally that this condition persists, although the periodic nature of the errors can make the effect small in some directions.

It seems that the most severe errors are associated with the arrays having the larger tilts. We suspect that the causes lie in the use of the array center as the acoustic center and the assumption of constant sound speed for the entire array. The z-phone is about 30 ft higher than the others. Also, the tilt correction method is but approximate (see Appendix B.)

We are disinclined to attach great importance to the other source, the isospeed ray tracing. The former was considered in Section 3 and cannot

Table 3. Error Structure - Current Methodology

10/27/88 Array #1 Acoustic Center Depth = 1308.76 Sound Source Depth = 250

	$h_1 = 2000$	$\theta = 0.483579$	$t_5 = 0.4639118$			$h_1 = 3000$	$\theta = 0.334327$	$t_5 = 0.6521831$		
ϕ	ϕ_{er}	θ_{er}	tim_{er}	h_{er}	z_{er}	ϕ_{er}	θ_{er}	tim_{er}	h_{er}	z_{er}
.0000000	.0017878	.0009728	.0000966	-.47	-1.87	.0018177	.0007312	.0000908	-.41	-2.44
.4188790	.0023100	.0006887	.0001706	.14	-1.48	.0023335	.0005428	.0001704	.15	-2.01
.8377580	.0020063	.0003597	.0002181	.69	-.93	.0020193	.0003178	.0002208	.62	-1.42
1.2566370	.0010939	.0002388	.0002293	.87	-.71	.0010944	.0002425	.0002320	.75	-1.22
1.6755160	.0001933	.0004279	.0002062	.57	-1.04	.0001812	.0003906	.0002073	.48	-1.62
2.0943951	-.0000828	.0008080	.0001561	-.04	-1.68	-.0001053	.0006718	.0001551	-.05	-2.37
2.5132741	.0004645	.0011156	.0000859	-.67	-2.13	.0004353	.0008889	.0000816	-.62	-2.90
2.9321531	.0014834	.0011180	.0000039	-1.02	-1.95	.0014525	.0008694	-.0000056	-1.00	-2.70
-2.9321531	.0023000	.0007739	-.0000750	-.99	-1.08	.0022728	.0005861	-.0000911	-1.08	-1.71
-2.5132741	.0023678	.0002686	-.0001326	-.70	.05	.0023491	.0001824	-.0001541	-.94	-.40
-2.0943951	.0016317	-.0001035	-.0001566	-.41	.84	.0016246	-.0001161	-.0001806	-.74	.52
-1.6755160	.0005621	-.0001271	-.0001476	-.34	.87	.0005677	-.0001448	-.0001710	-.66	.59
-1.2566370	-.0001532	.0001992	-.0001127	-.54	.14	-.0001358	.0000993	-.0001336	-.75	-.19
-.8377580	-.0000576	.0006640	-.0000574	-.80	-.90	-.0000311	.0004578	-.0000746	-.87	-1.35
-.4188790	.0007752	.0009805	.0000150	-.83	-1.70	.0008061	.0007135	.0000029	-.79	-2.25

10/27/88 Array #1 Acoustic Center Depth = 1308.76 Sound Source Depth = 250

	$h_1 = 4000$	$\theta = 0.252155$	$t_5 = 0.8482453$			$h_1 = 5000$	$\theta = 0.200409$	$t_5 = 1.0477325$		
ϕ	ϕ_{er}	θ_{er}	tim_{er}	h_{er}	z_{er}	ϕ_{er}	θ_{er}	tim_{er}	h_{er}	z_{er}
.0000000	.0018328	.0005733	.0000869	-.27	-2.60	.0018424	.0004691	.0000842	-.20	-2.77
.4188790	.0023452	.0004483	.0001686	.24	-2.21	.0023525	.0003869	.0001670	.28	-2.45
.8377580	.0020255	.0002923	.0002201	.65	-1.66	.0020293	.0002773	.0002188	.64	-1.96
1.2566370	.0010941	.0002464	.0002311	.75	-1.49	.0010939	.0002508	.0002297	.72	-1.84
1.6755160	.0001747	.0003658	.0002058	.50	-1.93	.0001705	.0003501	.0002041	.49	-2.31
2.0943951	-.0001171	.0005795	.0001530	.02	-2.71	-.0001244	.0005176	.0001511	.05	-3.09
2.5132741	.0004203	.0007354	.0000785	-.49	-3.24	.0004109	.0006315	.0000762	-.42	-3.58
2.9321531	.0014369	.0007016	-.0000107	-.87	-2.99	.0014270	.0005880	-.0000139	-.80	-3.26
-2.9321531	.0022592	.0004601	-.0000990	-1.02	-1.91	.0022506	.0003756	-.0001035	-.98	-2.11
-2.5132741	.0023399	.0001263	-.0001644	-.96	-.50	.0023341	.0000900	-.0001703	-.98	-.61
-2.0943951	.0016214	-.0001214	-.0001922	-.82	.51	.0016193	-.0001223	-.0001989	-.88	.47
-1.6755160	.0005710	-.0001523	-.0001825	-.74	.62	.0005731	-.0001542	-.0001892	-.80	.62
-1.2566370	-.0001265	.0000373	-.0001441	-.77	-.17	-.0001206	-.0000012	-.0001502	-.78	-.18
-.8377580	-.0000174	.0003244	-.0000835	-.80	-1.39	-.0000087	.0002374	-.0000887	-.76	-1.43
-.4188790	.0008220	.0005391	-.0000035	-.66	-2.35	.0008320	.0004239	-.0000075	-.58	-2.45

Table 3. (Continued)

10/27/88 Array #56 Acoustic Center Depth = 1218.84 Sound Source Depth = 250

$h_1 = 2000$ $\theta = 0.447900$ $t_5 = 0.4556447$ $h_1 = 3000$ $\theta = 0.307561$ $t_5 = 0.6463758$

ϕ	ϕ_{er}	θ_{er}	$time_{er}$	h_{er}	z_{er}	ϕ_{er}	θ_{er}	$time_{er}$	h_{er}	z_{er}
.0000000	-.0017890	.0005318	.0002299	.52	-1.46	-.0018021	.0004311	.0002035	.58	-1.39
.4188790	-.0013984	.0007249	.0001651	.05	-1.70	-.0014151	.0005548	.0001355	.14	-1.66
.8377580	-.0006555	.0007152	.0000899	-.26	-1.52	-.0006730	.0005262	.0000557	-.19	-1.45
1.2566370	-.0000518	.0004745	.0000218	-.32	-.90	-.0000670	.0003282	-.0000168	-.33	-.74
1.6755160	.0000096	.0001303	-.0000263	-.19	-.11	-.0000006	.0000586	-.0000682	-.30	.14
2.0943951	-.0005179	-.0001141	-.0000505	-.06	.42	-.0005216	-.0001297	-.0000939	-.23	.74
2.5132741	-.0012953	-.0001104	-.0000512	-.06	.42	-.0012916	-.0001258	-.0000946	-.24	.73
2.9321531	-.0018198	.0001405	-.0000275	-.21	-.12	-.0018094	.0000693	-.0000695	-.31	.11
-2.9321531	-.0017540	.0004885	.0000212	-.33	-.92	-.0017387	.0003432	-.0000173	-.35	-.79
-2.5132741	-.0011477	.0007297	.0000902	-.27	-1.55	-.0011301	.0005422	.0000562	-.20	-1.50
-2.0943951	-.0004055	.0007372	.0001654	.04	-1.73	-.0003888	.0005690	.0001358	.13	-1.70
-1.6755160	-.0000185	.0005403	.0002296	.51	-1.47	-.0000055	.0004414	.0002030	.56	-1.42
-1.2566370	-.0002368	.0002988	.0002710	.93	-1.08	-.0002298	.0002745	.0002456	.93	-.98
-.8377580	-.0009066	.0001914	.0002853	1.10	-.90	-.0009067	.0001984	.0002602	1.07	-.78
-.4188790	-.0015747	.0002946	.0002716	.94	-1.07	-.0015818	.0002692	.0002464	.94	-.97

10/27/88 Array #56 Acoustic Center Depth = 1218.84 Sound Source Depth = 250

$h_1 = 4000$ $\theta = 0.231211$ $t_5 = 0.8438392$ $h_1 = 5000$ $\theta = 0.183359$ $t_5 = 1.0442213$

ϕ	ϕ_{er}	θ_{er}	$time_{er}$	h_{er}	z_{er}	ϕ_{er}	θ_{er}	$time_{er}$	h_{er}	z_{er}
.0000000	-.0018086	.0003668	.0001872	.60	-1.31	-.0018125	.0003250	.0001765	.62	-1.20
.4188790	-.0014235	.0004465	.0001182	.20	-1.55	-.0014285	.0003753	.0001071	.24	-1.39
.8377580	-.0006818	.0004064	.0000367	-.14	-1.29	-.0006870	.0003278	.0000247	-.09	-1.07
1.2566370	-.0000747	.0002365	-.0000378	-.32	-.52	-.0000792	.0001768	-.0000508	-.29	-.23
1.6755160	-.0000058	.0000153	-.0000906	-.34	.42	-.0000089	-.0000117	-.0001045	-.36	.76
2.0943951	-.0005234	-.0001367	-.0001171	-.32	1.06	-.0005245	-.0001395	-.0001313	-.36	1.43
2.5132741	-.0012897	-.0001328	-.0001178	-.32	1.05	-.0012886	-.0001356	-.0001320	-.36	1.41
2.9321531	-.0018041	.0000261	-.0000919	-.36	.38	-.0018010	-.0000009	-.0001057	-.37	.71
-2.9321531	-.0017311	.0002518	-.0000383	-.33	-.58	-.0017265	.0001922	-.0000513	-.31	-.31
-2.5132741	-.0011214	.0004231	.0000372	-.15	-1.36	-.0011162	.0003448	.0000252	-.11	-1.16
-2.0943951	-.0003805	.0004615	.0001186	.18	-1.61	-.0003755	.0003909	.0001074	.23	-1.47
-1.6755160	.0000009	.0003779	.0001867	.59	-1.36	.0000048	.0003366	.0001759	.61	-1.26
-1.2566370	-.0002262	.0002587	.0002295	.91	-.93	-.0002241	.0002491	.0002187	.90	-.86
-.8377580	-.0009067	.0002028	.0002442	1.04	-.72	-.0009067	.0002066	.0002334	1.02	-.66
-.4188790	-.0015854	.0002529	.0002304	.92	-.91	-.0015875	.0002430	.0002197	.92	-.83

Table 3. (Continued)

3/22/89 Array #1 Acoustic Center Depth = 1308.76 Sound Source Depth = 250

$h_1 = 2000$ $\theta = 0.482345$ $t_5 = 0.4652331$ $h_1 = 3000$ $\theta = 0.332511$ $t_5 = 0.6540366$

ϕ	ϕ_{er}	θ_{er}	$time_{er}$	h_{er}	z_{er}	ϕ_{er}	θ_{er}	$time_{er}$	h_{er}	z_{er}
.0000000	.0017867	.0009788	.0000963	-.44	-1.81	.0018168	.0007400	.0000907	-.41	-2.46
.4188790	.0023079	.0006881	.0001701	.18	-1.40	.0023317	.0005436	.0001700	.15	-2.00
.8377580	.0020040	.0003511	.0002175	.75	-.83	.0020174	.0003088	.0002203	.64	-1.38
1.2566370	.0010925	.0002221	.0002287	.93	-.60	.0010933	.0002241	.0002315	.78	-1.14
1.6755160	.0001937	.0004044	.0002057	.64	-.91	.0001817	.0003650	.0002069	.51	-1.52
2.0943951	-.0000804	.0007800	.0001559	.02	-1.55	-.0001031	.0005419	.0001548	-.01	-2.27
2.5132741	.0004680	.0010857	.0000859	-.60	-2.00	.0004386	.0008578	.0000815	-.58	-2.80
2.9321531	.0014866	.0010891	.0000040	-.95	-1.82	.0014554	.0008399	-.0000054	-.96	-2.60
-2.9321531	.0023015	.0007490	-.0000747	-.92	-.96	.0022741	.0005607	-.0000907	-1.05	-1.62
-2.5132741	.0023674	.0002503	-.0001321	-.64	.16	.0023484	.0001637	-.0001535	-.91	-.32
-2.0943951	.0016301	-.0001134	-.0001561	-.35	.94	.0016227	-.0001263	-.0001799	-.72	.58
-1.6755160	.0005606	-.0001284	-.0001471	-.30	.95	.0005661	-.0001457	-.0001704	-.65	.62
-1.2566370	-.0001538	.0002048	-.0001123	-.50	.21	-.0001364	.0001065	-.0001331	-.75	-.19
-.8377580	-.0000575	.0006737	-.0000572	-.77	-.85	-.0000310	.0004701	-.0000743	-.88	-1.37
-.4188790	.0007751	.0009902	.0000150	-.80	-1.64	.0008061	.0007264	.0000031	-.80	-2.27

3/22/89 Array #1 Acoustic Center Depth = 1308.76 Sound Source Depth = 250

$h_1 = 4000$ $\theta = 0.249797$ $t_5 = 0.8506490$ $h_1 = 5000$ $\theta = 0.197561$ $t_5 = 1.0506906$

ϕ	ϕ_{er}	θ_{er}	$time_{er}$	h_{er}	z_{er}	ϕ_{er}	θ_{er}	$time_{er}$	h_{er}	z_{er}
.0000000	.0018316	.0005823	.0000868	-.27	-2.61	.0018406	.0004768	.0000842	-.19	-2.75
.4188790	.0023433	.0004488	.0001683	.25	-2.18	.0023503	.0003860	.0001667	.29	-2.38
.8377580	.0020237	.0002822	.0002197	.67	-1.58	.0020274	.0002656	.0002184	68	-1.83
1.2566370	.0010932	.0002266	.0002307	.78	-1.37	.0010931	.0002295	.0002293	.77	-1.66
1.6755160	.0001753	.0003390	.0002055	.54	-1.79	.0001714	.0003224	.0002039	.54	-2.10
2.0943951	-.0001147	.0005492	.0001528	.06	-2.56	-.0001218	.0004871	.0001509	.10	-2.88
2.5132741	.0004237	.0007046	.0000785	-.45	-3.09	.0004147	.0006012	.0000762	-.37	-3.37
2.9321531	.0014399	.0006725	-.0000105	-.83	-2.85	.0014305	.0005597	-.0000136	-.75	-3.07
-2.9321531	.0022606	.0004349	-.0000985	-.98	-1.78	.0022525	.0003505	-.0001030	-.94	-1.92
-2.5132741	.0023393	.0001070	-.0001637	-.93	-.38	.0023338	.0000698	-.0001696	-.94	-.43
-2.0943951	.0016196	-.0001327	-.0001915	-.79	.61	.0016177	-.0001355	-.0001980	-.84	.62
-1.6755160	.0005694	-.0001545	-.0001818	-.72	.68	.0005714	-.0001587	-.0001884	-.77	.73
-1.2566370	-.0001272	.0000436	-.0001435	-.76	-.15	-.0001217	.0000028	-.0001495	-.76	-.11
-.8377580	-.0000175	.0003366	-.0000830	-.80	-1.40	-.0000093	.0002477	-.0000882	-.75	-1.41
-.4188790	.0008217	.0005523	-.0000033	-.66	-2.37	.0008311	.0004357	-.0000073	-.58	-2.45

Table 3. (Continued)

3/22/89 Array #56 Acoustic Center Depth = 1218.84 Sound Source Depth = 250

	$h_1 = 2000$	$\theta = 0.446542$	$t_5 = 0.4569723$			$h_1 = 3000$	$\theta = 0.305570$	$t_5 = 0.6482545$		
ϕ	ϕ_{er}	θ_{er}	tim_{er}	h_{er}	z_{er}	ϕ_{er}	θ_{er}	tim_{er}	h_{er}	z_{er}
.0000000	-.0017923	.0005007	.0002303	.47	-1.57	-.0018058	.0003725	.0002037	.50	-1.61
.4188790	-.0014023	.0006844	.0001653	.01	-1.80	-.0014196	.0004854	.0001356	.08	-1.85
.8377580	-.0006594	.0006649	.0000900	-.29	-1.60	-.0006775	.0004460	.0000556	-.24	-1.61
1.2566370	-.0000549	.0004158	.0000217	-.35	-.95	-.0000708	.0002393	-.0000171	-.38	-.88
1.6755160	.0000077	.0000659	-.0000266	-.22	-.15	-.0000030	-.0000358	-.0000687	-.34	.01
2.0943951	-.0005183	-.0001808	-.0000509	-.08	.38	-.0005220	-.0002263	-.0000945	-.27	.62
2.5132741	-.0012941	-.0001759	-.0000515	-.09	.37	-.0012901	-.0002212	-.0000952	-.28	.61
2.9321531	-.0018174	.0000794	-.0000278	-.24	-.18	-.0018065	-.0000216	-.0000700	-.36	-.02
-2.9321531	-.0017509	.0004347	.0000211	-.37	-.99	-.0017350	.0002596	-.0000177	-.40	-.94
-2.5132741	-.0011442	.0006852	.0000903	-.31	-1.64	-.0011261	.0004683	.0000561	-.26	-1.67
-2.0943951	-.0004020	.0007023	.0001656	-.00	-1.83	-.0003848	.0005056	.0001359	.06	-1.91
-1.6755160	-.0000155	.0005136	.0002300	.45	-1.59	-.0000021	.0003874	.0002032	.48	-1.66
-1.2566370	-.0002351	.0002773	.0002715	.87	-1.21	-.0002278	.0002267	.0002459	.84	-1.24
-.8377580	-.0009067	.0001709	.0002858	1.03	-1.03	-.0009068	.0001520	.0002605	.98	-1.04
-.4188790	-.0015765	.0002706	.0002721	.88	-1.20	-.0015840	.0002188	.0002467	.85	-1.22

3/22/89 Array #56 Acoustic Center Depth = 1218.84 Sound Source Depth = 250

	$h_1 = 4000$	$\theta = 0.228642$	$t_5 = 0.8462835$			$h_1 = 5000$	$\theta = 0.180284$	$t_5 = 1.0472331$		
ϕ	ϕ_{er}	θ_{er}	tim_{er}	h_{er}	z_{er}	ϕ_{er}	θ_{er}	tim_{er}	h_{er}	z_{er}
.0000000	-.0018133	.0002785	.0001874	.51	-1.69	-.0018185	.0002049	.0001765	.50	-1.78
.4188790	-.0014291	.0003471	.0001182	.11	-1.88	-.0014356	.0002445	.0001069	.13	-1.91
.8377580	-.0006874	.0002964	.0000365	-.21	-1.58	-.0006942	.0001869	.0000243	-.19	-1.54
1.2566370	-.0000795	.0001182	-.0000382	-.39	-.78	-.0000855	.0000287	-.0000514	-.39	-.67
1.6755160	-.0000089	-.0001077	-.0000912	-.41	.17	-.0000130	-.0001638	-.0001052	-.45	.33
2.0943951	-.0005240	-.0002614	-.0001177	-.38	.82	-.0005254	-.0002927	-.0001321	-.44	1.00
2.5132741	-.0012878	-.0002563	-.0001184	-.39	.80	-.0012862	-.0002877	-.0001328	-.45	.98
2.9321531	-.0018004	-.0000935	-.0000925	-.43	.12	-.0017961	-.0001498	-.0001065	-.47	.26
-2.9321531	-.0017262	.0001387	-.0000387	-.41	-.86	-.0017202	.0000489	-.0000518	-.42	-.77
-2.5132741	-.0011161	.0003191	.0000370	-.23	-1.67	-.0011093	.0002095	.0000249	-.22	-1.65
-2.0943951	-.0003753	.0003680	.0001185	.09	-1.96	-.0003688	.0002655	.0001073	.11	-2.01
-1.6755160	.0000052	.0002942	.0001867	.49	-1.75	.0000102	.0002208	.0001758	.48	-1.86
-1.2566370	-.0002239	.0001815	.0002297	.80	-1.35	-.0002212	.0001400	.0002188	.77	-1.49
-.8377580	-.0009070	.0001272	.0002444	.93	-1.15	-.0009071	.0000992	.0002335	.88	-1.31
-.4188790	-.0015882	.0001732	.0002306	.81	-1.32	-.0015912	.0001315	.0002198	.78	-1.45

Table 4. Error Structure - Proposed Methodology

10/27/88	Array #1	Acoustic Center Depth = 1308.76			Sound Source Depth = 250			
	$h_1 = 2000$	$\theta = 0.489930$	$t_4 = 0.4654736$		$h_1 = 3000$	$\theta = 0.339157$	$t_4 = 0.6532862$	
ϕ	ϕ_{er}	θ_{er}	h_{er}	z_{er}	ϕ_{er}	θ_{er}	h_{er}	z_{er}
.0000000	.00002258	.00006163	-.07	-.12	.00001590	.00006335	-.07	-.19
.4188790	.00003532	.00004005	-.04	-.08	.00002490	.00004109	-.04	-.12
.8377580	.00004159	.00000997	-.01	-.02	.00002924	.00000960	-.01	-.03
1.2566370	.00004007	-.00002200	.02	.04	.00002802	-.00002369	.03	.07
1.6755160	.00003132	-.00004904	.05	.10	.00002171	-.00005135	.06	.15
2.0943951	.00001754	-.00006587	.07	.13	.00001201	-.00006775	.07	.20
2.5132741	.00000186	-.00007002	.08	.14	.00000126	-.00007047	.08	.21
2.9321531	-.00001258	-.00006218	.07	.12	-.00000820	-.00006092	.07	.18
-2.9321531	-.00002356	-.00004547	.05	.09	-.00001486	-.00004348	.05	.13
-2.5132741	-.00003016	-.00002363	.03	.05	-.00001853	-.00002295	.03	.07
-2.0943951	-.00003232	.00000056	.00	-.00	-.00001982	-.00000153	.00	.00
-1.6755160	-.00002989	.00002534	-.03	-.05	-.00001885	.00002127	-.02	-.06
-1.2566370	-.00002235	.00004820	-.05	-.10	-.00001469	.00004464	-.05	-.13
-.8377580	-.00000973	.00006478	-.07	-.13	-.00000662	.00006356	-.07	-.19
-.4188790	.00000632	.00007019	-.08	-.14	.00000441	.00007116	-.08	-.21

10/27/88	Array #1	Acoustic Center Depth = 1308.76			Sound Source Depth = 250			
	$h_1 = 4000$	$\theta = 0.255966$	$t_4 = 0.8490844$		$h_1 = 5000$	$\theta = 0.203535$	$t_4 = 1.0484023$	
ϕ	ϕ_{er}	θ_{er}	h_{er}	z_{er}	ϕ_{er}	θ_{er}	h_{er}	z_{er}
.0000000	.00001262	.00006511	-.07	-.26	.00001070	.00006692	-.08	-.34
.4188790	.00001971	.00004209	-.05	-.17	.00001660	.00004306	-.05	-.22
.8377580	.00002304	.00000926	-.01	-.04	.00001930	.00000895	-.01	-.04
1.2566370	.00002197	-.00002525	.03	.10	.00001832	-.00002670	.03	.13
1.6755160	.00001693	-.00005352	.06	.21	.00001407	-.00005557	.06	.28
2.0943951	.00000928	-.00006961	.08	.28	.00000768	-.00007145	.08	.36
2.5132741	.00000097	-.00007102	.08	.28	.00000081	-.00007167	.08	.36
2.9321531	-.00000606	-.00005967	.07	.24	-.00000482	-.00005837	.07	.29
-2.9321531	-.00001058	-.00004127	.05	.17	-.00000807	-.00003877	.04	.19
-2.5132741	-.00001271	-.00002212	.02	.09	-.00000923	-.00002101	.02	.11
-2.0943951	-.00001351	-.00000407	.00	.02	-.00000967	-.00000727	.01	.04
-1.6755160	-.00001335	.00001629	-.02	-.07	-.00001008	.00001000	-.01	-.05
-1.2566370	-.00001095	.00004049	-.04	-.16	-.00000881	.00003551	-.04	-.18
-.8377580	-.00000511	.00006230	-.07	-.25	-.00000425	.00006100	-.07	-.31
-.4188790	.00000350	.00007226	-.08	-.29	.00000299	.00007353	-.08	-.37

Table 4. (Continued)

10/27/88 Array #56 Acoustic Center Depth = 1218.84 Sound Source Depth = 250

	$h_1 = 2000$	$\theta = 0.453929$	$t_4 = 0.4569741$		$h_1 = 3000$	$\theta = 0.312071$	$t_4 = 0.6473052$	
ϕ	ϕ_{er}	θ_{er}	h_{er}	z_{er}	ϕ_{er}	θ_{er}	h_{er}	z_{er}
.0000000	-.00002534	-.00004423	.04	.09	-.00001609	-.00004670	.05	.14
.4188790	-.00003175	-.00002062	.02	.04	-.00002056	-.00002438	.02	.07
.8377580	-.00003311	.00000761	-.01	-.02	-.00002197	.00000353	-.00	-.01
1.2566370	-.00002836	.00003575	-.04	-.07	-.00001934	.00003280	-.03	-.10
1.6755160	-.00001774	.00005766	-.06	-.12	-.00001235	.00005670	-.06	-.17
2.0943951	-.00000311	.00006756	-.07	-.13	-.00000218	.00006774	-.07	-.20
2.5132741	.00001211	.00006258	-.06	-.12	.00000845	.00006179	-.06	-.19
2.9321531	.00002430	.00004438	-.04	-.09	.00001658	.00004134	-.04	-.12
-2.9321531	.00003109	.00001822	-.02	-.04	.00002058	.00001359	-.01	-.04
-2.5132741	.00003191	-.00000987	.01	.02	.00002052	-.00001428	.01	.04
-2.0943951	.00002755	-.00003494	.03	.07	.00001732	-.00003791	.04	.11
-1.6755160	.00001929	-.00005397	.05	.11	.00001195	-.00005528	.06	.17
-1.2566370	.00000841	-.00006515	.06	.13	.00000519	-.00006540	.07	.20
-.8377580	-.00000365	-.00006738	.07	.13	-.00000227	-.00006759	.07	.20
-.4188790	-.00001542	-.00006026	.06	.12	-.00000965	-.00006136	.06	.18

10/27/88 Array #56 Acoustic Center Depth = 1218.84 Sound Source Depth = 250

	$h_1 = 4000$	$\theta = 0.234753$	$t_4 = 0.8445435$		$h_1 = 5000$	$\theta = 0.186264$	$t_4 = 1.0447819$	
ϕ	ϕ_{er}	θ_{er}	h_{er}	z_{er}	ϕ_{er}	θ_{er}	h_{er}	z_{er}
.0000000	-.00001139	-.00004909	.05	.20	-.00000852	-.00005136	.05	.26
.4188790	-.00001482	-.00002816	.03	.11	-.00001126	-.00003192	.03	.16
.8377580	-.00001625	-.00000080	.00	.00	-.00001265	-.00000539	.01	.03
1.2566370	-.00001471	.00002949	-.03	-.12	-.00001181	.00002573	-.03	-.13
1.6755160	-.00000963	.00005559	-.06	-.22	-.00000795	.00005426	-.06	-.27
2.0943951	-.00000172	.00006799	-.07	-.27	-.00000143	.00006832	-.07	-.34
2.5132741	.00000662	.00006086	-.06	-.24	.00000551	.00005969	-.06	-.30
2.9321531	.00001263	.00003774	-.04	-.15	.00001017	.00003339	-.03	-.17
-2.9321531	.00001513	.00000842	-.01	-.03	.00001169	.00000255	-.00	-.01
-2.5132741	.00001461	-.00001896	.02	.08	.00001090	-.00002389	.02	.12
-2.0943951	.00001207	-.00004086	.04	.16	.00000882	-.00004379	.05	.22
-1.6755160	.00000824	-.00005653	.06	.23	.00000598	-.00005772	.06	.29
-1.2566370	.00000357	-.00006568	.07	.26	.00000259	-.00006597	.07	.33
-.8377580	-.00000158	-.00006782	.07	.27	-.00000116	-.00006807	.07	.34
-.4188790	-.00000674	-.00006239	.06	.25	-.00000498	-.00006336	.07	.32

Table 4. (Continued)

3/22/89 Array #1 Acoustic Center Depth = 1308.76 Sound Source Depth = 250

	$h_1 = 2000$	$\theta = 0.711452$	$t_4 = 0.5438750$		$h_1 = 3000$	$\theta = 0.337225$	$t_4 = 0.6551362$	
ϕ	ϕ_{er}	θ_{er}	h_{er}	z_{er}	ϕ_{er}	θ_{er}	h_{er}	z_{er}
.0000000	.00003985	.00006864	-.12	-.14	.00002163	.00008688	-.09	-.26
.4188790	.00006200	.00004455	-.08	-.09	.00003395	.00005637	-.06	-.17
.8377580	.00007302	.00001161	-.02	-.02	.00003989	.00001347	-.01	-.04
1.2566370	.00007069	-.00002346	.04	.05	.00003830	-.00003181	.03	.09
1.6755160	.00005579	-.00005365	.09	.11	.00002986	-.00006968	.08	.21
2.0943951	.00003169	-.00007333	.13	.15	.00001668	-.00009251	.10	.28
2.5132741	.00000343	-.00007943	.14	.16	.00000193	-.00009663	.11	.29
2.9321531	-.00002363	-.00007193	.13	.14	-.00001116	-.00008341	.09	.25
-2.9321531	-.00004518	-.00005335	.09	.11	-.00002024	-.00005939	.06	.18
-2.5132741	-.00005863	-.00002743	.05	.05	-.00002516	-.00003159	.03	.09
-2.0943951	-.00006280	.00000209	-.00	-.00	-.00002692	-.00000317	.00	.01
-1.6755160	-.00005718	.00003173	-.06	-.06	-.00002586	.00002745	-.03	-.08
-1.2566370	-.00004173	.00005753	-.10	-.11	-.00002045	.00005986	-.07	-.18
-.8377580	-.00001775	.00007479	-.13	-.15	-.00000943	.00008666	-.09	-.26
-.4188790	.00001127	.00007919	-.14	-.16	.00000584	.00009771	-.11	-.29

3/22/89 Array #1 Acoustic Center Depth = 1308.76 Sound Source Depth = 250

	$h_1 = 4000$	$\theta = 0.253446$	$t_4 = 0.8514820$		$h_1 = 5000$	$\theta = 0.200474$	$t_4 = 1.0513520$	
ϕ	ϕ_{er}	θ_{er}	h_{er}	z_{er}	ϕ_{er}	θ_{er}	h_{er}	z_{er}
.0000000	.00001680	.00008781	-.10	-.35	.00001385	.00008844	-.10	-.44
.4188790	.00002631	.00005682	-.06	-.23	.00002162	.00005702	-.06	-.28
.8377580	.00003080	.00001303	-.01	-.05	.00002516	.00001270	-.01	-.06
1.2566370	.00002948	-.00003288	.04	.13	.00002403	-.00003348	.04	.17
1.6755160	.00002294	-.00007091	.08	.28	.00001871	-.00007149	.08	.36
2.0943951	.00001279	-.00009314	.10	.37	.00001048	-.00009323	.11	.47
2.5132741	.00000157	-.00009564	.11	.38	.00000135	-.00009423	.11	.47
2.9321531	-.00000806	-.00008011	.09	.32	-.00000623	-.00007645	.09	.38
-2.9321531	-.00001408	-.00005503	.06	.22	-.00001044	-.00004999	.06	.25
-2.5132741	-.00001677	-.00002991	.03	.12	-.00001169	-.00002791	.03	.14
-2.0943951	-.00001784	-.00000760	.01	.03	-.00001226	-.00001347	.02	.07
-1.6755160	-.00001801	.00001845	-.02	-.07	-.00001333	.00000667	-.01	-.03
-1.2566370	-.00001520	.00005177	-.06	-.21	-.00001224	.00004166	-.05	-.21
-.8377580	-.00000736	.00008284	-.09	-.33	-.00000630	.00007855	-.09	-.39
-.4188790	.00000443	.00009744	-.11	-.39	.00000356	.00009699	-.11	-.48

Table 4. (Continued)

3/22/89	Array #56		Acoustic Center Depth = 1218.84			Sound Source Depth = 250		
	h_1 = 2000	θ = 0.452549	t_4 = 0.4583009		h_1 = 3000	θ = 0.309991	t_4= 0.6491808	
ϕ	ϕ_{er}	θ_{er}	h_{er}	z_{er}	ϕ_{er}	θ_{er}	h_{er}	z_{er}
.0000000	-.00003537	-.00006070	.06	.12	-.00002153	-.00006076	.06	.18
.4188790	-.00004398	-.00002798	.03	.06	-.00002708	-.00003140	.03	.09
.8377580	-.00004567	.00001082	-.01	-.02	-.00002868	.00000469	-.00	-.01
1.2566370	-.00003907	.00004953	-.05	-.10	-.00002512	.00004263	-.04	-.13
1.6755160	-.00002430	.00007979	-.08	-.16	-.00001584	.00007385	-.07	-.22
2.0943951	-.00000389	.00009328	-.09	-.19	-.00000226	.00008781	-.09	-.26
2.5132741	.00001726	.00008583	-.09	-.17	.00001180	.00007868	-.08	-.24
2.9321531	.00003398	.00005998	-.06	-.12	.00002219	.00005037	-.05	-.15
-2.9321531	.00004307	.00002352	-.02	-.05	.00002695	.00001363	-.01	-.04
-2.5132741	.00004398	-.00001501	.01	.03	.00002653	-.00002208	.02	.07
-2.0943951	.00003788	-.00004933	.05	.10	.00002229	-.00005202	.05	.16
-1.6755160	.00002639	-.00007547	.07	.15	.00001530	-.00007429	.07	.22
-1.2566370	.00001128	-.00009081	.09	.18	.00000635	-.00008739	.09	.26
-.8377580	-.00000553	-.00009361	.09	.19	-.00000361	-.00008975	.09	.27
-.4188790	-.00002183	-.00008334	.08	.17	-.00001332	-.00008074	.08	.24

3/22/89	Array #56		Acoustic Center Depth = 1218.84			Sound Source Depth = 250		
	h_1 = 4000	θ = 0.235058	t_4 = 0.8469817		h_1 = 5000	θ = 0.183019	t_4= 1.0477857	
ϕ	ϕ_{er}	θ_{er}	h_{er}	z_{er}	ϕ_{er}	θ_{er}	h_{er}	z_{er}
.0000000	-.00001438	-.00005913	.06	.24	-.00000981	-.00005569	.06	.28
.4188790	-.00001806	-.00003375	.03	.13	-.00001218	-.00003487	.04	.17
.8377580	-.00001942	-.00000166	.00	.01	-.00001316	-.00000825	.01	.04
1.2566370	-.00001739	.00003401	-.03	-.14	-.00001201	.00002314	-.02	-.12
1.6755160	-.00001110	.00006516	-.07	-.26	-.00000769	.00005246	-.05	-.26
2.0943951	-.00000123	.00007900	-.08	-.32	-.00000038	.00006500	-.07	-.33
2.5132741	.00000893	.00006768	-.07	-.27	.00000701	.00005078	-.05	-.25
2.9321531	.00001574	.00003703	-.04	-.15	.00001123	.00001837	-.02	-.09
-2.9321531	.00001805	.00000136	-.00	-.01	.00001187	-.00001400	.01	.07
-2.5132741	.00001701	-.00002969	.03	.12	.00001057	-.00003790	.04	.19
-2.0943951	.00001394	-.00005396	.06	.22	.00000846	-.00005498	.06	.27
-1.6755160	.00000944	-.00007185	.07	.29	.00000567	-.00006792	.07	.34
-1.2566370	.00000373	-.00008260	.08	.33	.00000203	-.00007617	.08	.38
-.8377580	-.00000270	-.00008440	.09	.34	-.00000220	-.00007731	.08	.39
-.4188790	-.00000900	-.00007648	.08	.31	-.00000634	-.00007033	.07	.35

support errors of this magnitude. (The calculations in this section apply the polynomial extrapolation prior to the development of isospeed layers. In this way the DV table extension is not an issue in the present comparisons.)

Accordingly, the author has proposed and tested a method that treats the two main issues. The acoustic center is moved to the C-phone. (Visualize Figure 3 with the C-phone on the axis of the cylinder.) In this way the transit time that stops the ray tracing is t_4, a directly measured quantity. Also the sound speed in the layer containing the (X, Y, C) phones (Z-phone omitted) is assumed constant in order to determine (ϕ_p, θ_p), the azimuth and elevation angles of the proposed method. In this way the change in sound speed at the Z-phone is taken out of the computation. Details appear in Appendix F.

Computations using this technique appear in Table 4. The improvement is dramatic. Let us repeat the earlier exemplary computations 10/22/88, Array No. 1, $h_1 = 5000$ and $\phi = 0.418879$. This time the inputs come from Table 4: specifically $\sqrt{(.22)^2 + (0.5)^2 + (5 \cdot 0.04306)^2} = 0.31$ ft., a value dramatically smaller than 12 ft. A scan of Table 4 and comparison with Table 3 shows that these improvements are quite consistent.

These computations also have the advantage that the five-foot layer isogradient ray tracing was used together with the exact tilt corrections, eq. (B.5.)

5. CONCLUSIONS

Generally there are a number of sources of systematic error. In some the effects are small, e.g., isogradient vs. isospeed raytracing, 5 foot versus 25 foot layer thicknesses. None the less they are systematic and certainly no longer necessary. The presence of systematic errors tends to build up idiosyncracies

that frustrate the use of standard statistical methodology when troubleshooting other aspects of the data.

The discovery of the periodic nature of the errors was a surprise. Its presence adds another dimension to the interpretation of the data. No doubt it is the source of some deception.

The major sources of error related to ray tracing (see pages 5, 6) are believed to be associated with

(i) the conversion of transit times to the direction of the sound source
(ii) the constant speed extrapolation of the DV profile below 1300 ft.
(iii) the use of approximations for tilt corrections.

Of course the effects of these errors are directional because of their periodic nature. We have documented errors of 12 ft. or so due to (i). We can speculate 10 or more feet because of (ii). Moreover the combined effects could be additive. The effect of (iii) increases as the tilts increase.

It is further noted that the above errors apply to single arrays. At this point we have no comment about how they may combine to produce mismatches in the array overlap regions. It would be more comfortable to treat this issue by introducing the changes and then collecting more data.

6. ADDENDUM

It came to the author's attention during the final editing phase of this report, that the approximate tilt corrections, eq. (B.4), are not the ones currently employed by the software. Rather, the system is using

$$\begin{Bmatrix} X(1) \\ X(2) \\ X(3) \end{Bmatrix} = \begin{Bmatrix} c_2 & 0 & -s_2 \\ 0 & c_1 & -s_1 \\ s_2 & s_1 & c_1 c_2 \end{Bmatrix} \begin{Bmatrix} X_0(1) \\ X_0(2) \\ X_0(3) \end{Bmatrix} \tag{6.1}$$

Accordingly the author made some specialized computations for purposes of indicating the effect. Referring to Tables 3 and 4, we have chosen to treat the exemplary case: water column of 10/27/88, array number 1, h_1 = 5000 ft, z_1 = 250, and ϕ = 0.418879 radians. The table below contains the four errors and total offset for each of four algorithms:

(i) the isospeed method (from Table 3)
(ii) the isospeed method using (6.1) vice (B.4)
(iii) the isospeed method using (B.5) vice (B.4)
(iv) the proposed method (from Table 4)

TABLE 5. EFFECT OF TILT CORRECTION METHOD

10/27/88, Array #1, h_1 = 5000 ft, z_1 = 250 ft, ϕ = 0.418879 rad., a_2 = 1308.76 ft.

	ϕ_{er}	θ_{er}	h_{er}	z_{er}	d
(i)	.0023525	.0003869	.28	–2.45	12.02
(ii)	.0021174	–.0001567	1.47	2.95	11.09
(iii)	–.0000161	–.0000077	1.26	2.19	2.53
(iv)	.0000166	.0000430	–.05	– 22	0.31

The results of Table 5 suggest the following: there is little distinction between the use of (B.4) and (6.1) for the tilt correcting (compare (i) and (ii)). However case (iii) suggests that there is much to be gained by use of the exact tilt correct (B.5) even if isospeed ray tracing is used with 25 ft layer thickness. Finally case (iv) suggests that considerable gains are available if, in addition, we use the proposed methodology.

All of these systematic errors are mathematical, i.e., due to choice of algorithms. There is no longer any reason not to use the best.

APPENDIX A

The twelve depth velocity profiles used in this study are recorded here in graphical form. They include the profiles used in [7]. Generally the measured values stop at a depth of about 1300 feet and it is necessary to extrapolate, in several instances to depths greater than 1350 feet (see Table B-2).

The insets of the graphs illustrate two different extrapolation schemes. The constant value extrapolation is the one currently in use, [5]. But there is a slight deception. Current methodology utilizes isospeed profiles, see Figure 2, and 25 foot layer thicknesses. The constant value extrapolation is the value of the deepest 25 foot layer appearing in an isospeed profile.

The other extrapolation is based upon fitting a second order polynomial to the deepest hundred feet of the original profile (five foot layer thicknesses). There are two steps in this process. First is fitting the curve by least squares. Because of the equally spaced depth increments, the fitting takes an especially simple form. Using the equation,

$$\upsilon = a + b(u - \bar{u}) + c(u - \bar{u})^2 \tag{A.1}$$

where υ is velocity, u is layer depth, and $\bar{u}$ = average depth, the normal equations take the form

$$\begin{aligned}
\Sigma\upsilon &= \Sigma a - \Sigma b(u - \bar{u}) - c\Sigma(u - \bar{u})^2 \\
\Sigma\upsilon(u - \bar{u}) &= \Sigma a(u - \bar{u}) - \Sigma b(u - \bar{u})^2 - c\Sigma(u - \bar{u})^3 \\
\Sigma\upsilon(u - \bar{u})^2 &= \Sigma a(u - \bar{u})^2 - \Sigma b(u - \bar{u})^3 - c\Sigma(u - \bar{u})^4
\end{aligned}$$

Using the notation $S_v = \Sigma v$, $S_{vu} = \Sigma v\,(u-\overline{u})$, $S_{vuu} = \Sigma v\,(u-\overline{u})^2$. $S_{u2} = \Sigma\,(u-\overline{u})^2$, $S_{u4} = \Sigma(u-\overline{u})^4$ and recognizing $\Sigma(u-\overline{u}) = \Sigma(u-\overline{u})^3 = 0$ because of the uniform spacing, the above equations assume the reduced form

$$
\begin{aligned}
Sv &= na + cS_{u2} \\
S_{vu} &= bS_{u2} \\
S_{vuu} &= aS_{u2} + cS_{u4}
\end{aligned}
\tag{A.2}
$$

and we solve for the coefficient of the quadratic term

$$
c = \left(nS_{vuu} - S_v S_{u2}\right) / \left(nS_{u4} - S_{u2}^2\right) \tag{A.3}
$$

(This done, values for a and b come easily from the first two equations.)

We note in passing that if n = 2K+1, an odd number, and Δ is the spacing between consecutive values of {u}, then $\overline{u}$ is an integer and

$$
\begin{aligned}
S_{u2} &= \frac{\Delta^2}{3} K(K+1)(2K+1), \\
S_{u4} &= \frac{\Delta^4}{2}\left[K(K+1)\right]^2, \\
nS_{u4} - S_{u2}^2 &= \Delta^4 K^2 (K+1)^2 (2K+1)(7-4K)/18
\end{aligned}
\tag{A.4}
$$

Such formulas expedite the computation of c in (A.3).

The second step deals with the issue of how to use this quadratic for extrapolation purposes. Generally, the direct use of the equation (A.1) would lead to a visual discontinuity between the last measured value and the first extrapolated one. We have chosen not to do this. Instead we recognize that $\Delta \cdot c$ represents the first difference of the gradient sequence $\{v_1(i)\}$, see Figure 2. So to preserve continuity, the extrapolation is enabled by using successive updates

$$\upsilon_1(i) = \upsilon_1(i-1) + \Delta \cdot c$$
$$\upsilon(i+1) = \upsilon(i) + \Delta \upsilon_1(i)$$
$$\upsilon_0(i) = \left[u(i+1)\upsilon(i) - u(i)\upsilon(i+1)\right] / \Delta$$

where $\upsilon(i)$ is the estimated sound speed at $u(i)$; $\upsilon_0(i)$ and $\upsilon_1(i)$ are the intercept and slope values of the straight line fit for the i^{th} layer. It is this continuity preserving step that explains the occasional appearance of "crooked" extrapolations in the insets.

The use of isogradient ray tracing with 25 foot layer thicknesses was used in Section 3. If extrapolation of the water column was required, then a different second order polynomial method was used, and after the conversion to 25 foot layers. Basically the quantity $\Delta \cdot c$ was estimated by averaging the difference of the last five values of υ_1 (last 100 feet), and then proceeding in the same way as stated above. No graphs showing the effect of this have been prepared. But the choice does have an effect upon the d_g values computed for Table 2.

We take this opportunity to note that the visual appeal of the quadratic extrapolation is rather good in instances 1, 2, 3, 4, 6 and 11. The others are easily challenged. This information may influence the reader's interpretation of some values appearing in Table 2.

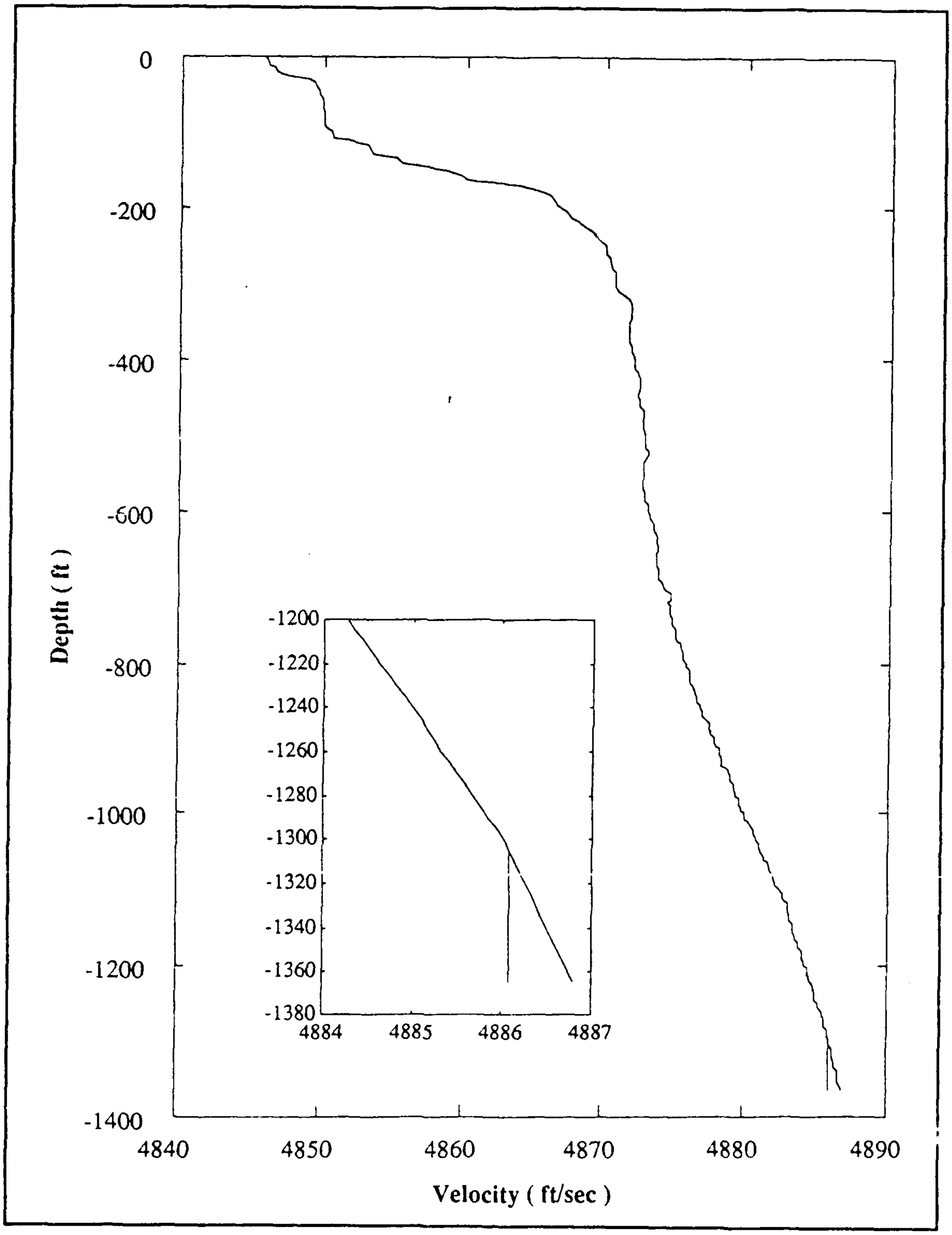

Depth Velocity Profile—5/12/88

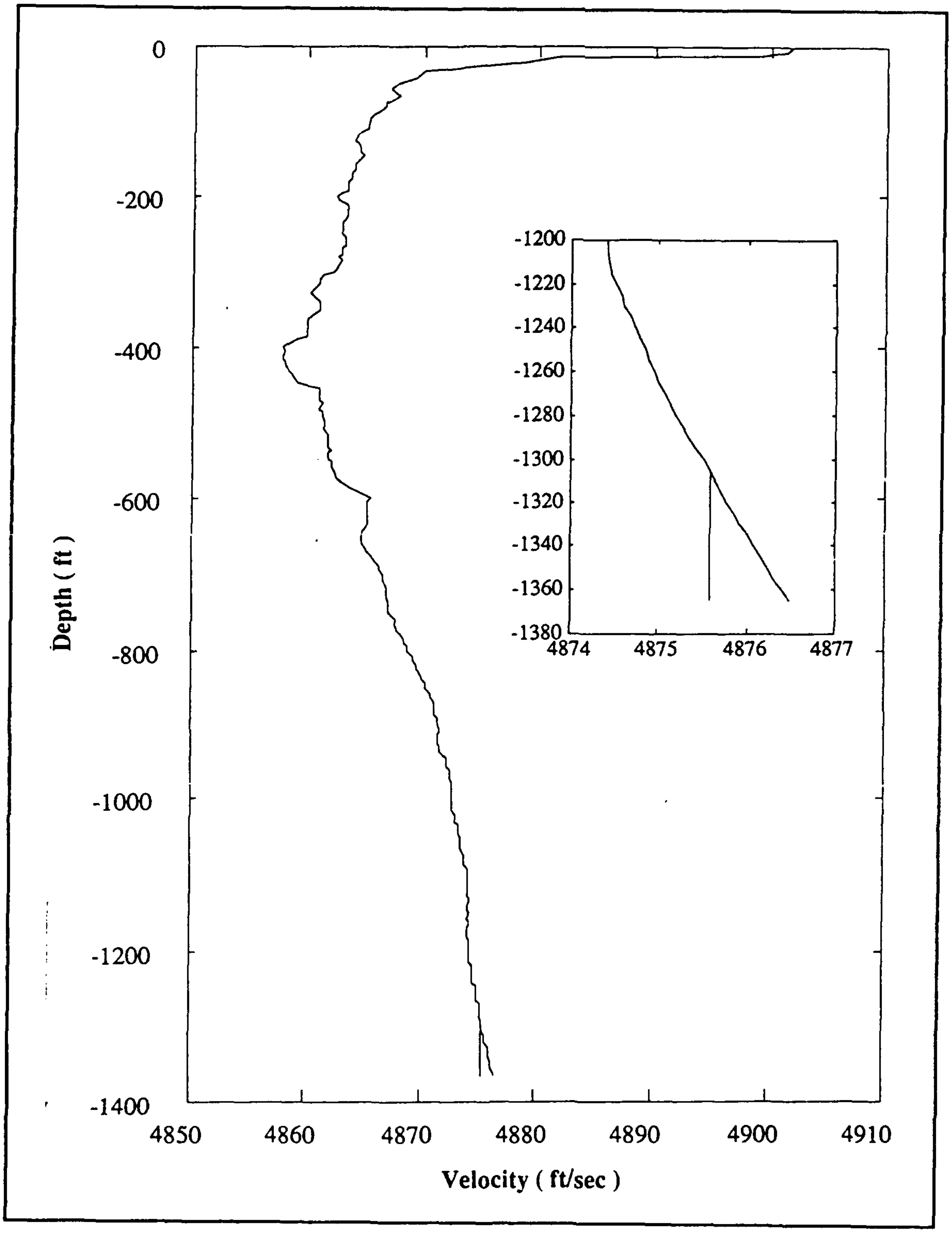

Depth Velocity Profile—6/22/88

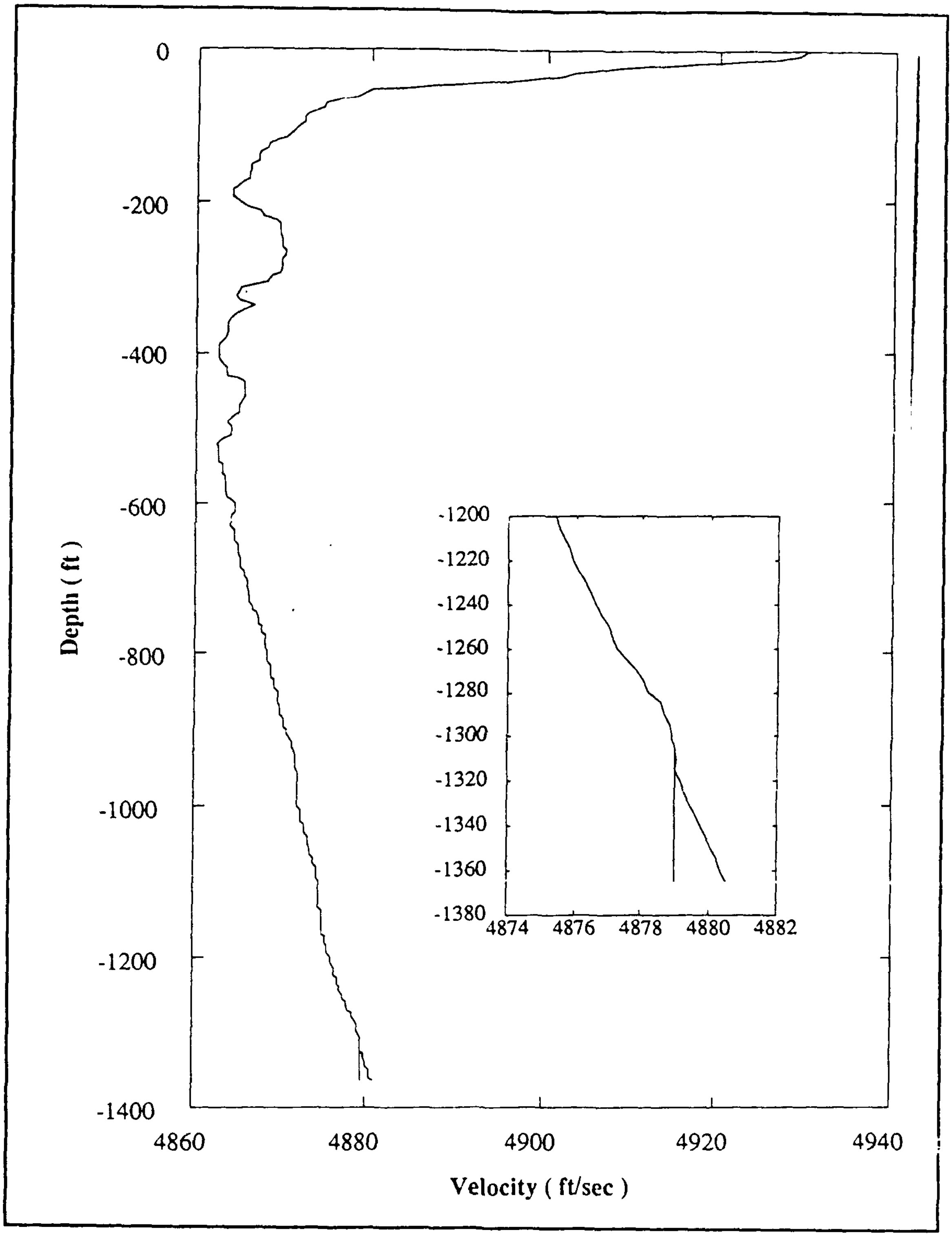

Depth Velocity Profile—7/21/88

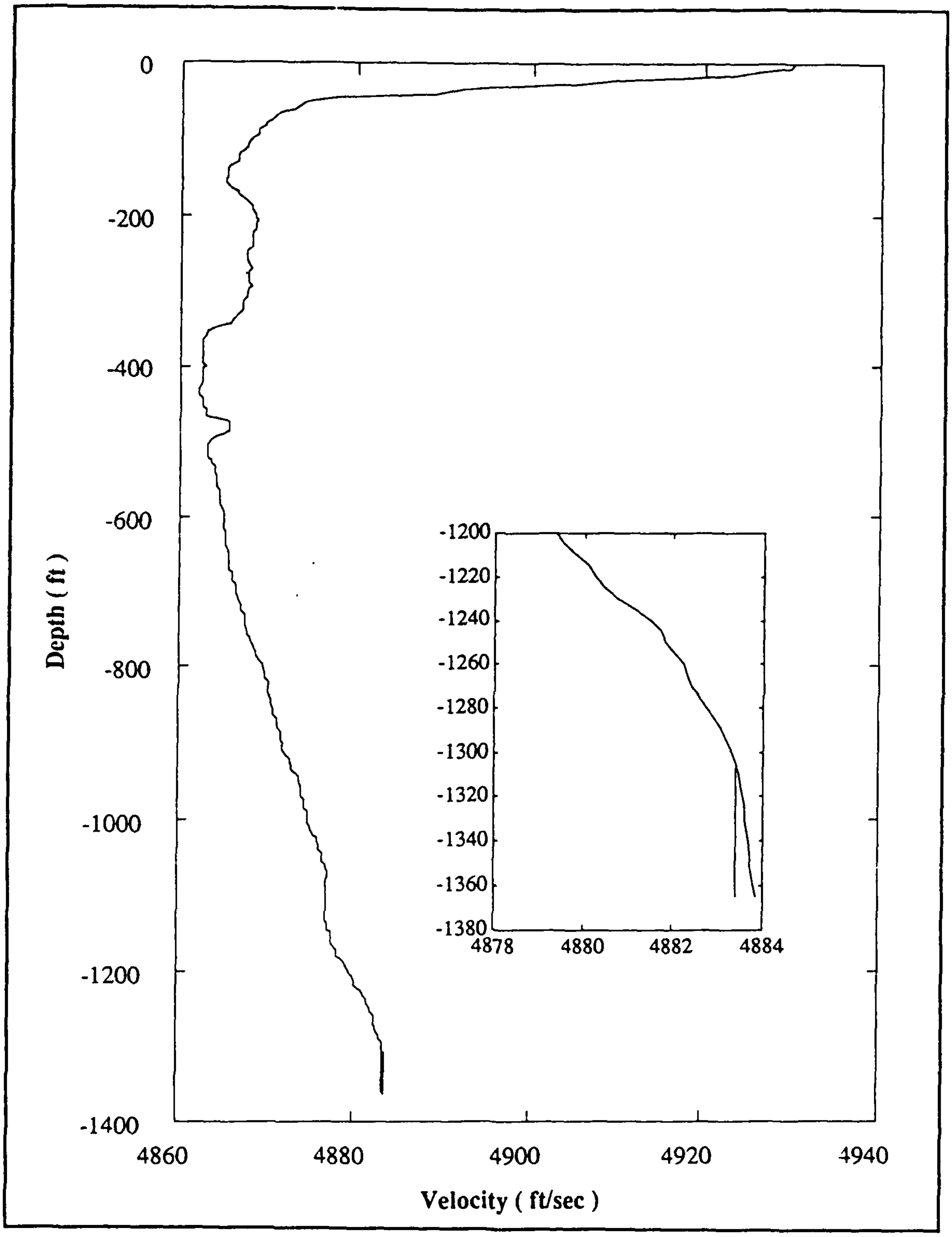

Depth Velocity Profile—8/03/88

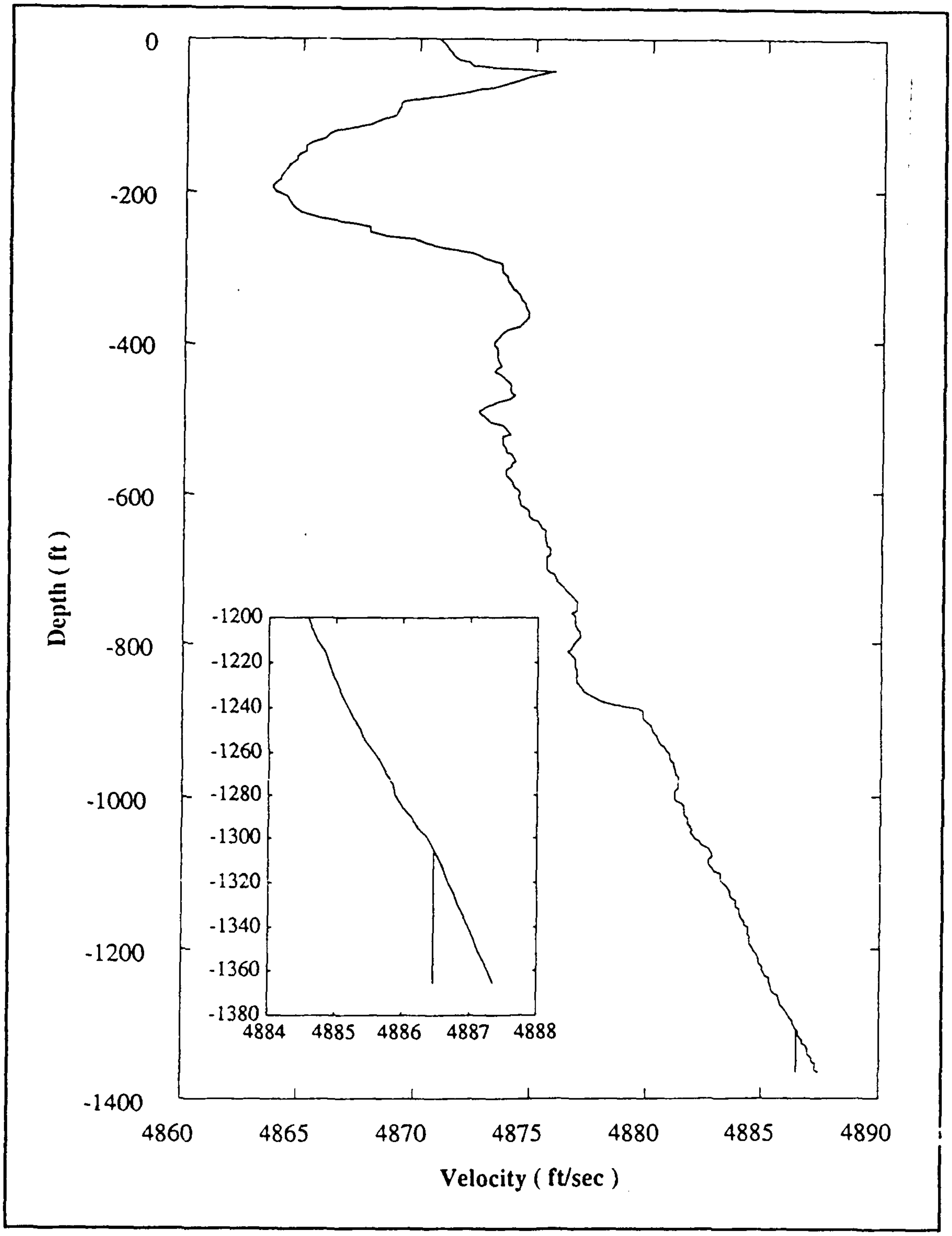

Depth Velocity Profile—10/27/88

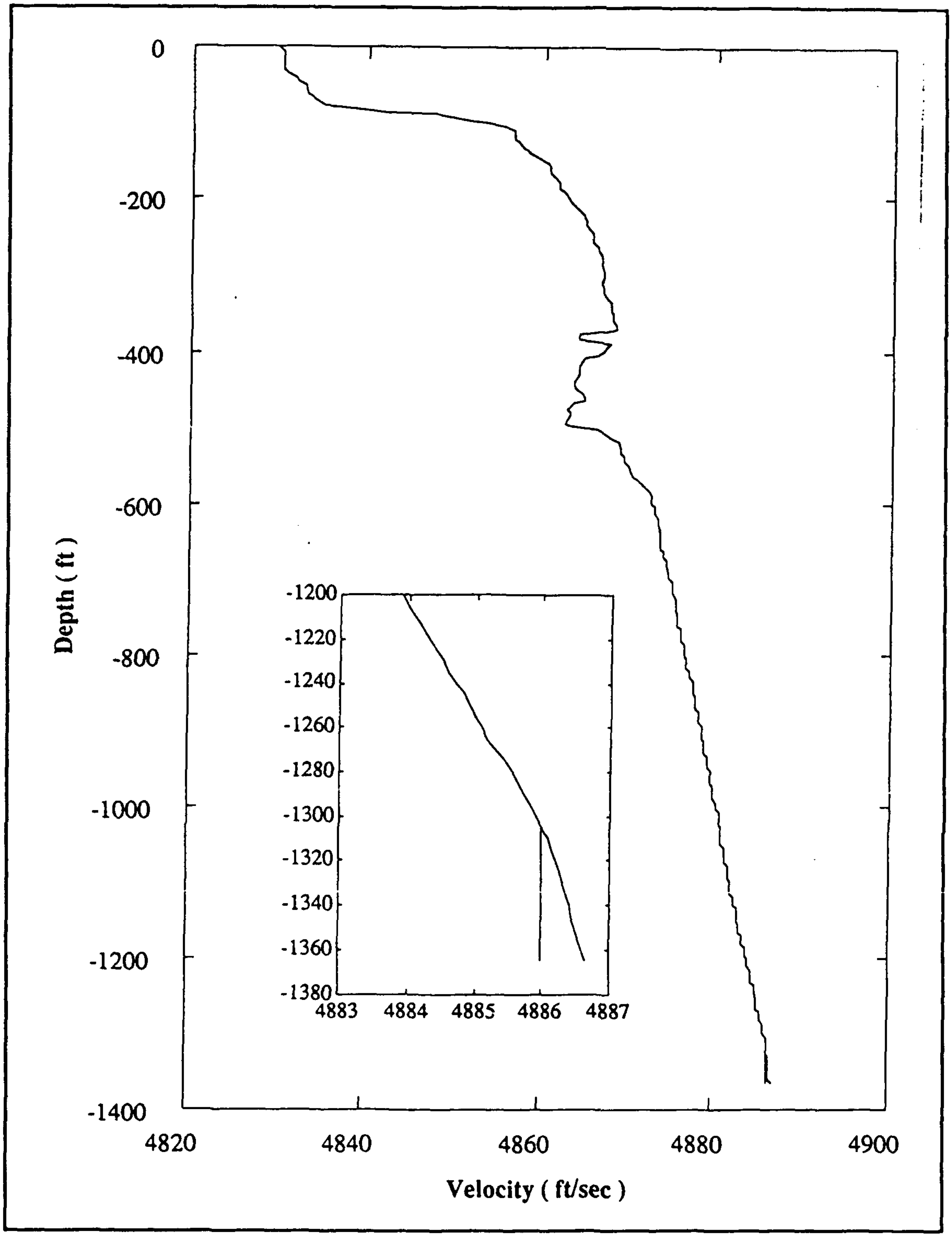

Depth Velocity Profile—1/13/89

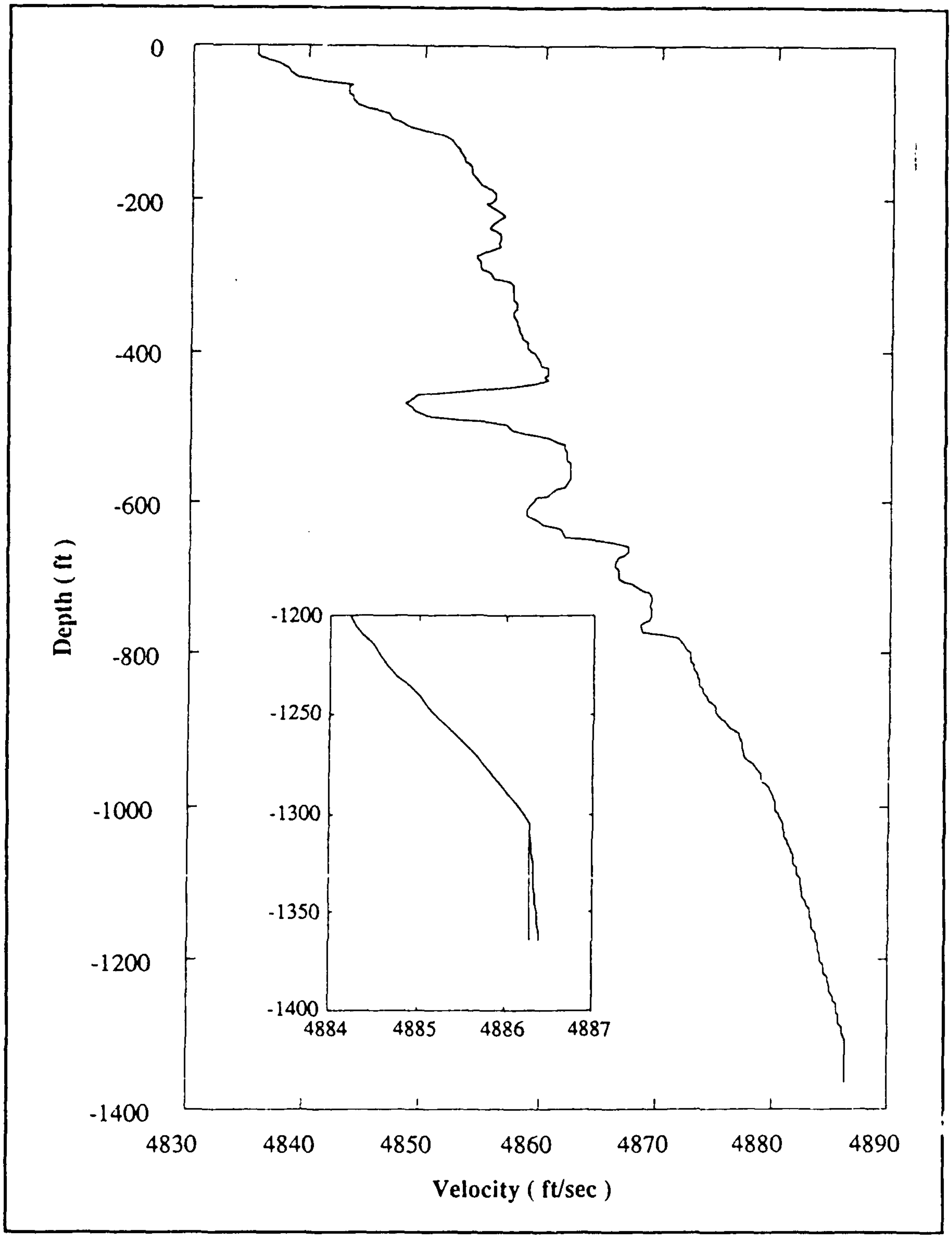

Depth Velocity Profile—3/08/89

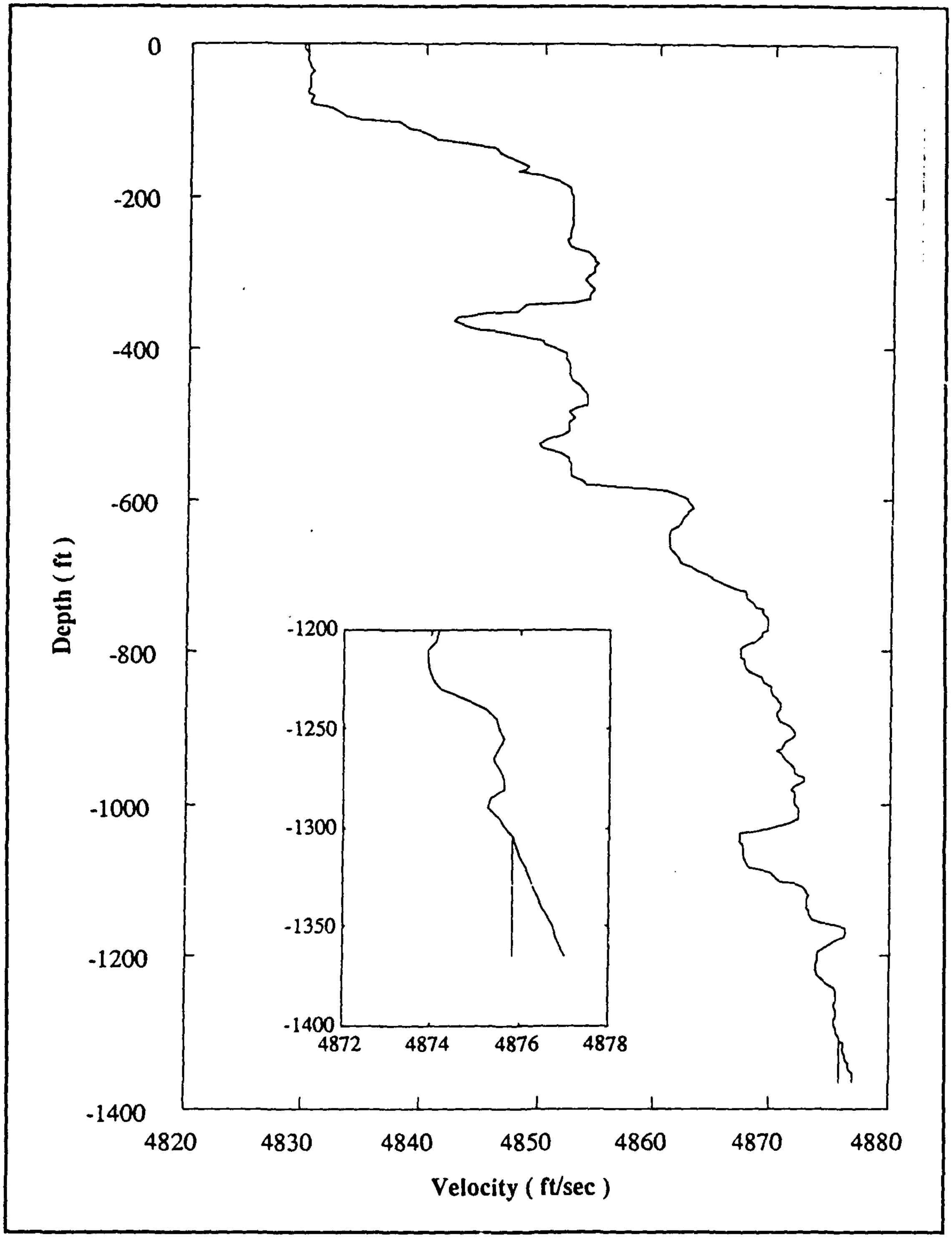

Depth Velocity Profile—3/22/89

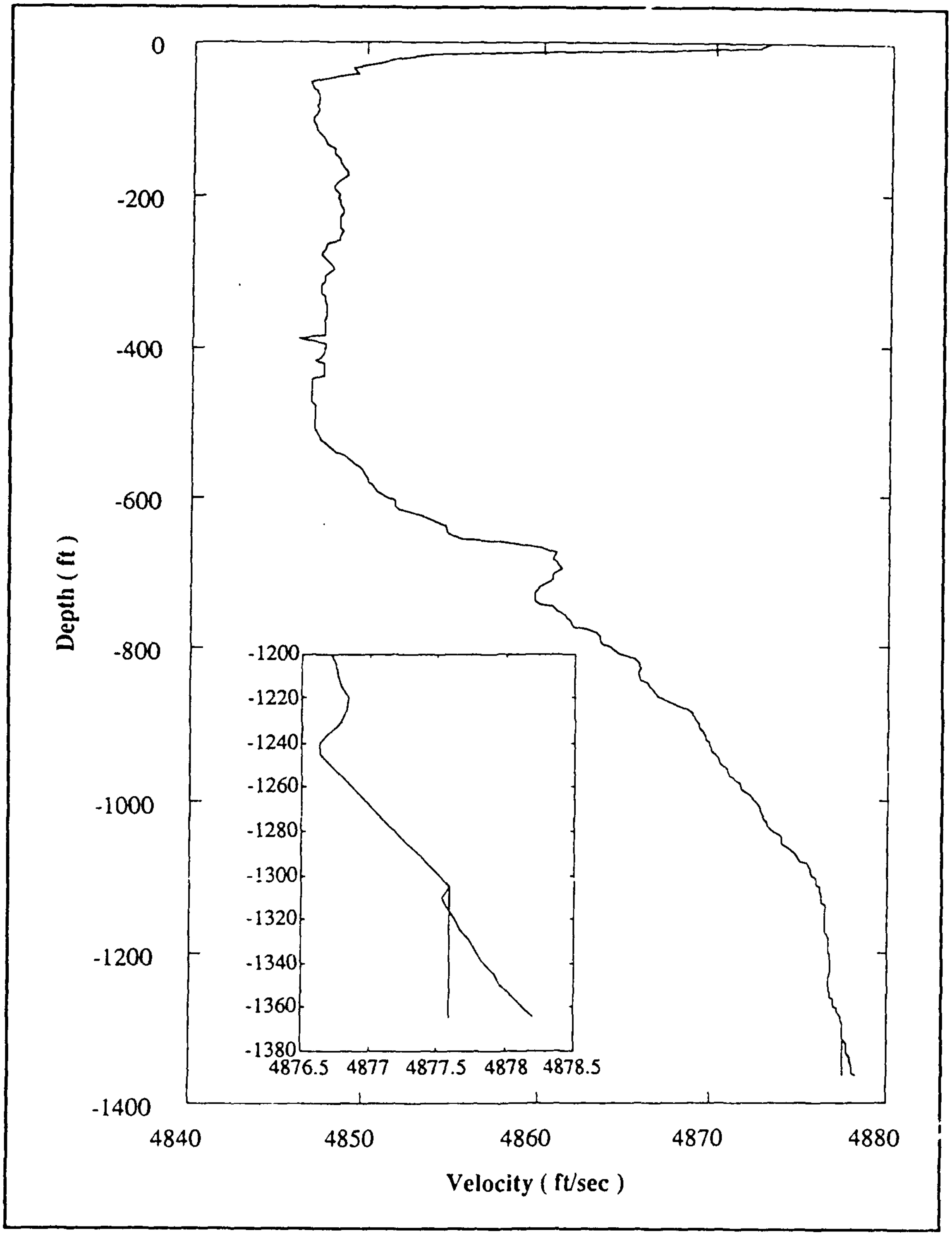

Depth Velocity Profile—4/26/89

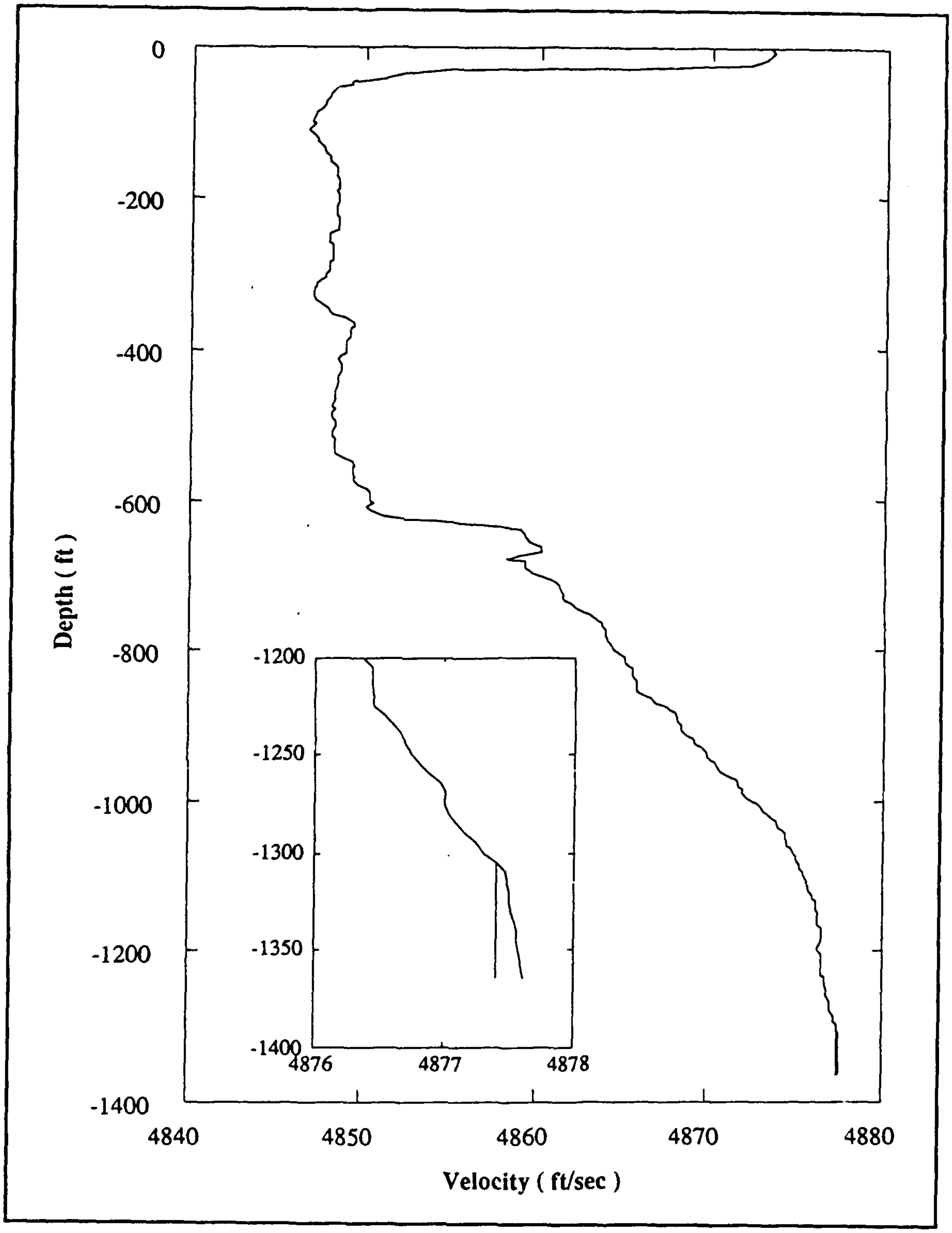

Depth Velocity Profile—4/27/89

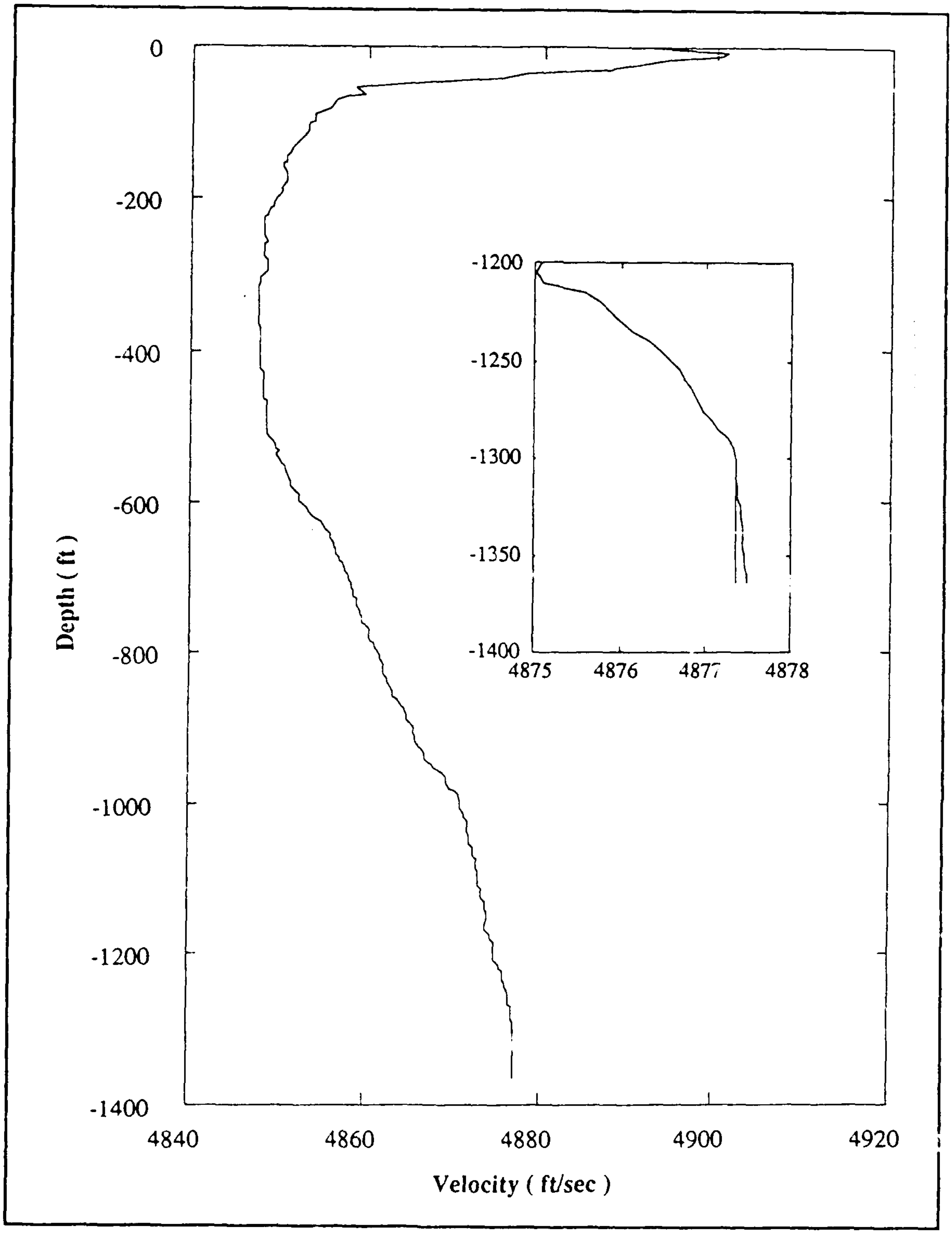

Depth Velocity Profile—5/10/89

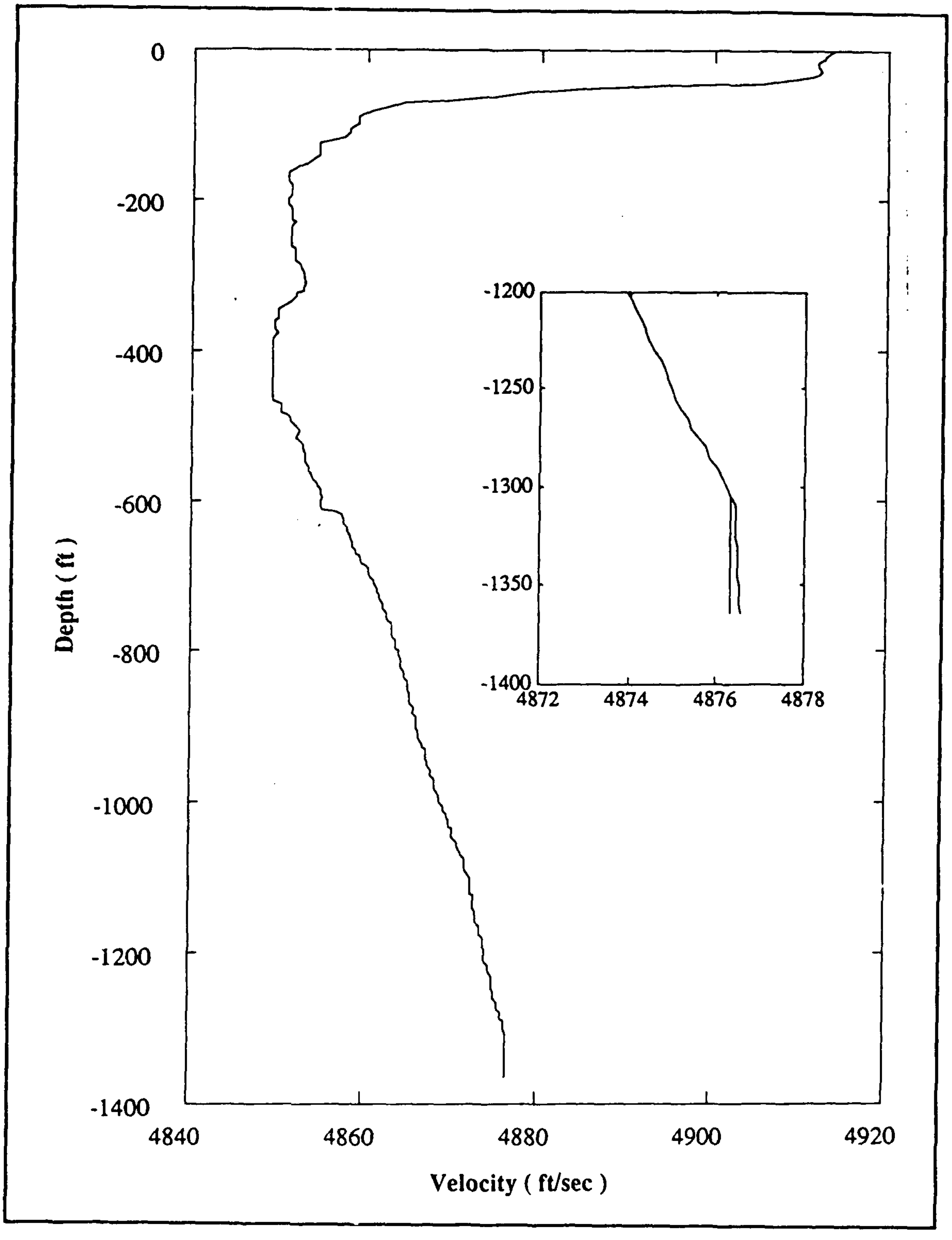

Depth Velocity Profile—6/06/89

APPENDIX B

COORDINATE SYSTEMS

The developments that follow deal with several coordinate systems and we need efficient ways to distinguish among them. First of all is the right handed system defined by the X, Y, Z and C hydrophones of the array. All incoming transit times must be interpreted in this system and we call it cs(a), or the coordinate system of the array. The origin is at the c hydrophone.

Since this system is generally tilted with respect to a "flat earth surface" system there is need to rotate cs(a) into alignment with a common coordinate system for all arrays, or a range coordinate which has horizontal directions consistent with the earth's surface. Such a resultant system will be called cs(b) and, for convenience of terminology, the X arm of cs(a) is rotated to a position called *east*; the Y arm to a position called *north*, and the Z arm to a position called vertical or zenith. The origin is still at the c hydrophone.

The ray tracing methodology of Ref [5] attempts to locate the sound source in relation to a specific point termed the acoustic center. This center is the geometric center of the array cube. The resulting coordinate system is a translation of cs(a), and will be called cs(ac). In this system the four hydrophone positions are specified by D/2 times the vectors

$$\begin{pmatrix} 1 \\ -1 \\ -1 \end{pmatrix} \quad \begin{pmatrix} -1 \\ 1 \\ -1 \end{pmatrix} \quad \begin{pmatrix} -1 \\ -1 \\ 1 \end{pmatrix} \quad \begin{pmatrix} -1 \\ -1 \\ -1 \end{pmatrix} \qquad (B.1)$$

respectively, whereas in cs(a) these four vectors would be the three unit basis vectors and the origin. Conversion from cs(ac) to cs(a) is a direct translation.

The conversion of a point located in cs(a) to the cs(b) system requires a three-dimensional rotation based upon the tilt angles and the "ZROT" horizontal direction correction. It is convenient to describe this in terms of the three Euler angles ϕ_1, ϕ_2, ϕ_3, or roll, pitch and yaw. Letting

$$s_i = \text{sine}\,(\phi_i) \quad \text{and} \quad c_i = \text{cosine}\,(\phi_i) \qquad i = 1, 2, 3 \tag{B.2}$$

we define three successive rotations which, when applied sequentially to a point in cs(a), will in the end describe it in cs(b). First hold the X arm fixed and rotate the Y-Z plane through an angle ϕ_1; the matrix of this transform is

$$\rho_1 = \begin{bmatrix} 1 & 0 & 0 \\ 0 & c_1 & -s_1 \\ 0 & s_1 & c_1 \end{bmatrix}$$

Next hold the (current position of) Y-arm fixed and rotate the X-Z plane through an angle of ϕ_2; this transformation has matrix

$$\rho_2 = \begin{bmatrix} c_2 & 0 & -s_2 \\ 0 & 1 & 0 \\ s_2 & 0 & c_2 \end{bmatrix}$$

Finally hold the (current position of) Z-arm fixed and rotate the X-Y plane through an angle of ϕ_3; the transform is

$$\rho_3 = \begin{bmatrix} c_3 & -s_3 & 0 \\ s_3 & c_3 & 0 \\ 0 & 0 & 1 \end{bmatrix}$$

The successive applications of these three rotations is a unitary transformation, (i.e., its inverse is equal to its transpose),

$$B = \rho_3 \rho_2 \rho_1 \tag{B.3}$$

and if a is a three vector in cs(a), then b = Ba is the same vector referenced in cs(b).

The determination of the Euler angles is accomplished as follows. The submerged arrays have tilt indicators on the X and Y arms which, individually, measure the angles that these arms make with the horizontal. An accounting for these tilts must be made when the ray trace azimuth and elevation angles are converted to a horizontal based coordinate system. The technique currently in use takes the apparent position, X_0, and applies the transformation

$$\begin{Bmatrix} X(1) \\ X(2) \\ X(3) \end{Bmatrix} = \begin{Bmatrix} 1 & 0 & -\sin(XTILT) \\ 0 & 1 & -\sin(YTILT) \\ \sin(XTILT) & \sin(YTILT) & 1 \end{Bmatrix} \begin{Bmatrix} X_0(1) \\ X_0(2) \\ X_0(3) \end{Bmatrix} \tag{B.4}$$

so that the new apparent position, X, is referenced in a plane level with the earth. This transformation is an approximation which simply rotates the two arms to the horizontal as if they were separate unconnected arms and the rotation of one does not affect the rotation of the other. That is, the first two rows of the coefficient matrix are not orthogonal. The result is an approximation whose success depends upon the smallness of the tilt angles.

The exact way to accomplish this goal involves the direct replacement of the coefficient matrix with the product rotation $\rho_2\rho_1$:

$$\begin{Bmatrix} X(1) \\ X(2) \\ X(3) \end{Bmatrix} = \begin{Bmatrix} c_2 & -s_1 s_2 & -c_1 s_2 \\ 0 & c_1 & -s_1 \\ s_2 & s_1 c_2 & c_1 c_2 \end{Bmatrix} \begin{Bmatrix} X_0(1) \\ X_0(2) \\ X_0(3) \end{Bmatrix} \tag{B.5}$$

Upon comparing these two coefficient matrices, one sees there is choice in identifying the two tilt angles with these two Euler angles. We have chosen to match the first two elements of the third row:

$$s_2 = \sin(XTILT) \qquad s_1 = \sin(YTILT)/c_2. \tag{B.6}$$

The geometric interpretation is as follows. First hold the X arm fixed and rotate the plane of the Y-Z arms so that the Y arm is horizontal. This is not a vertical projection. The division by c_2 shows that one must rotate through an angle greater than YTILT in order to maintain orthogonality of the coordinate system when making the Y arm parallel to the earth's surface. This done, we next hold the Y arm fixed in its new position and rotate the plane of the X-Z arms so that the X arm is horizontal. Since the new Y arm is already horizontal this second rotation is a vertical projection through an angle of XTILT.

This latter method is exact. The nature of the original approximation can be assessed by comparing the two coefficient matrices, using numerical inputs. The effect is not great for most of the tilts present at Nanoose.

To complete the conversion of cs(a) to cs(b) we must find the third Euler angle in terms of ZROT, the rotatic of the horizontal plane determined by array survey. In [5], ZROT is defined as the angle from the horizontally projected X arm to the range center line (east). The comparison of this definition with that of ϕ_3 (see ρ_3) leads to

$$s_3 = -\sin(ZROT) \tag{B.7}$$

The subsequent application of ρ_3 to $\rho_2\rho_1$ will bring the point a into east-north orientation.

Finally the position location system prefers to specify an object's position in terms of east, north, and depth (positive) below the sea surface. This system is a left-handed one with origin on the sea surface directly above the acoustic center of the array.

Table B-1 contains the positions of the Nanoose arrays at the time of their most recent survey dates. These are the positions of the acoustic centers in the range coordinate system. It is both useful and instructive to use our coordinate system superstructure and locate the hydrophones of each array in the range coordinate system.

Let α be the 3-vector locating the acoustic center of an array in the range coordinate system, see Table B-1. Let a be the location of one of the phones in cs(a) and let f,

$$f = (D/2)\begin{pmatrix}1\\1\\1\end{pmatrix} \tag{B.8}$$

be the position of the acoustic center in cs(a). In the system cs(b) these vectors are Ba and Bf, and the location of the phone relative to the acoustic center is B(a-f). The position p of the phone in the range coordinate system is

$$p = \alpha + B(a-f) \tag{B.9}$$

Since the C-phone is the origin in cs(a), its range coordinate position is α – Bf. the result of this computation is in Table B-2.

TABLE B-1. NANOOSE ARRAY COORDINATES AND ORIENTATION ANGLES

(Distances in feet; angles in radians)

Survey	Date	X	Y	Z	XTILT	YTILT	ZROT
AR 0	6/20/85	12188.01	−131.52	−1295.33	0.002909	0.014835	−0.208183
AR 1	6/20/85	19463.16	−174.99	−1308.76	0.061523	−0.036070	1.362579
AR 2	7/12/85	26991.39	−109.83	−1323.25	0.000145	0.005236	2.670336
AR 3	1/7/88	34505.10	−80.76	−1323.32	0.027925	−0.011345	2.928139
AR 4	10/24/88	42005.19	−55.17	−1318.28	0.001164	−0.040288	−2.315877
AR 5	6/20/85	49497.00	−25.23	−1315.58	−0.000291	−0.004072	1.668535
AR 6	6/20/85	56972.28	−21.21	−1308.50	0.013817	0.041161	−0.703420
AR 7	7/30/85	64680.66	15.33	−1353.39	0.034907	0.022835	−0.574144
AR 8	11/16/88	71969.73	−29.28	−1300.89	−0.005963	−0.012217	−1.577341
AR 9	5/7/84	3.00	3.00	1.00	0.000000	0.000000	0.000000
AR 10	3/12/84	47100.00	−3600.00	−1300.00	0.000000	0.000000	0.000000
AR 11	7/18/85	23173.89	−6488.40	−1312.09	−0.004654	0.000436	2.784376
AR 12	6/20/85	30731.25	−6553.05	−1312.90	0.002036	0.001745	−3.042179
AR 13	6/20/85	38213.61	−6640.77	−1323.05	0.000291	0.006254	1.373522
AR 14	6/20/85	45647.07	−6513.18	−1324.78	0.001309	0.002327	−2.348044
AR 15	6/19/85	53249.43	−6354.60	−1316.66	0.003345	0.004509	0.581544
AR 16	9/13/85	60859.74	−6356.07	−1313.42	0.014835	0.036943	2.303276
AR 17	6/16/87	68217.93	−6524.10	−1313.43	0.008290	0.034761	2.158449
AR 54	2/2/88	38029.95	5401.98	−1212.69	0.007709	−0.003782	−1.056919
AR 55	6/20/85	45645.75	6369.66	−1188.12	0.027634	0.039415	−0.728553
AR 56	7/30/85	53180.13	6417.96	−1218.84	0.037525	0.048142	−1.392651
AR 57	7/30/85	60745.71	6419.40	−1088.24	0.006981	0.001891	−3.108606
AR 23	6/20/85	41605.14	−12150.18	−1268.23	−.002182	0.003200	−1.845214
AR 24	4/17/89	49572.00	−12966.00	−1300.00	−0.007272	0.055269	−1.343904
AR 25	10/24/88	56993.79	−12999.33	−1205.48	0.000291	−0.002182	−0.593726
AR 26	8/8/88	64442.94	−12971.04	−1255.35	−0.014835	−0.012654	3.134192
AR 27	7/15/80	22119.60	−15908.70	83.00	0.000000	0.000000	0.000000
AR 28	5/4/83	45000.00	1500.00	−1350.00	0.000000	0.000000	0.000000
AR 29	2/2/79	0.00	0.00	0.00	0.000000	0.000000	0.000000

TABLE B-2. LOCATIONS OF THE C-HYDROPHONES

AR	Date	XC	YC	ZC
0	6/20/85	12170.190	−143.316	−1310.105
1	6/20/85	19473.791	−192.189	−1325.075
2	7/12/85	27011.563	−103.354	−1338.287
3	1/7/88	34522.511	−69.103	−1338.681
4	10/24/88	42004.318	−33.398	−1332.413
5	6/20/85	49513.397	−38.633	−1330.630
6	6/20/85	56950.933	−23.551	−1323.123
7	7/30/85	64659.408	10.557	−1367.552
8	11/16/88	71954.918	−13.999	−1315.793
9	5/7/84	−12.000	−12.000	−14.000
10	3/12/84	47085.000	−3615.000	−1315.000
11	7/18/85	23193.258	−6479.598	−1327.004
12	6/20/85	30744.657	−6536.662	−1327.956
13	6/20/85	38225.375	−6658.513	−1337.943
14	6/20/85	45646.877	−6492.002	−1339.829
15	6/19/85	53245.085	−6375.441	−1331.552
16	9/13/85	60880.699	−6357.757	−1328.681
17	6/16/87	68238.605	−6528.792	−1328.448
54	2/2/88	38009.399	5407.725	−1227.510
55	6/20/85	45624.165	6367.887	−1202.470
56	7/30/85	53162.159	6429.360	−1233.742
57	7/30/85	60760.102	6434.858	−1103.370
23	3/20/85	41594.799	−12131.725	−1283.312
24	4/17/89	49554.120	−12955.612	−1315.728
25	10/24/88	56972.961	−13003.338	−1220.483
26	9/8/88	64458.271	−12955.966	−1269.935
27	7/15/80	22108.374	−15890.700	68.000
28	5/4/83	44985.000	1485.000	−1365.000
29	2/2/79	−15.000	−15.000	−15.000

APPENDIX C

2. RAY FITTING AND RAY TRACING

A "ping" sound source produces a wave front that travels through the water and is detectable by the receiving transducers. A ray is the path generated by the normal to the wave front. Ray tracing is the activity of following a ray from a receiver for a fixed amount of time in order to locate the sound source. Ray fitting is the activity of recreating the ray path from the positions of the source and the receiving sensor. The latter is needed to study the error performance of the former.

The speed of sound in water is assumed to vary with depth, but remain homogeneous in the horizontal. Thus a single depth-velocity profile is valid throughout the field.

We begin with some preliminaries followed by the development of a ray fitting algorithm, which may be viewed as an inverse to ray tracing. It is certainly more difficult. All paths are direct paths. That is, no provision is made for reflections or refractions that produce non monotone rays connecting source and receiver. Also our interest lies in the greater ranges and no adjustments are presented for sources that are directly above the receiver.

The notation is chosen to be consistent with that used in the Fortran source codes. We are given a speed-depth profile in the form of pairs lm_i and vel_i.

lm_i = depth of ith water layer, positive down.
vel_i = speed of sound at the depth lm_i.

Digression. The water speed processing system at NUWES produces average velocity values for a large number of equally spaced points. These averages are intended to serve as constant values for the entire layer, eq. (3.1). Thus the information is provided in the form, for i = 1, ..., m

l_i = depth of water layer boundary
vel_i = velocity constant for layer (l_i, l_{i+1})

The values used for lm_i above are the layer midpoints:

$lm_i = .5 \times (l_i + l_{i+1})$ for $i=1, ..., m-1$

The algorithms developed below do not require layers of equal thickness. Thus they can accommodate the user who wants to use thin layers at depths of rapid change and thick layers at depths of slow changes. All computations should be in double precision arithmetic.

Occasionally as application leads to a receiver whose depth is greater than the largest $\{lm_i\}$. For these cases we have been using an extrapolation of the sound speed profile that adjoins a sufficient number of layers, all of the same thickness as the deepest of the original layers. The corresponding velocities are extrapolated using a second order polynomial calculated from a fixed second difference whose value is the average of the four deepest second differences. (Use of the coefficient of the quadratic term in a least square fit has also been employed as an option.)

Since ray fitting is a rather delicate operation we use the isogradient technique. I.e., straight lines are fitted to the speed for each layer; the constant gradient of slope is computed; the profile itself is then a continuous function of connected straight line segments. See Figure 2. I.e., if

$$lm_i \le z \le lm_{i+1}$$

then

$$vel(z) = v_0(i) + v_1(i)z$$

where

$$v_0(i) = lm_{i+1} \cdot vel_i - lm_i \cdot vel_{i+1}$$

$$v_1(i) = (vel_{i+1} - vel_i)/dz_i$$

$$dz_i = lm_{i+1} - lm_i$$

Typically the values of $\{v_0(i)\}$ are positive and large compared to the $\{v_1(i)\}$ which are small and of either sign or zero. Snell's law comes into play and the ray invariant will be denoted rv. The ray path in each layer will be a circle arc ($v_1(i) \neq 0$) or a straight line ($v_1(i) = 0$).

Now we are positioned to describe our ray fitting algorithm. It is two dimensional (horizontal, vertical) and given the endpoints

(a_1, a_2) receiver
(p_1, p_2) sound source

the goal is to compute

θ_0 entrance angle at the receiver
θ_1 exit angle at the sound source
t transit time of sound from source to receiver

There is no loss in placing the origin on the water surface directly over the receiver. Thus, $a_1 = 0$ and $p_2 < a_2$ (depth of receiver).

The algorithm is an iterative one that operates as follows. Initialize the entrance angle θ_0. Use this angle to ray trace upward through the layers until the vertical value of p_2 is achieved. Compute the current horizontal value h,

and compare it with p_1. If this is within a preassigned small number, ε, stop

Figure C-1. Details of single layer processing

$v(z) = v_0 + v_1 z$ (linear profile) $z_1 < z < z_0$

Given: $\theta_0, z_0, z_1, v_0, v_1$, and

the ray invariant $rv = \dfrac{\cos(\theta_0)}{v(z_0)}$

Case $v_1 = 0$

$$dz = z_1 - z_0$$

$$dw = dz/\sin(\theta_0)$$

$$h_1 = h_0 + dw \cdot \cos(\theta_0)$$

$$dt = dw/v_0$$

$$\cos(\theta_1) = rv \cdot v(z_1)$$

Case $v_1 \neq 0$

$$q_2 = -v_0/v_1$$

$$s = \sin(\theta_0)$$

$$c = \cos(\theta_0)$$

$$q_1 = h_0 + (q_2 - z_0)s/c$$

$$r = \mathrm{signum}(q_2)(q_2 - z_0)/c$$

$$h = q_1 - \mathrm{signum}(q_2)\, r \cdot \sin(\theta)$$

$$dt = \frac{1}{v_1}\int_{\theta_0}^{\theta_1} \frac{d\theta}{\cos(\theta)}$$

$$= \frac{1}{v_1}\ln\left(\frac{1+\sin(\theta)}{\cos(\theta)}\right)\Big/_{\theta_0}^{\theta_1}$$

$$\cos(\theta_1) = rv \cdot v(z_1)$$

and compute the transit time. Otherwise, adjust the entrance angle θ_0 according to the ratio of the current rise over run, $\frac{h}{a_2 - p_2}$, to the desired one, $\frac{p_1}{a_2 - p_2}$, and repeat the algorithm using the new initialization.

ALGORITHM RAYFIT

Initialize

(i) Determine the layers that contain the source and receiver. Choose j, n so that

$$lm_j \leq p_2 < lm_{j+1}$$

$$lm_n \leq a_2 < lm_{n+1}$$

(ii) Make thickness corrections for the extreme layers

$$dz_j = lm_{j+1} - p_2$$

$$dz_n = a_2 - lm_n$$

(iii) Compute the sound speed at depths a_2, p_2

$$va_2 = v_0(n) + v_1(n) \cdot a_2$$

$$vp_2 = v_0(j) + v_1(j) \cdot p_2$$

(iv) Unless a "previous" value for θ_0 is available, fit a straight line through the depth-velocity profile in the range (p_2, a_2) and use θ_0 corresponding to the circle arc (or line) of that approximate profile. I.e.,

If $va_2 = vp_2$ then $\theta_0 = \tan^{-1}((a_2 = p_2)/p_1)$, else

$$q_2 = \frac{va_2 \cdot p_2 - vp_2 \cdot a_2}{(a_2 - p_2)}$$

$$q_1 = .5 \cdot p_1 + .5 \cdot (p_2 - a_2)(p_2 + a_2 - 2q_2)/p_1$$

$$\theta_0 = \tan^{-1}\{q_1/(q_2-a_2)\}$$

endif

Set initial values for iteration

A. $i = n,$ $s = \sin(\theta_0),$ $c = \sqrt{1-s^2}$

$rv = c/va_2,$ $h = 0,$ $z = a_2$

Main raytracing code

B. If $v_1(i) = 0$, then

$dw = dz_i/s$

$h = h + c \cdot dw$

else

$q_2 = -v_0(i)/v_1(i)$

$q_1 = h + (q_2 - z) \cdot s/c$

$r = \sqrt{(h-q_1)^2 + (z-q_2)^2}$

$c = rv \cdot vel(i)$

$s = \sqrt{1-c^2}$

$h = q_1 - \mathrm{signum}(q_2) \cdot r \cdot s$

endif

If $i = j$, goto TEST

$z = lm_i$

$i = i-1$

goto B

TEST: $\theta_1 = \cos^{-1}(rv \cdot vp_2)$

If $v_1(j) \neq 0$ $h=q_1-\mathrm{signum}(q_2) \cdot r \cdot \sin(\theta_1)$

If $|h-p_2| < \epsilon$, goto FINI

Re-estimate θ_0

$\theta_o = \tan^{-1}\{\tan(\theta_0) \cdot h/p_1\}$

goto A

FINI:

$ang(j) = \theta_i$

$ang_{n+1} = \theta_0$

$ang_i = \cos^{-1}(rv \cdot vel(i))$ for $i = j+1, \ldots, n$

Compute transit time

$t = 0$

Do TC $i = j, n$

If $v_1(i) = 0$

$t = t + dz_i/(v_0(i) \cdot \sin(ang_i))$

else

$$t = \frac{1}{v_1(i)} \ln\left\{\frac{\cos(ang_{i+1})(1+\sin(ang_i))}{(1+\sin(ang_{i+1}))\cos(ang_i)}\right\}$$

endif

TC continue

Remove extreme layer thickness corrections

$dz_i = lm_{j+1} - lm_j$

$dz_n = lm_{n+1} - lm_n$

end

This algorithm has been quite useful to us. Using $\epsilon = 10^{-6}$ we typically have 8 to 10 iterations through A.

Raytracing algorithms are less sensitive, but since a good one is readily available by merely modifying the above, let us do that. The process is an inverse one in that the goal is to compute p_1, p_2 given θ_0 and t_0, where t_0 is the transit time.

ISOGRAD

Initialize by locating the layer containing the receiver, establishing the ray invariant, etc.

Choose n so that $lm_n \leq a_2 < lm_{n+1}$

$i = n,$ $h = 0,$ $z = a_2,$ $t = 0$

$s = \sin(\theta_0),$ $c = \cos(\theta_0)$

$va_2 = v_0(i) + v_1(i) \cdot a_2$

$rv = c/va_2$

$dz_n = a_2 - lm_n$

AA: If $v_1(i) = 0$, then

$dw = dz_i/s$

$dt = dw/v_0(i)$

$h = h + c \cdot dw$

else

$q_2 = -v_0(i)/v_1(i)$

$q_1 = h + (q_2 - z) \cdot s/c$

$r = \sqrt{(h-q_1)^2 + (z-q_2)^2}$

$cp = rv/v_1(i)$

$sp = \sqrt{1-cp^2}$

$$dt = \frac{1}{v_1(i)} \ln \left\{\frac{c}{1+s} \frac{1+sp}{cp}\right\}$$

$h = q_1 - \text{signum}(q_2)\, sp$

endif

$t = t + dt$

If $t \geq t_0$ goto FINAL

$z = lm_i$

$s = sp$ $c=cp$ $i = i-1$ goto AA

FINAL

$dt = t_0 + dt - t$

If $v_1(i) = 0$

$dz_i = v_0(i) \cdot dt$

$dw = dz_i/sp$

$p_1 = h + dw \cdot cs$

$p_2 = z - dz_i$

else

$x = \exp[dt \cdot v_1(i)](1+s)/c$

$cp = 2 \cdot x/(1+x^2)$

$sp = \sqrt{1-cp^2}$

$p_1 = q_1 + r \cdot sp$

$p_2 = q_2 + r \cdot cp$

endif

Restore layer integrity

$$dz_i = lm_{i+1} - lm_i$$
$$dz_n = lm_{n+1} - lm_n$$

Compute exit angle

$$\theta_1 = \cos^{-1}(cp)$$

APPENDIX D. EFFECT OF SOUND SPEED OSCILLATION WITHIN A LAYER OF WATER

Suppose a water layer of thickness Δ_z has an average sound speed of υ feet per second. Suppose further that the speed profile within the layer is an oscillation of frequency K and amplitude δ. We address the question of how this profile can affect the nominal calculation of the ray's horizontal distance and transit time through the layer.

The question is most easily treated using isospeed ray tracing and modeling the oscillations as follows: Partition the layer into 2K equithick sublayers and assume the sound speed alternates between the values $\upsilon+\delta$ and $\upsilon-\delta$ as we move through these layers. Let θ_1 be the elevation angle for the $\upsilon+\delta$ speed layers and θ_2 for the $\upsilon-\delta$ layers.

According to isospeed ray tracing formulation, the horizontal distance advanced in the layer is

$$H = \frac{\Delta_z}{2K}\sum_{j=1}^{2K}\cot\left(\theta_j\right) = \frac{\Delta_z}{2}\left[\cot(\theta_1)+\cot(\theta_2)\right]$$

and the transit time

$$\begin{aligned} T &= \frac{\Delta_z}{2K}\sum_{1}^{2K}\frac{1}{\upsilon_j \sin\left(\theta_j\right)} \\ &= \frac{\Delta_z}{2}\left[\frac{1}{(\upsilon+\delta)\sin(\theta_1)}+\frac{1}{(\upsilon-\delta)\sin(\theta_2)}\right] \end{aligned}$$

The nominal values are found by using υ as the speed and θ_1 as the angle throughout the layer. Thus the error in these two values is

$$\Delta H = \frac{\Delta_z}{2}\left[\cot(\theta_2) - \cot(\theta_1)\right],$$

$$\Delta T = \frac{\Delta_z}{2}\left[\frac{1}{(\upsilon+\delta)\sin(\theta_1)} + \frac{1}{(\upsilon-\delta)\sin(\theta_2)} - \frac{2}{\upsilon\sin(\theta_1)}\right],$$

and θ_1 and θ_2 are related by the ray invariant equation

$$\frac{\cos(\theta_1)}{\upsilon+\delta} = \frac{\cos(\theta_2)}{\upsilon-\delta}$$

The error ΔH is affected by velocity only through this equation. Notice that the errors do not depend upon the frequency K. Using δ/υ as the proportion of the speed appearing in the amplitude, we can rewrite

$$\begin{aligned}
\Delta T &= \frac{\Delta_z}{2\upsilon}\left[\frac{1}{(1+\delta/\upsilon)\sin(\theta_1)} + \frac{1}{(1-\delta/\upsilon)\sin(\theta_2)} - \frac{2}{\sin(\theta_1)}\right] \\
&\doteq \frac{\Delta_z}{2\upsilon}\left[\frac{1-\delta/\upsilon}{\sin(\theta_1)} + \frac{1+\delta/\upsilon}{\sin(\theta_2)} - \frac{2}{\sin(\theta_1)}\right] \\
&= \frac{\Delta_z}{2\upsilon}\left[\left(\frac{1}{\sin(\theta_2)} + \frac{1}{\sin(\theta_1)}\right)(1+\delta/\upsilon)\right]
\end{aligned}$$

since the proportion δ/υ is believed small.

Some speculative calculations appear in Table (D-1) for Δ_z = 5 feet and υ = 4800 feet/second.

The calculation is not very sensitive to values of υ, but quite responsive to the elevation angle. It should be noted that the signs of ΔH, ΔT change if the modeled oscillations are in reverse order. This is equivalent to replacing with $-\delta$.

This author is not qualified to judge the reality of the suggested values of δ/υ. Certainly the question deserves more attention. It is common to process

some 200 of these 5 foot layers in a ray computation. The error buildup, even if the signs change randomly, could be significant, perhaps 15 times ΔH.

TABLE D-1. EFFECT OF OSCILLATION
(υ = 4800 feet/second; Δ_z = 5 feet)

δ/υ	θ_1	ΔH	ΔT
.0001	0.1	0.48	–.0001006
	0.15	0.15	–.0000301
	0.2	0.06	–.0000127
	0.3	0.02	–.0000037
	0.4	0.01	–.0000015
.0005	0.1	2.18	–.0004517
	0.15	0.70	–.0001432
	0.2	0.30	–.0000615
	0.3	0.009	–.0000181
	0.4	0.04	–.0000074
.001	0.1	3.87	–.0008032
	0.15	1.31	–.0002699
	0.2	0.58	–.0001189
	0.3	0.18	–.0000357
	0.4	0.08	–.0000147

The support for this calculation proceeds as follows: Suppose X is a random variable uniformly distributed on the interval $(-\Delta H, \Delta H)$. Then the mean of X is zero and the variance is $(\Delta H)^2/3$. If there are n layers to be processed then the error in determining the horizontal distance is the sum of N independent and identical such X's. It will have mean zero and standard deviation $\Delta H\sqrt{n/3}$; zero plus or minus two standard deviations could be a significant amount, especially for small elevation angles.

APPENDIX E. CONVERSION OF FOUR TRANSIT TIMES TO INPUTS FOR THE RAY TRACING ALGORITHM

The method in current use for converting the four transit times (t_1, ..., t_4) into an azimuth angle, ϕ_c, an elevation angle, θ_c and t_{ac} an estimated transit time from the source to the acoustic center is outlined and critiqued below.

The two angles ϕ_c and θ_c are generated from a description that assumes a constant value υ for the speed of sound for all points in the array. Then the concept of an "apparent position," (X,Y,Z) relative to the acoustic center for the sources in a constant speed median is utilized for purposes of estimating the two angles. The apparent position must satisfy the system of equations

$$\begin{aligned}
(X+D/2)^2+(Y-D/2)^2+(Z-D/2)^2 &= \upsilon^2 t_1^2 \\
(X-D/2)^2+(Y+D/2)^2+(Z-D/2)^2 &= \upsilon^2 t_2^2 \\
(X-D/2)^2+(Y-D/2)^2+(Z+D/2)^2 &= \upsilon^2 t_3^2 \\
(X-D/2)^2+(Y-D/2)^2+(Z-D/2)^2 &= \upsilon^2 t_4^2
\end{aligned} \qquad (E.1)$$

This is a system of four equations in three unknowns. Unless the values of t_1, ..., t_4 are singularly coherent, there are an infinity of solutions for X, Y, Z.

The current policy is to obtain a unique solution by subtracting the fourth equation successively from each of the other three, leaving a three by three system remaining. I.e.,

$$\begin{aligned}
2XD &= \upsilon^2\left(t_1^2 - t_4^2\right) \\
2YD &= \upsilon^2\left(t_2^2 - t_4^2\right) \\
2ZD &= \upsilon^2\left(t_3^2 - t_4^2\right)
\end{aligned} \qquad (E.2)$$

and a unique solution. Other rationales supporting this approach can be found in [5].

At this point an adjustment is made under the name of a direction cosine correction (DCC). The quantity D/2 is added to each component of the apparent position (in effect making the position relative to the C–phone) and the length of the new vector is computed and divided by υt_4. Call this

$$DCC = \sqrt{(X+D/2)^2+(Y+D/2)^2+(Z+D/2)^2} \;/\; \upsilon t_4 \tag{E.3}$$

The translated values are normalized by DCC prior to returning the origin to the acoustic center:

$$\begin{aligned} X_c &= \frac{X+D/2}{DCC} - D/2 \\ Y_c &= \frac{Y+D/2}{DCC} - D/2 \\ Y_c &= \frac{Y+D/2}{DCC} - D/2 \end{aligned} \tag{E.4}$$

Next come the tilt corrections, required because the corrected apparent position is in the coordinate system cs(ac), see Appendix B. This is accomplished by applying the approximation of eq. (B.4), i.e., that coefficient matrix (instead of the exact one (B.5)) to the vector (X_c, Y_c, Z_c): The Z rotation can also be applied at this point, i.e., multiplying by ρ_3. Let us call the result of all this (X,Y,Z) and form the functions

$$\begin{aligned} \sin(\theta_c) &= Z / \sqrt{X^2+Y^2+Z^2} \\ \sin(\phi_c) &= Y / \sqrt{X^2+Y^2} \\ \cos(\phi_c) &= X / \sqrt{X^2+Y^2} \end{aligned} \tag{E.5}$$

and, from these, the angles θ_c and ϕ_c can be found.

Finally, there is need to construct a transit time to the acoustic center because it is not measured. Calling the values t_{ac}, the proportionality adjustment with t_4 is used.

$$t_{ac} = t_4\sqrt{X^2+Y^2+Z^2} / \sqrt{(X+D/2)^2+(Y+D/2)^2+(Z+D/2)^2} \qquad (E.6)$$

APPENDIX F. ALTERNATIVE INITIALIZATION OF RAY TRACING

Current methodology utilizes the four measured ray transit times (t_1, t_2, t_3, t_4) from source to the X, Y Z, C hydrophones (respectively), and converts them to ϕ_c, θ_c, and t_{ac}, the azimuth and elevation angles and an estimated transit time from source to the acoustic center. It is seen in Section 5 that there can be considerable error in this, especially for ϕ_c. Our alternative is to shift the acoustic center to the C–phone and to ignore t_3. The resulting angles will have much smaller error, and the transit time t_4 is used directly.

We proceed to develop the ray azimuth (spherical coordinate longitude) and elevation (spherical coordinate latitude) angles from times t_1, t_2, t_4, in the range coordinate system. (See Appendix B for a general discussion of coordinate systems.) The conversion of those times is influenced by the array orientation.

Let s_i,c_i be the sine and cosine of the i^{th} Euler angle in the orientation of the 3–D sensor array j; i = 1, 2, 3. The conversion of XTILT, YTILT, and ZROT into Euler angles is explained in Appendix B, together with methodology for locating the positions of the phones at the ends of the array arms.

Having moved the acoustic center to the C–phone, we are using the coordinate system cs(a). Letting B_j represent the j^{th} column of the matrix B, eq. (B.3), the locations of the X,Y,Z phones are, respectively,

$$D \cdot B_1 \qquad D \cdot B_2 \qquad D \cdot B_3$$

and, of course, the C–phone is at the origin. These locations in the range coordinate system can be found by adding the location of the C–phone as indicated in Table B–2.

Typically there is very little difference in the depths (3^{rd} component) of the X,Y, and C–phones. Hence there is small variability if the speed of sound at these three depths and the use of a constant common value, say υ, is more tenable than the previous use.

Again we adopt the concept of an apparent position (X,Y,Z) of the sound source and the first two direction cosines can be found by applying the law of cosines (see the figure) for j = 1, 2.

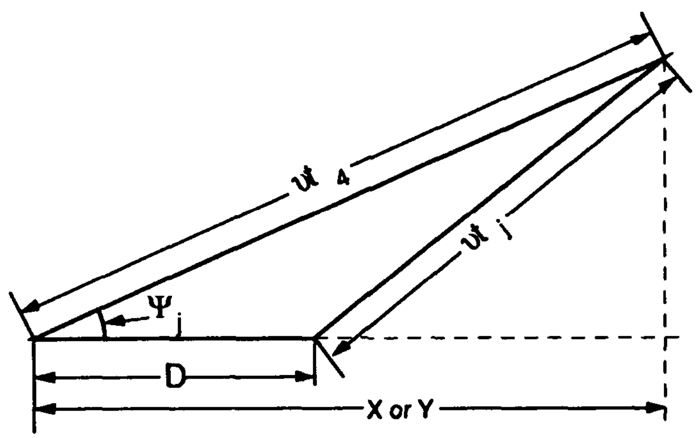

where t_1, t_2, t_4 are the signal transit times to the X, Y and C phones, respectively.

For j = 1, the cosine of the marked angle is $X/\upsilon t_4$ and by the law of cosines

$$(v \cdot t_1)^2 = D^2 + (\upsilon t_4)^2 - 2D \cdot t_4 \cos(\Psi_1)$$

It follows that

$$X = \frac{D}{2} + (\upsilon \cdot t_4 - \upsilon \cdot t_1)(\upsilon \cdot t_4 + \upsilon \cdot t_1)/(2D)$$

and a like equation for j = 2, leading to

$$Y = D/2 + (\upsilon t_4 - \upsilon t_2)\,(\upsilon t_4 + \upsilon t_2) \,/\, 2D.$$

The third direction cosine is obtained from

$$\cos(\Psi_3) = \sqrt{1 - \cos^2(\Psi_1) - \cos^2(Y_2)} = \sqrt{1 - (X^2 + Y^2) \,/\, \upsilon^2 t_4^2}$$

Next we rotate these values into alignment with the test range coordinate system, i.e., apply the matrix B, eq. (B.3)

$$\begin{bmatrix} X_c \\ Y_c \\ Z_c \end{bmatrix} = B \begin{bmatrix} X \\ Y \\ Z \end{bmatrix} \qquad (F.1)$$

The proposed ray elevation (θ) and azimuth (ϕ_p) angles can be found from

$$\cos\left(\theta_p\right) = Z_c \,/\, \sqrt{X_c^2 + Y_c^2 + Z_c^2} \qquad (F.2)$$

and

$$\begin{aligned} \sin\left(\phi_p\right) &= Y_c \,/\, \sqrt{X_c^2 + Y_c^2} \\ \cos\left(\phi_p\right) &= X_c \,/\, \sqrt{X_c^2 + Y_c^2} \end{aligned} \qquad (F.3)$$

Comment. This technique was designed to treat the speculated shortcomings of the procedure currently in use. The results are quite successful, especially in reducing azimuth error. It has the curious property of not using information provided by the Z-phone. It seems wasteful not to use this information. Yet any system that does use it must be required to perform at least as well as this one.

Appendix G.

```
      SUBROUTINE ERRCUR(H1,Z1,K,A2,XTILT,YTILT,ZROT,D,L,VEL,M,
     * THR,THC,THER,PHR,PHC,PHER,HC,HER,ZC,ZER,TEE,TIMER)
C****************************************************************
C                                                        08/10/90
C    COMPUTES THE TRUE ELEVATION ANGLES AND THE ESTIMATED ELEVATION
C  ANGLES FOR K SOUND SOURCE DISTRIBUTED EQUALLY ON A CIRCLE OF RADIUS
C  H1 AT DEPTH Z1 FOR A RECIEVING ARRAY AT DEPTH A2 BUT OTHERWISE AT THE
C  CENTER OF THE CIRCLE. THE ACCOUSTIC CENTER IS THE GEOMETRIC CENTER OF
C  THE ARRAY CUBE. THE CURRENTLY USED METHODOLOGY IS APPLIED.
C
C****************************************************************
C
C  INPUTS:
C     H1:     RADIUS OF CIRCLE IN FEET
C     Z1:     DEPTH OF SOUND SOURCE IN FEET
C     K:      NUMBER OF SOURCES ON THE CIRCLE
C     A2:     DEPTH OF THE C-HYDROPHONE
C     XTILT,YTILT,ZROT:  ORIENTATION INFORMATION ABOUT THE
C             SENSING  ARRAY  (RADIANS)
C     D:      LENGTH OF ARRAY EDGES.
C     L:      DEPTH OF LAYER BOUNDARIES.
C     M:      NUMBER OF RECORDS IN THE VELOCITY DEPTH PROFILE.
C     VEL:    AVERAGE SPEED OF SOUND IN THE LAYERS.
C
C  OUTPUTS:
C     THR:    ACTUAL ELEVATION ANGLE (THETA)
C     THC:    THETA ESTIMATES AT ACCOUSTIC CENTER, CURRENT METHOD
C     THER:   THETA ERROR AT THE ACCOUSTIC CENTER, CURRENT METHOD
C     PHR:    ACTUAL AZIMUTH ANGLE (PHI).
C     PHC:    PHI ESTIMATES AT ACCOUSTIC CENTER, CURRENT METHOD.
C     PHER:   PHI ERROR AT ACCOUSTIC CENTER.
C     HC:     HORIZONTAL ESTIMATE, CURRENT METHOD.
C     HER:    HORIZONTAL ERROR.
C     ZC:     VERTICAL ESTIMATE, CURRENT METHOD.
C     ZER:    VERTICAL ERROR.
C     T:      TRANSIT TIME TO ACCOUSTIC CENTER.
C     TIMC:   ESTIMATE OF TIME TO ACCOUSTIC CENTER, CURRENT METHOD.
C     TIMER:  TRANSIT TIME ERROR.
C****************************************************************

      DIMENSION B(5,3),DZ(300),THER(30),HD(5),HC(30),ZC(30)
      DIMENSION L(300),LM(300),LL(300),PX(30),PY(30),T(5),TEE(30)
      DIMENSION THC(30),THR(30),V0(300),V1(300),VEL(300),VV(300)
      DIMENSION HX(5),HY(5),HER(30),ZER(30),TIMER(30)
      DIMENSION X0(3),PHC(30),PHR(30),PHER(30),TIMC(30)

      REAL*8 A1,A2,A2M,ANG,B,C1,C2,C3,D,DP,DW,DZ,THER,CG
      REAL*8 H,H0,H1,HD,L,LM,LL,LPZ,PIE,P1,P2,PX,PY,S1,S2,S3
      REAL*8 T,T0,THEC,TH0,TH1,THC,THR,HC,ZC,HER,ZER
      REAL*8 V,V0,V1,VEL,VV,X,X0,XTILT,Y,YTILT,Z,Z0,Z1,ZROT
      REAL*8 CC1,CC2,VV1,VV0,HX,HY,SC,DCC,RAC,RC,TEE
      REAL*8 CAZ,SAZ,PHC,PHR,PHER,LH,C,T3P,TIMC,TIMER
      REAL*8 SR,SRER,LB,SV,SVU2,SVU,SU2,SU4,G1,G

      PIE = 3.14159265359D0
```

```
      IEST = 0
      M1 = M
C  DISTRIBUTE THE K SOURCES EQUALLY AROUND THE CIRCLE COUNTER
C  CLOCKWISE FROM THE EAST.
      DO 10 I = 1,K
         ANG = 2*PIE*(I-1)/K
         PX(I) = H1*DCOS(ANG)
         PY(I) = H1*DSIN(ANG)
         PHR(I) = ANG
         IF(ANG.GT.PIE) PHR(I) = ANG - 2*PIE
 10   CONTINUE
C  FORM SINES AND COSINES OF ALL THE EULER ANGLES:ROLL,PITCH,YAW
      S2 = DSIN(XTILT)
      C2 = DSQRT(1 - S2**2)
      S1 = DSIN(YTILT)/C2
      C1 = DSQRT(1 - S1**2)
      S3 = -DSIN(ZROT)
      C3 = DCOS(ZROT)
C  IN THE COORDINATE SYSTEM HAVING CENTER AT THE C-HYDROPHONE
C  AND POSITIVE-UPWARD, THE LOCATIONS OF THE FOUR HYDROPHONES
C  (RELATIVE TO THE ARM LENGTH D) ARE DEVELOPED NEXT.  THIS IS
C  THE TRANSPOSE OF THE MATRIX B IN APPENDIX B.
      B(1,1) = C2*C3
      B(1,2) = C2*S3
      B(1,3) = S2
      B(2,1) = -S1*S2*C3 - C1*S3
      B(2,2) = -S1*S2*S3 + C1*C3
      B(2,3) = S1*C2
      B(3,1) = -C1*S2*C3 + S1*S3
      B(3,2) = -C1*S2*S3 - S1*C3
      B(3,3) = C1*C2
C  LIKE NOTATION WILL BE USED TO LOCATE THE C-HYROPHONE AND THE
C  ACCOUSTIC CENTER (AC).
      DO 12 J = 1,3
         B(4,J) = 0.0D0
         B(5,J) = 0.5*(B(1,J) + B(2,J) + B(3,J))
 12   CONTINUE

      A1 = 0.0D0
      P2 = Z1
C  LOCATE THE HYDROPHONE HORIZONTAL COMPONENTS IN THE COORDINATE
C  SYSTEM CENTERED AT AC.
      DO 14 J = 1,5
         HX(J) = D*(B(J,1) - B(5,1))
         HY(J) = D*(B(J,2) - B(5,2))
 14   CONTINUE
C  DETERMINE THE DEPTHS OF THE FOUR HYDROPHONES AND THE AC.
      HD(1) = A2 + D*(B(5,3) - B(1,3))
      HD(2) = A2 + D*(B(5,3) - B(2,3))
      HD(3) = A2 + D*(B(5,3) - B(3,3))
      HD(4) = A2 + D*(B(5,3) - B(4,3))
      HD(5) = A2
```

```
C  FIND THE DEEPEST HYDROPHONE
      A2M = 0.D0
      DO 51 J=1,4
         IF(HD(J).GT.A2M) A2M = HD(J)
 51   CONTINUE

C  FORM THE SET OF LAYER MIDPOINTS.
      DO 105 I = 1,M-1
         LM(I) = .5*(L(I) + L(I+1))
 105  CONTINUE
      LM(M) = LM(M-1) + L(M) - L(M-1)

C   FORM DEPTH INCREMENTS, AND ALL SOUND VELOCITY SLOPE
C   INTERCEPTS.
      DO 110 I=1,M-1
         DZ(I)=LM(I+1)-LM(I)
         V0(I)=(LM(I+1)*VEL(I) - LM(I)*VEL(I+1))/DZ(I)
         V1(I)=(VEL(I+1)-VEL(I))/DZ(I)
 110  CONTINUE
C
      IF(A2M.LT.LM(M-2)) GOTO 126

C  IF A2M IS DEEPER THAN THE LAST LAYER MIDPOINT, THEN WE EXTRAPOLATE
C  THE SOUND VELOCITY PROFILE BY USING A QUADRATIC FUNCTION OVER THE
C  DEEPEST 100 FEET.

C  FIRST COUNT THE NUMBER OF LAYERS (OF THICKNESS DZ(M-2)) TO
C  BE ADJOINED.  ALSO MUST EXTEND THE L ARRAY.
      K0 = 2 + MAX(0,NINT((A2M-LM(M-1))/DZ(M-1)))
      MC = 21

C  FIND THE AVERAGE DEPTH FOR THE LAST 100 FEET
      LB = 0.0D0
      DO 200 J = M+1-MC,M
 200     LB = LB + LM(J)
      LB = LB/MC

C  FORM SUM OF POWERS AND PRODUCTS.
      SV = 0.0D0
      SVU2 = 0.0D0
      SVU = 0.0D0
      SU2 = 0.0D0
      SU4 = 0.0D0
      G1 = 0.0D0
      DO 210 J = M+1-MC,M
         U = LM(J) - LB
         SV = SV + VEL(J)
         SVU = SVU + U*VEL(J)
         SVU2 = SVU2 + U**2 * VEL(J)
         SU2 = SU2 + U**2
         SU4 = SU4 + U**4
         G1 = G1 + V1(J)
 210  CONTINUE

      G1 = G1/MC
      G = SVU/SU2
      GG = (MC*SVU2 - SU2*SV)/(SU4*MC - SU2**2)
```

```
      IF(GG.LT.0.0D0) GG = 0.0D0
      IF(V1(M-1).LT.0.0D0) V1(M-1) = G1

C  PERFORM THE EXTRAPOLATION.
      DO 125 I=M,M+K0
          V1(I) = V1(I-1) + GG*DZ(M-1)
          LM(I+1) = LM(!) + DZ(M-1)
          VEL(I+1) = VEL(I) + DZ(M-1)*V1(I)
          V0(I) = (LM(I+1)*VEL(I) - LM(I)*VEL(I+1))/DZ(M-1)
          L(I+1) = L(I) + DZ(M-1)
          DZ(I) = DZ(M-1)
 125  CONTINUE

C  UPDATE M, THE NUMBER OF LAYERS
      M = M+K0
 126  CONTINUE

C  THE OUTER LOOP WILL PERFORM COMPUTATIONS FOR THE K SOUND
C  SOURCES.

C  ADJUST DV TABLE TO 25 FT. INCREMENTS.
      CALL VELMOD(L,VEL,M1,LL,VV,MM)

C  RAYFITTING
C  THE INNER LOOP WILL FIT RAYS TO THE FOUR HYDROPHONES
C  AND THE AC IN THE ORDER X,Y,Z,C AND AC.
      DO 50 I = 1,K
      WRITE(*,*)' OUTER LOOP  I = ',I,' K = ',K
          DO 35 J = 1,5
              P1 = DSQRT((PX(I)-HX(J))**2 + (PY(I)-HY(J))**2)
              Z0 = HD(J)
              CALL RAYFIT1(A1,Z0,P1,P2,M,VEL,LM,DZ,V0,V1,T0,TH0,
     *        TH1,IEST)

C  COLLECT THE FIVE TRANSIT TIMES.
              T(J) = T0

C  IN THIS PROGRAM WE KEEP ONLY THE TRUE ELEVATION ANGLE AT AC.
              THR(I) = TH0
 35       CONTINUE
C  INNER LOOP COMPLETED.

C  LOCATE THE WATER LAYER, N, CONTAINING THE ARRAY.  USE THIS
C  TO DEVELOP THC, THE CURRENTLY USED ESTIMATE OF TH0.
          N = MM
          DO 37 J = 2,MM
              IF((LL(J-1).LE.A2).AND.(LL(J).GT.A2)) N = J-1
 37       CONTINUE
C
          V = VV(N)

C  USE THE FOUR TRANSIT TIMES TO PRODUCE ESTIMATES OF THE
C  ENTRANCE ANGLE. CALCULATE THE PRE-TILT CORRECTED APPARENT
C  POSITION AND INCLUDE THE DIRECTION COSINE CORRECTION.
          DO 40 J = 1,3
              X0(J)=((V*T(4)-V*T(J))*(V*T(4)+V*T(J)))/(2*D)
              X0(J) = 0.5*D + X0(J)
 40       CONTINUE
```

```
          SC = V*T(4)
          DCC = (DSQRT(X0(1)**2 + X0(2)**2 + X0(3)**2))/SC
          DO 41 J = 1,3
             X0(J) = (X0(J)/DCC) - 0.5*D
 41       CONTINUE

C  NEXT MAKE TILT CORRECTIONS
          X = X0(1) - X0(3)*DSIN(XTILT)
          Y = X0(2) - X0(3)*DSIN(YTILT)
          Z = X0(3) + X0(1)*DSIN(XTILT) + X0(2)*DSIN(YTILT)

          RAC = DSQRT(X**2 + Y**2 + Z**2)
          RC = DSQRT((X + D/2)**2 + (Y + D/2)**2 + (Z + D/2)**2)
          T0 = T(4)*RAC/RC
          TIMC(I) = T0

C  PERFORM Z ROTATION IN THE (X,Y) PLANE.
          X0(1) = C3*X - S3*Y
          X0(2) = S3*X + C3*Y

C  COMPUTE THEC: THE ESTIMATE OF THETA CURRENTLY IN USE.
          THEC = DASIN(Z/DSQRT(X**2 + Y**2 + Z**2))

C  COMPUTE SINES AND COSINES OF AZIMUTH.
          SAZ = X0(2)/DSQRT(X**2 + Y**2)
          CAZ = X0(1)/DSQRT(X**2 + Y**2)
          PHC(I) = DATAN2(SAZ,CAZ)
          PHER(I) = PHC(I) - PHR(I)
          IF(ABS(PHER(I)).GT.PIE) PHER(I) = PHC(I) + PHR(I)
          IFG = 0

C  RAYTRACE BY THE ISOSPEED METHOD.
          CALL ISOSPEED(A1,Z0,T0,THEC,LL,VV,MM,H,Z,TH1)

          HC(I) = H
          ZC(I) = Z

C  NOW FINISH THE OUTPUT.
          THC(I) = THEC

C  AND THE ERRORS
          TEE(I) = T(5)
          THER(I) = THC(I) - THR(I)
          TIMER(I) = TIMC(I) - T(5)
          HER(I) = HC(I) - H1
          ZER(I) = ZC(I) - Z1
          SR = DSQRT(H1**2 + (A2 - Z1)**2)
          SRER = DSQRT(HC(I)**2 + (A2 - Z1)**2) - SR
 50    CONTINUE
C  OUTER LOOP COMPLETED!

       RETURN

 100   FORMAT(3(5X,E13.6))
 120   FORMAT(3(5X,F15.12))
 130   FORMAT(3(F12.8,2X))
       END
```

```
C     *************************************************************
C  LIBRARY FILE: LIB12.FOR                                  2/22/90
C     *************************************************************
C     *************************************************************
      SUBROUTINE ISOGRAD1(A1,A2,T0,TH0,N,LM,VEL,V0,V1,DZ,H,Z,TH1)
C****************************************************************
C                                                           09/25/89
C     T0 :     TRANSIT TIME (SEC).
C     TH0 :    ELEVATION ANGLE AT SENSOR (RAD).
C     A1 :     HORIZONTAL COORDINATE OF SENSOR.
C     A2 :     VERTICAL COORDINATE OF SENSOR, POSITIVE DOWN.
C     V0,V1 : ARRAYS CONTAINING SOUND VELOCITY PARAMETERS.
C     LM :     ARRAY CONTAINING LAYER MIDPOINTS.
C     N :      INDEX OF DEEPEST LAYER USED.
C
C****************************************************************

      DIMENSION LM(300),V0(300),V1(300),DZ(300),VEL(300)
      REAL*8 T0,H,H0,Z,A1,A2,TH0,TH1,VEL
      REAL*8 LM,V0,V1,DZ,Q1,Q2
      REAL*8 VA2,R,VP2,TH,RV,DW,DT,X,T
      INTEGER N,IS

      I = N
      T = 0.0D0
      TH=TH0
      H0 = A1
      VA2=V0(I)+V1(I)*A2
      RV=DCOS(TH)/VA2
      Z = A2
      DZ(N) = Z - LM(N)
 50   IF(V1(I).EQ.0.0) THEN
          DW = DZ(I)/DSIN(TH)
          DT = DW/V0(I)
          H = H0 + DW*DCOS(TH)
          TH1 = TH
      ELSE
          Q2=-V0(I)/V1(I)
          IF (Q2) 51,52,53
 51       IS = -1
          GOTO 54
 52       IS = 0
          GOTO 54
 53       IS = 1
 54       CONTINUE
          Q1=H0 + (Q2-Z)*DTAN(TH)
          R=DSQRT((Q2-Z)**2 + (Q1-H0)**2)
          TH1=DACOS(RV*VEL(I))
          DT=DLOG((DCOS(TH)/(1+DSIN(TH)))*((1+DSIN(TH1))/
     *        DCOS(TH1)))/V1(I)
          H=Q1 - IS*R*DSIN(TH1)
      ENDIF
      T=T+DT
      IF (T.GE.T0) GOTO 60
      Z=LM(I)
      H0 = H
      TH=TH1
```

```
      I=I-1
      GOTO 50

 60   DT=T0+DT-T
      IF(V1(I).EQ.0.0) THEN
          DW = V0(I)*DT
          DZ(I) = DW*DSIN(TH1)
          H = H0 + DW*DCOS(TH1)
          Z = Z - DZ(I)
      ELSE
          X=(EXP(DT*V1(I)))*(1+DSIN(TH))/DCOS(TH)
          TH1=DACOS((2*X)/(1+X**2))
          H = Q1 - IS*R*DSIN(TH1)
          Z = Q2 - IS*R*DCOS(TH1)
      ENDIF

C  RESTORE THE END LAYERS.

      DZ(I) = LM(I+1) - LM(I)
      DZ(N) = LM(N+1) - LM(N)

      RETURN
      END
C*****************************************************************
C*****************************************************************


      SUBROUTINE ISOSPEED(A1,A2,T0,TH0,L,VEL,M,H,Z,TH1)
C*****************************************************************
C                                                        08/09/89
C    This is a 2-D ray tracing algorithm that mimics the one in
C  Proceedure 5181.  It utilizes the assumption that the speed
C  of sound in water is constant for the entire layer encompassed
C  by the layer boundaries.  A fixed ray invariant is used
C   throughout the entire migration.
C*****************************************************************
C  INPUTS:
C     A1,A2   - POSITION OF SENSOR (A2>0 DOWN)
C     T0      - TRANSIT TIME
C     TH0     - ELEVATION ANGLE (OF THE RAY AT THE SENSOR,
C                 ALSO CALLED THE ENTRANCE ANGLE)
C     L       - ARRAY CONTAINING LAYER BOUNDARIES
C     VEL     - ARRAY CONTAINING SOUND VELOCITY AT THE
C                 THE LAYER MIDPOINTS
C  OUTPUTS:
C     H,Z     - POSITION OF TARGET (SOUND SOURCE)
C     TH1     - ELEVATION ANGLE AT TARGET
C*****************************************************************
      DIMENSION L(300),VEL(300)
      REAL*8 A1,A2,C,S,T,DT,DW,TH,DZ,RV,TH1,Z,H,L,VEL,TH0,T0
      Z = A2
      H = A1
      T = 0.0

C  CHOOSE N SUCH THAT L(N) <= A2 < L(N+1).  IF A2 IS DEEPER
C  THAN LOWEST LAYER THEN N = M, THE INDEX OF THE DEEPEST LAYER
C  BOUNDARY
      N = M
```

```
      DO 5 I = 2,M
         IF ((L(I-1).LE.A2).AND.(L(I).GT.A2)) N = I - 1
  5   CONTINUE
      RV = DCOS(TH0)/VEL(N)
      J = N
      TH = TH0
      S = DSIN(TH0)
      C = DSQRT(1 - S**2)
 10   DZ = Z - L(J)

C  COMPUTE THE INCREMENTAL SLANT RANGE
      DW = DZ/S

C  COMPUTE THE INCREMENTAL TRAVEL TIME
      DT = DW/VEL(J)

C  ACCUMULATE TOTAL TRAVEL TIME AND TEST
      T = T + DT
      IF (T.GE.T0) GOTO 50

C  UPDATE THE HORIZONTAL AND VERTICAL ACCUMULATIONS
      H = H + DW*C
      Z = Z - DZ

C  USE SNELL'S LAW TO UPDATE THE LAYER ENTRANCE ANGLE AND
C  THE TRIG FUNCTIONS.
      J = J - 1
      C = RV * VEL(J)
      S = DSQRT(1 - C**2)
      GOTO 10

 50   T = T - DT
      DT = T0 - T
      DW = VEL(J)*DT
      DZ = DW*S
      H = H + DW*C
      Z = Z - DZ
      TH1 = DASIN(S)

      RETURN
      END
C*****************************************************************
C*****************************************************************


      SUBROUTINE RAYFIT1(A1,A2,P1,P2,M,VEL,LM,DZ,V0,V1,T0,TH0,
     *          TH1,IEST)
C  **************************************************************
C                          09/12/89
C  NEW SUBROUTINE TO REPLACE TGEN, RAYTRACING ALGORITHM.
C  **************************************************************
C  INPUTS:
C    A1,A2  - POSITION OF SENSOR (A2 > 0 DOWN)
C    P1,P2  - POSITION OF SOUND SOURCE ( P2 > 0 DOWN )
C    LM     - ARRAY CONTAINING LAYER MIDPOINTS
C    M      - NUMBER OF LAYER MIDPOINTS
C    VEL    - ARRAY CONTAINING SOUND VELOCITY AT THE
C               LAYER MIDPOINTS.
```

```
C     V0      - SPEED INTERCEPT VALUES
C     V1      - SPEED SLOPE VALUES
C     DZ      - DEPTH INCREMENTS
C     IEST  - FLAG FOR INITIALIZING THE ANGLE
C   OUTPUTS:
C     T0      - TRANSIT TIME
C     TH0     - ELEVATION ANGLE AT THE SENSOR
C     TH1     - ELEVATION ANGLE AT THE SOUND SOURCE
C     ***************************************************************

      DOUBLE PRECISION VEL(300),DZ(300),LM(300),V0(300)
      DOUBLE PRECISION V1(300),ANG(300),G(300)
      REAL*8 A1,A2,P1,P2,T0,TH0,TH1,EP,S,C
      REAL*8 H,H0,DW,VA2,VP2,GG,R,Z,TH,RV,Q1,Q2
      INTEGER M,IS

      EP = 1D-6

C   DETERMINE LAYERS INVOLVED IN RAY FITTING
      N = M
      J = M
      DO 30 I=1,M - 1
          IF ((LM(I).LE.A2).AND.(LM(I+1).GT.A2)) N=I
          IF ((LM(I).LE.P2).AND.(LM(I+1).GT.P2)) J=I
  30 CONTINUE

C   MAKE END CORRECTIONS FOR THE LAYERS
      DZ(N) = A2 - LM(N)
      DZ(J) = LM(J+1) - P2

C     COMPUTE SPEED OF SOUND AT A2 AND P2
      VA2 = V0(N) + V1(N)*A2
      VP2 = V0(J) + V1(J)*P2
      IF(IEST.NE.0) GOTO 50

C   INITIALIZE THE ELEVATION ANGLE AT THE SENSOR, TH0, BY
C   FITTING A STRAIGHT LINE SPEED PROFILE BETWEEN P2 AND A2.
      IF(VEL(N).EQ.VEL(J)) THEN
          TH0 = DATAN((A2-P2)/(P1-A1))
      ELSE
          Q2 = (VEL(N)*LM(J) - VEL(J)*LM(N)) / (VEL(N)-VEL(J))
          Q1 = 0.5*(P1+A1)+(0.5*(P2-A2)*(P2+A2-2*Q2))/(P1-A1)
          TH0 = DATAN((Q1-A1)/(Q2-A2))
      ENDIF

C   OUTER LOOP: SET UP RAY FITTING FOR TH0 = ELEVATION ANGLE
  50  S = DSIN(TH0)
      C = DSQRT(1.0 - S**2)
      I = N
      RV = C/VA2
      H0 = A1
      Z = A2

  60  IF(V1(I).EQ.0.0) THEN
          DW = DZ(I)/S
          H = H0 + DW*C
      ELSE
          Q2 = -V0(I)/V1(I)
```

```
          IF (Q2) 61,62,63
 61       IS = -1
          GOTO 64
 62       IS = 0
          GOTO 64
 63       IS = 1
 64       CONTINUE
          Q1 = H0 + (Q2-Z)*S/C
          R = DSQRT((Q2-Z)**2 + (Q1-H0)**2)
          C = RV*VEL(I)
          S = DSQRT(1.0-C**2)
          H = Q1 - IS*R*S
      ENDIF

      IF (I.EQ.J) GOTO 80
      H0 = H
      Z = LM(I)
      I = I - 1
      GOTO 60

 80   TH1 = DACOS(RV*VP2)

C  FRACTIONAL LAYER CORRECTION
      IF(V1(J).NE.0.0) H = Q1 - IS*R*DSIN(TH1)
      IF (ABS(H-P1).LT.EP) GOTO 90

C  RE-ESTIMATE TH0
      TH0 = DATAN(DTAN(TH0)*H/P1)
      GOTO 50

C  PREPARE FOR COMPUTATION OF TRANSIT TIME.
C  COLLECT EXIT AND ENTRANCE ANGLES.
 90   ANG(J) = TH1
      ANG(N+1) = TH0
      DO 95 I = J+1,N
          ANG(I) = DACOS(RV*VEL(I))
 95   CONTINUE

C  COMPUTE TRANSIT TIME
      T0 = 0.0D0
      DO 100 I = J,N
          IF(V1(I).EQ.0.0) THEN
              T0 = T0 + DZ(I)/(V0(I)*DSIN(ANG(I)))
          ELSE
              T0=T0 + DLOG((DCOS(ANG(I+1))*(1+DSIN(ANG(I))))/
     *          ((1+DSIN(ANG(I+1)))*DCOS(ANG(I))))/V1(I)
          ENDIF
 100  CONTINUE

C  REMOVE THE END CORRECTIONS.
      DZ(J) = LM(J+1) - LM(J)
      DZ(N) = LM(N+1) - LM(N)
      IEST = 1

      RETURN
      END
C*****************************************************************
C*****************************************************************
```

```
      SUBROUTINE VELMOD(L,VEL,M,LL,VV,MM)
C*********************************************************************
C                               02/22/90
C  THIS PROGRAM TAKES THE VELOCITY SOUND PROFILE GIVEN IN FIVE (5)
C  FOOT INCREMENTS AND CONVERTS IT INTO TWENTYFIVE (25) FOOT INCREMENT
C  PROFILE.
C*********************************************************************
C
C  INPUT:
C     L:     DEPTH IN 5 FT INCREMENTS
C     VEL:   SOUND VELOCITY IN 5 FT. INCREMENTS
C     M:     NUMBER OF ELEMENTS IN DEPTH ARRAY
C  OUTPUT
C     LL:    DEPTH IN 25 FT INCREMENTS
C     VV:    SOUND VELOCITY IN 25 FT INCREMENTS
C     MM:    NUMBER OF ELEMENTS IN DEPTH ARRAY
C*********************************************************************

      DIMENSION L(300),LL(300),VEL(300),VV(300)
      REAL*8 L,LL,VEL,VV,VS

      MM = INT(M/5)
      MREM = M - 5*MM
      VS = 0.0D0
      DO 10 J = 1,MM
          LL(J) = L(5*J-4)
          VV(J) = 0.2*(VEL(5*J-4) + VEL(5*J-3) + VEL(5*J-2) +
     *         VEL(5*J-1) + VEL(5*J))
 10   CONTINUE
      DO 20 J = 1,MREM
          VS = VS + VEL(M+1-J)
 20   CONTINUE
      LL(MM+1) = L(5*MM + 1)
      VV(MM+1) = VS/MREM
      RETURN
      END


      SUBROUTINE ERRPROP(H1,Z1,K,A2,XTILT,YTILT,ZROT,D,L,VEL,M,
     *  THR,THCER,TH1ER,PHR,PHER,PH1ER,H2ER,Z2ER,T4)
C****************************************************************
C                                                        08/22/90
C    POSITION ERROR ANALYSIS WHEN THE ORIGIN IS OVER THE C-HYDROPHONE
C  AND THE PROPOSED SYSTEM IS APPLIED. COMPUTES THE TRUE ELEVATION
C  ANGLES AND ESTIMATED ELEVATION ANGLES FOR K SOUND SOURCES
C  DISTRIBUTED EQUALLY ON A CIRCLE OF RADIUS H1 AT DEPTH Z1 FOR A
C  RECIEVING ARRAY AT DEPTH A2 BUT OTHERWISE AT THE CENTER OF THE
C  CIRCLE.  A2 IS DEPTH OF THE GEOMETRIC CENTER OF THE ARRAY CUBE.  THE
C  ACCOUSTIC CENTER IS THE C-HYDROPHONE.  BECAUSE OF DIRECT
C  MEASUREMENT THERE IS NO TRANSIT TIME ERROR.
C
C****************************************************************
C
C  INPUTS:
C     H1:     RADIUS OF CIRCLE IN FEET
```

```
C     Z1:      DEPTH OF SOUND SOURCE IN FEET
C     K:       NUMBER OF SOURCES ON THE CIRCLE
C     A2:      DEPTH OF THE CENTER OF THE ARRAY
C     XTILT,YTILT,ZROT:  ORIENTATION INFORMATION ABOUT THE
C              SENSING ARRAY (RADIANS)
C     D:       LENGTH OF ARRAY EDGES.
C     L:       DEPTH OF LAYER BOUNDARIES.
C     M:       NUMBER OF RECORDS IN THE VELOCITY DEPTH PROFILE.
C     VEL:     AVERAGE SPEED OF SOUND IN THE LAYERS.
C
C  OUTPUTS:
C     THR:      ACTUAL ELEVATION ANGLE (THETA)
C     THONE: THETA ESTIMATE, PROPOSED METHOD
C     THER:  THETA ERROR, PROPOSED METHOD
C     PHR:      ACTUAL AZIMUTH ANGLE (PHI).
C     PH1:      PHI ESTIMATES, PROPOSED METHOD.
C     PH1ER: PHI ERROR, PROPOSED METHOD.
C     HC:       HORIZONTAL ESTIMATE, CURRENT METHOD.
C     HER:      HORIZONTAL ERROR.
C     ZC:       VERTICAL ESTIMATE, CURRENT METHOD.
C     ZER:      VERTICAL ERROR.
C     T:        TRANSIT TIME TO THE C-HYDROPHONE.
C
C*****************************************************************

      DIMENSION B(5,3),DZ(300),HD(5),HX(5),HY(5),ITH2(20),L(300)
      DIMENSION LM(300),PH1(20),PH1ER(20),PHC(20),PHER(20)
      DIMENSION PHR(20),PX(20),PY(20),T(4),TH1ER(20),TH2(20)
      DIMENSION TH2ER(20),THC(20),THCER(20),THONE(20),THR(20)
      DIMENSION V0(300),V1(300),VEL(300),X0(30),PZ(2,2),PC(2)
      DIMENSION PP(2,3),E(3),TH3(20),TH3ER(20),TT3(3)
      DIMENSION IFL(2),SSC(2),SP(2),H2(20),Z2(20),H2ER(20)
      DIMENSION Z2ER(20),T4(30)

      REAL*8 B,DZ,HD,HX,HY,L,LM,PH1,PH1ER,PHC,PHER,PHR,PX
      REAL*8 PY,T,TH1ER,TH2,TH2ER,THC,THCER,THONE,THR,V0,V1
      REAL*8 VEL,X0,PONE,T4

      REAL*8 A1,A2,A2M,ALPH1,ANG,C,C1,C2,C3,CAZ,CT,CX,CX0,CY,CY0
      REAL*8 CZ,CZ0,D,DR,DR1,DP1,DP2,DTDS,EPS,F,FT,GG,H1,HH1,P1
      REAL*8 P2,PIE,Q1,Q2,Q1P,R0,R1,S,S0,S1,S2,S3,SAZ,ST,SS,T0,T3
      REAL*8 T3P,TH0,TH1,THEC,V,VV0,VV1,X,XTILT,Y,Y0,Y1,YTILT
      REAL*8 Z,Z0,Z1,ZROT,ZZ1,SC,DT

      REAL*8 PP,E,DEL,A,TH3,TH3ER,TT3,SSC,SP,PZ,PC
      REAL*8 A11,A12,A21,A22,B1,B2,H2,H2ER,Z2,Z2ER,THE
      REAL*8 LB,SV,SVU,SU2,SU4,SVU2,G,U
      INTEGER ITH2,IFL

      PIE = 3.14159265359D0
      EPS = 1D-6
      IEST = 0
      M1 = M

C  DISTRIBUTE THE K SOURCES EQUALLY AROUND THE CIRCLE COUNTER-
C  CLOCKWISE FROM THE EAST.
      DO 10 I = 1,K
         ANG = 2*PIE*(I-1)/K
```

```
      PX(I) = H1*DCOS(ANG)
      PY(I) = H1*DSIN(ANG)
      PHR(I) = ANG
      IF(ANG.GT.PIE) PHR(I) = ANG - 2*PIE
 10   CONTINUE

C  FORM SINES AND COSINES OF ALL THE EULER ANGLES:ROLL,PITCH,YAW
    S2 = DSIN(XTILT)
    C2 = DSQRT(1 - S2**2)
    S1 = DSIN(YTILT)/C2
    C1 = DSQRT(1 - S1**2)
    S3 = -DSIN(ZROT)
    C3 = DCOS(ZROT)

C  IN THE COORDINATE SYSTEM HAVING CENTER AT THE C-HYDROPHONE
C  AND POSITIVE-UPWARD, THE LOCATIONS OF THE FOUR HYDROPHONES
C  (RELATIVE TO THE ARM LENGTH D) ARE DEVELOPED NEXT.
    B(1,1) = C2*C3
    B(1,2) = C2*S3
    B(1,3) = S2
    B(2,1) = -S1*S2*C3 - C1*S3
    B(2,2) = -S1*S2*S3 + C1*C3
    B(2,3) = S1*C2
    B(3,1) = -C1*S2*C3 + S1*S3
    B(3,2) = -C1*S2*S3 - S1*C3
    B(3,3) = C1*C2

C  LIKE NOTATION WILL BE USED TO LOCATE THE C-HYROPHONE AND THE
C   ARRAY CENTER.
    DO 12 J = 1,3
      B(4,J) = 0.0D0
      B(5,J) = 0.5*(B(J,1) + B(J,2) + B(J,3))
 12 CONTINUE

    A1 = 0.0D0
    P2 = Z1

C  LOCATE THE HYDROPHONE HORIZONTAL COMPONENTS IN THE COORDINATE
C  SYSTEM CENTERED AT C-HYDROPHONE.
    DO 14 J = 1,5
      HX(J) = D*B(J,1)
      HY(J) = D*B(J,2)
 14 CONTINUE

C  DETERMINE THE DEPTHS OF THE FOUR HYDROPHONES AND THE ARRAY CENTER.
    HD(1) = A2 + D*(B(5,3) - B(1,3))
    HD(2) = A2 + D*(B(5,3) - B(2,3))
    HD(3) = A2 + D*(B(5,3) - B(3,3))
    HD(4) = A2 + D*(B(5,3) - B(4,3))
    HD(5) = A2

C  FIND THE DEEPEST HYDROPHONE
    A2M = 0.D0
    DO 51 J=1,4
      IF(HD(J).GT.A2M) A2M = HD(J)
 51 CONTINUE

C  FORM THE SET OF LAYER MIDPOINTS.
```

```
      DO 105 I = 1,M-1
          LM(I) = .5*(L(I) + L(I+1))
105   CONTINUE

C   FORM DEPTH INCREMENTS, AND ALL SOUND VELOCITY SLOPES AND
C   INTERCEPTS.
      DO 110 I=1,M-2
          DZ(I)=LM(I+1)-LM(I)
          V0(I)=(LM(I+1)*VEL(I) - LM(I)*VEL(I+1))/DZ(I)
          V1(I)=(VEL(I+1)-VEL(I))/DZ(I)
110   CONTINUE
      LM(M) = LM(M-1) + DZ(M-2)
C
      IF(A2M.LT.LM(M-1)) GOTO 126

C  IF A2M IS DEEPER THAN THE LAST LAYER MIDPOINT, THEN WE EXTRAPOLATE
C  THE SOUND VELOCITY PROFILE BY USING A QUADRATIC FUNCTION OVER
C  THE DEEPEST 100 FEET.

C  FIRST COUNT THE NUMBER OF LAYERS (OF THICKNESS DZ(M-2)) TO
C  BE ADJOINED.  ALSO MUST EXTEND THE L ARRAY.

      K0 = 2 + MAX(0,NINT((A2-LM(M-1))/DZ(M-2)))

C  FIND AVERAGE DEPTH OF LAST 100 FEET.
      LB = 0.0D0
      DO 43 I = M-21,M-1
          LB = LB + LM(I)
 43   CONTINUE
      LB = LB/21

C  FORM SUMS OF POWERS AND PRODUCTS.
      SV = 0.0D0
      SVU2 = 0.0D0
      SVU = 0.0D0
      SU2 = 0.0D0
      SU4 = 0.0D0
      DO 45 I = M-21,M-1
          U = LM(I) - LB
          SV = SV + VEL(I)
          SVU = SVU + U*VEL(I)
          SVU2 = SVU2 + U**2 * VEL(I)
          SU2 = SU2 + U**2
          SU4 = SU4 + U**4
 45   CONTINUE

      G = SVU/SU2
      GG = (21*SVU2 - SU2*SV)/(SU4 - SU2**2)
      V1(M-1) = G

C  PERFORM THE EXTRAPOLATION.
      DO 125 I=M,M+K0
          V1(I-1) = V1(I-2) + GG*DZ(M-1)
          LM(I) = LM(I-1) + DZ(M-2)
          VEL(I) = VEL(I-1) + DZ(M-2)*V1(I-1)
          V0(I-1) = (LM(I)*VEL(I-1) - LM(I-1)*VEL(I))/DZ(M-2)
          L(I+1) = L(I) + DZ(M-2)
          DZ(I-1) = DZ(M-2)
```

```
 125  CONTINUE

C  UPDATE M, THE NUMBER OF LAYERS
      M = M+K0
 126  CONTINUE

C  LOCATE THE WATER LAYER, N, CONTAINING THE ARRAY.
      N = M
      DO 37 J = 2,M
          IF((LM(J-1).LE.HD(4)).AND.(LM(J).GT.HD(4))) N = J-1
 37   CONTINUE
C
      V = V0(N) + V1(N)*HD(4)

C  THE OUTER LOOP WILL PERFORM COMPUTATIONS FOR THE K SOUND
C  SOURCES.

C  RAYFITTING
C  THE INNER LOOP WILL FIT RAYS TO THE FOUR HYDROPHONES
C  IN THE ORDER X,Y,Z, AND C.
      DO 50 I = 1,K
          WRITE(*,*)' OUTER LOOP  I = ',I,' K = ',K
          IVV1 = 0
          DO 35 J = 1,4
              P1 = DSQRT((PX(I)-HX(J))**2 + (PY(I)-HY(J))**2)
              Z0 = HD(J)
              CALL RAYFIT1(A1,Z0,P1,P2,M,VEL,LM,DZ,V0,V1,T0,TH0,
     *          TH1,IEST)

C  COLLECT THE FOUR TRANSIT TIMES.
              T(J) = T0

C  IN THIS PROGRAM WE KEEP ONLY THE TRUE ELEVATION ANGLE AT THE
C  C-HYDROPHONE.
              THR(I) = TH0
              T4(I) = T(4)
 35       CONTINUE

C  CALCULATE THE PRE-TILT CORRECTED APPARENT POSITION
          DO 40 J = 1,3
              X0(J)=(D**2 + (V*T(4)-V*T(J))*(V*T(4)+V*T(J)))/(2*D)
 40       CONTINUE

C  COMPUTE DIRECTION COSINES .
          CX0 = X0(1)/(V*T(4))
          CY0 = X0(2)/(V*T(4))
          CZ0 = DSQRT(1 - CX0**2 - CY0**2)

C  PERFORM EXACT TILT CORRECTIONS AND THE ROTATIONAL ALIGNMENT.
 42       CX = B(1,1)*CX0 + B(2,1)*CY0 + B(3,1)*CZ0
          CY = B(1,2)*CX0 + B(2,2)*CY0 + B(3,2)*CZ0
          CZ = B(1,3)*CX0 + B(2,3)*CY0 + B(3,3)*CZ0
          IF(IVV1.EQ.1) THEN
              TH2(I) = 0.5*PIE - DACOS(CZ)
              GOTO 49
          ENDIF
          SAZ = CY/DSQRT(CX**2 + CY**2)
          CAZ = CX/DSQRT(CX**2 + CY**2)
```

```
      PH1(I) = DATAN2(SAZ,CAZ)
      PH1ER(I) = PH1(I) - PHR(I)
      IF(ABS(PH1ER(I)).GT.PIE) PH1ER(I) = PH1(I) + PHR(I)
      THONE(I) = 0.5*PIE - DACOS(CZ)
      TH1ER(I) = THONE(I) - THR(I)

49    CALL ISOGRAD1(A1,Z0,T0,THONE(I),N,LM,VEL,V0,V1,DZ,H2(I),
     *     Z2(I),THE)
      H2ER(I) = H2(I) - H1
      Z2ER(I) = Z2(I) - Z1

50  CONTINUE
C  OUTER LOOP COMPLETED!

    RETURN

100 FORMAT(3(5X,E13.6))
120 FORMAT(3(5X,F15.12))
130 FORMAT(4(F10.8,2X),F13.8,1X,F12.8,2X,2(F12.8,2X),F12.8)
140 FORMAT(5X,'The transit time to the z-phone is not bracketed')
    END
```

REFERENCES

[1] A. B. Coppens, *Comparison of Isogradient and Isospeed Layer Models for Ray Tracing*, NPS Technical Report NPS61–78–004, 1978.

[2] A. B. Coppens and J. V. Sanders, "Introduction to the Sonar Equations," class notes, NPS, April 1982.

[3] D. Main, *Alternative Models for Calculation of Elevation Angles and Ray Transit Times for Ray Tracing of Hydrophonic Tracking Data*, Master's thesis, USNPS, September, 1984.

[4] L. Nettleton, *Geophysical 'rospecting for Oil*, McGraw–Hill, 1940.

[5] NUWES, "Data Gathering and Processing Program (DGAP)," *Section 4, Procedure 5181*, Naval Undersea Weapons Engineering Station, Keyport, WA.

[6] R. Read, *Program for the Simultaneous Estimation of Displacement and Orientation Corrections for Several Short Baseline Arrays*, NPS Technical Report, NPS55–85–028.

[7] R. Read, *An Investigation of Timing Synchronization Errors for Tracking Underwater Vehicles*, NPS Technical Report NPS55–90–15, July 1990.

[8] J. Urich, "Sound Propagation in the Sea," *Defense Advanced Research Projects Agency, OSD*, 1979.

Department of Operations Research Naval Postgraduate School Monterey, CA 93943 ATTN: Prof. L. Johnson, Code OR-Jo	1
Naval Undersea Warfare Engineering Station Keyport, Washington 98345 ATTN: R. Mash, Code 50	1
Naval Undersea Warfare Engineering Station Keyport, Washington 98345 ATTN: R. D. Helander, Code 51	1
Naval Undersea Warfare Engineering Station Keyport, Washington 98345 ATTN: S. L. McKeel, Code 512	2
Naval Undersea Warfare Engineering Station Keyport, Washington 98345 ATTN: J. Knudsen, Code 5122	2
Naval Undersea Warfare Engineering Station Keyport, Washington 98345 ATTN: T. Ward, Code 5122	1
Naval Undersea Warfare Engineering Station Keyport, Washington 98345 ATTN: G. Olsen, Code 5122	1
Naval Undersea Warfare Engineering Station Keyport, Washington 98345 ATTN: J. Hall, Code 5121	1
Naval Undersea Warfare Engineering Station Keyport, Washington 98345 ATTN: R. Evans, Code 5113	1
Naval Undersea Warfare Engineering Station Keyport, Washington 98345 ATTN: L. Beer, Code 5113	1

Naval Undersea Warfare Engineering Station Keyport, Washington 98345 ATTN: L. Bogan, Code 5111	1
Naval Undersea Warfare Engineering Station Keyport, Washington 98345 ATTN: D. Hutchins, Code 5232	1
Naval Undersea Warfare Engineering Station Keyport, Washington 98345 ATTN: J. Cain, Code 70E2	1
Naval Undersea Warfare Engineering Station Keyport, Washington 98345 ATTN: E. Roberts, Code 70B1	1
Naval Undersea Warfare Engineering Station Keyport, Washington 98345 ATTN: J. Chase, Code 70B1	1
Naval Undersea Warfare Engineering Station Keyport, Washington 98345 ATTN: Cmdr Dewey, Code 80	1
Naval Undersea Warfare Engineering Station Keyport, Washington 98345 ATTN: A. Pickard, Code 801	1
Naval Undersea Weapons Engineering Station Keyport, Washington 98345 ATTN: Larry A. Anderson, Code 71E	1
Naval Undersea Warfare Engineering Station Keyport, Washington 98345 ATTN: P. Correa, Code VITRO	1
Naval Undersea Warfare Engineering Station Keyport, Washington 98345 ATTN: B. Boyer, Code VITRO	1
Center for Defense Analyses 1800 N. Beauregard St. Alexandria, VA 22311	1

Center for Naval Analyses 1
4401 Ford Ave.
Alexandria, VA 22302-0268